Region II Storm Surge Project – Joint Probability Analysis of Hurricane and Extratropical Flood Hazards

September 2014

FEMA

Federal Emergency Management Agency
Department of Homeland Security
500 C Street, SW
Washington DC, 20472

Contract: HSFEHQ-09-D-0369-003
Task Order: HSFE02-09-J-0001

This document was prepared by

RAMPP
8401 Arlington Blvd.
Fairfax, VA 22031

TABLE OF CONTENTS

Figures

Tables

1D	One-dimensional
ADCIRC	ADvanced CIRCulation Model for Oceanic, Coastal and Estuarine Waters
CVL	Cross-validated Likelihood
CVSE	Cross-validated Square Error
DNR	Department of Natural Resources (Florida)
GEV	Generalized Extreme Value
HURDAT	Atlantic Hurricane Database
JPM	Joint Probability Method
JPM-OS	Joint Probability Method Optimal Sampling
km	Kilometer
m	Meter
mb	Millibars
NCAR	National Center for Atmospheric Research
NCEP	National Centers for Environmental Prediction
NOAA	National Oceanic and Atmospheric Administration
NOS	National Ocean Service
NWS	National Weather Service
NY-NJ	New York-New Jersey
OWI	Oceanweather Inc.

SECTION ONE INTRODUCTION

This report documents the development of a probabilistic model to represent the occurrence rate and characteristics of future hurricanes capable of producing significant surge inundation along the coast of New Jersey (excluding Delaware Bay) and portions of New York. The analysis used available hurricane data and statistical tools that were developed for the offshore oil industry and in recent flood hazard studies. The report also documents the generation of a suite of synthetic storms, and associated recurrence rates, that provide an efficient representation of the population of possible future tropical cyclones and their characteristics for use as inputs to numerical wind, wave, and surge models. These synthetic storms are generated by means of a JPM-OS (Joint Probability Method—Optimal Sampling) scheme, which is also described in the report.

This study follows the approach initially developed in the Mississippi surge study (FEMA, 2008). It incorporates refinements introduced in subsequent surge studies, as well as data modifications to accommodate the conditions of tropical cyclones affecting the New York and New Jersey coast and to take into account the effects of astronomical tides.

This report also documents the investigation of statistical issues that arose in the analysis of extratropical storms.

1.1 PROJECT OBJECTIVES

The objective of the analysis documented here is to provide the following two inputs for the Region II New York-New Jersey (NY-NJ) storm surge study being performed by Risk Assessment, Mapping, and Planning Partners (RAMPP) for the Federal Emergency Management Agency (FEMA):

1. A probabilistic characterization of the occurrence and characteristics of future[1] tropical cyclones that may cause significant surge along the NY-NJ coast.

2. A set of representative synthetic storms and their associated recurrence rates, to be used for the numerical wind, wave, and surge calculations, and in the final probability calculations. These synthetic storms have characteristics (including starting times for the purpose of astronomical-tide calculations) and recurrence rates that make them representative of the population of possible future storms, for the purposes of surge inundation calculations.

An additional element in this report is the investigation of statistical issues that arose in the analysis of extratropical storms. These storms were not modeled using JPM-OS, but rather a historical-hindcast approach[2]. A number of statistical issues arise because the number of historical extratropical storms is not large.

[1] The report refers to future storms, in the sense that hazard analyses usually consider future events. However, the analysis only considered the current climatological regime, as represented by the storm population considered in Section 2.

[2] In the historical hindcast approach, the wind and pressure fields are reconstructed using all available data and then used to calculate surge throughout the study region. The surge values at each grid point are then fit to a distribution and used to determine the surge elevations associated with the desired recurrence intervals.

The numerical calculation of winds, waves, surge, and total inundation for these synthetic storms, the use of results from these calculations to compute elevations associated with recurrence intervals of interest, and the actual results from these calculations are documented under separate reports for the Region II Storm Surge Project.

1.2 APPROACH FOR JPM-OS

The NY-NJ surge study follows the Joint-Probability Method (JPM), as described by Resio (2007) and Toro et al. (2010b). This study incorporates the experience from the Mississippi Surge study (FEMA, 2008; Niedoroda et al., 2010), as well as subsequent FEMA flood studies, with the appropriate data and model modifications to capture the conditions in NY-NJ.

Following the approach used in these prior studies, it was decided to use the characteristics at or near landfall as the primary variables. This is justified by the following two arguments:

1. most of the coastal surge is generated by the storm in the last 90 nautical miles prior to landfall (Resio, 2007), and
2. more and better storm data are available at the coast than offshore, especially data for older storms.

For the purposes of the JPM method, the storm is described in terms of its characteristics at or near landfall, using the following parameters: pressure deficit[3] ΔP (representing storm intensity), radius of the exponential pressure profile[4] R_p (representing storm size), Holland's B parameter (which controls the shape of the pressure and wind fields), forward velocity V_f, storm heading θ[5], and the landfall location (or, equivalently, the minimum distance from the track to a reference point along the coast). These parameters, illustrated in Figure 1-1, represent the main storm characteristics affecting surge. They are treated explicitly as random variables in the JPM method. Other storm characteristics are not considered explicitly. Although tropical cyclones are much more complex than this parameterization allows for, and substantially more information is available for well-studied recent storms, it is necessary at present to utilize this simple storm parameterization for the probabilistic characterization of future storms.

The differences between real tropical cyclones and this simple parameterization are not ignored in the JPM formulation employed in this study. They are included in a statistical sense by means of the epsilon (ε) terms used in the JPM calculations, as will be explained in Section 4.2.

---

[3] In this project, ΔP is calculated from the central pressure P_C by assuming that the far-field pressure is always 1013 mb (i.e. $\Delta P = 1013 - P_C$).

[4] This project works exclusively with R_p, the radius of the exponential pressure profile. In particular, the data are collected in terms of R_p, the models are constructed in terms of R_p, and the synthetic storms are parameterized in terms of R_p. The difference between R_p and the radius to maximum winds $R_{\max}$ (sometimes written as RMW) is sometimes ignored, although the two are not necessarily identical for every storm. Wherever this report refers to $R_{\max}$, it should be understood as referring to R_p.

[5] Direction to, measured clockwise from North.

The maximum elevation of a storm surge is also affected by the tide phase and amplitude at the time of landfall. Consideration of these effects is necessary for coastal locations in NY-NJ because the average tidal range is on the order of 4 feet[6].

For the statistical analyses to determine the storm recurrence rate and probability distribution of ΔP, which are the most important quantities in the storm characterization, we follow the methodology developed by Chouinard and his colleagues (Chouinard, 1992; Chouinard and Liu, 1997; Chouinard et al., 1997). This methodology assigns weights to the historical storm data based on each storm's distance to the site of interest, in a manner that provides an optimal compromise between statistical precision and geographical resolution. For other parameters, this study follows simpler statistical approaches.

The JPM method considers all possible combinations of storm characteristics at landfall, with their associated probabilities; calculates the surge effects for each combination; and then combines these results to obtain the annual probability of exceeding any storm surge elevation of interest. Mathematically, this calculation is represented as a multi-dimensional integral (the JPM integral).

Given the number of factors affecting surge, and the computational effort required to compute winds, waves, and surge for one combination of these factors, implementation of the full JPM approach is not feasible. Recently two JPM-Optimal Sampling (JPM-OS) approaches have been developed to overcome this problem (Resio 2007, Toro et al., 2010a and b). The approach used in this study uses a quadrature procedure that approximates the multi-dimensional JPM integral by means of a weighted sum over a manageable number of discrete probability masses (see Toro et al., 2010a for details on this formulation). Each of these masses may be interpreted as the characteristics at landfall of a representative synthetic storm. These characteristics, together with some simple deterministic rules, are then used to specify the entire storm history, which is then used as input to the numerical wind, wave, and surge models. Once the total inundation is computed for each synthetic storm, calculation of the associated exceedance probabilities (or the inverse calculation of the surge associated with a certain exceedance probability) is straightforward.

An important consideration in designing and evaluating the JPM-OS formulation is that very little benefit is gained if the accuracy of the JPM-OS integration is significantly greater than the accuracy of the numerical wind and surge models. Based on the analysis of high-water marks and other tests performed in the Mississippi study (FEMA, 2008; Niedoroda et al., 2010), the accuracy of the combined wind and wave models may be characterized by a standard deviation of 1 to 2 feet. This value can be used to establish a criterion for the maximum tolerable bias and standard deviation when evaluating the adequacy of the JPM-OS storm set.

The maximum elevation of a storm surge is affected by the tide phase at the time of landfall. This effect is included in the analysis by assigning a random initial tide phase to the hydrodynamic model simulation of each of the synthetic storms. More detail on this treatment of the astronomical tide is given in Section 4.6. A similar approach was followed for extra-tropical storms, as described in Section 5.4.

[6] The treatment of tides is presented in Section 4.6 and is not discussed in relation to the tropical cyclone characteristics or the JPM formulation.

1.3 OVERALL CONTENT AND ORGANIZATION OF THIS REPORT

This report covers three major aspects of the joint probability analysis of tropical cyclone flood hazards for NY-NJ. First it explains, in some detail, the methods that have been used in other recent FEMA coastal flood studies and the adaptation of these methods to the specific conditions for NY-NJ. Second, it describes the development, testing, and verification of new or substantially altered methods that have been specifically developed to improve the accuracy and efficiency of the joint probability analysis or other aspects of the overall project. Third, it documents various project data and intermediate analysis results in order to provide a record of the work completed. It is often necessary to provide considerable background information and explanations in order to provide coherent descriptions of the steps conducted that led to particular results.

The organization of this report follows the natural progression of the steps required for the development of the JPM-OS synthetic storms. Section 2 documents the data used in this study. Section 3 documents the statistical analysis of these data to determine the storm rate and the probability distributions of ΔP, $R_{\max}$, V_f, and θ. Section 4 describes the JPM method in detail and documents the development of the quadrature procedure and the generation of synthetic storms. Section 5 investigates statistical issues that arose in the analysis of extratropical storms. Section 6 describes the procedure for calculating the surge elevations for each recurrence interval of interest using the results from the production runs.

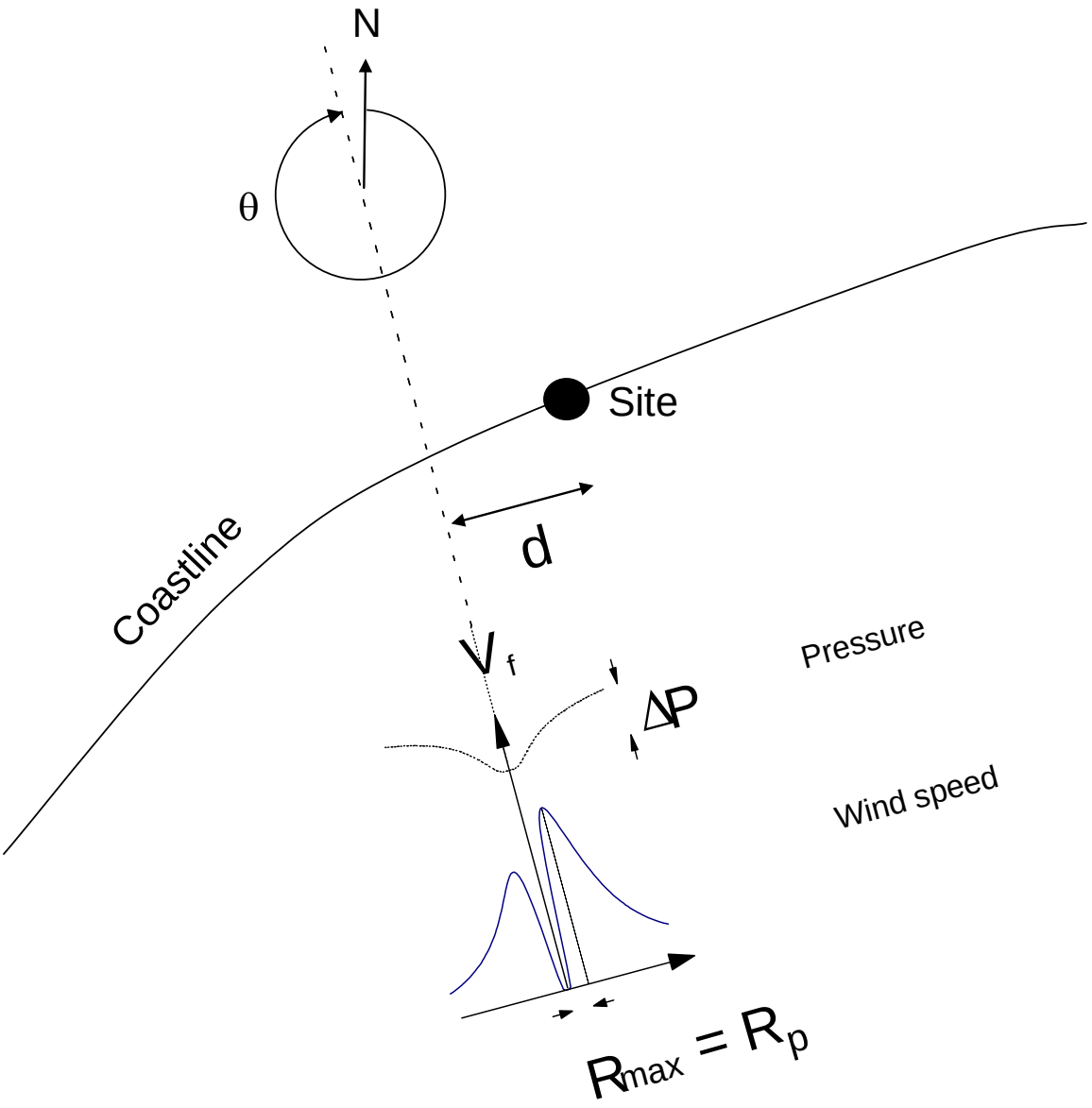

Figure 1-1. Characterization of a storm as it approaches the coast. Note that Holland's B parameter is not included in the figure. B changes the shape of the wind and pressure fields and affects the maximum wind speed for a given ΔP .

SECTION TWO DATA

2.1 INTRODUCTION

This section documents the tropical cyclone data used to develop the probabilistic model of storm occurrence and characteristics as described in Section 3. It also discusses some of the key decisions that were necessary as part of the data collection and selection.

2.2 DATA SOURCES USED

The tropical cyclone data for this study were developed by Oceanweather, Inc. (OWI) and are documented in a separate report (RAMPP, 2014a).

These data consist of two overlapping data sets, as follows:

1. A data set of all tropical cyclones passing within the study area (defined as latitudes 38-42 North and longitudes 64 to 82 West[7]) during the period 1900-2010. This data set includes track coordinates and central pressure taken every 6 hours, and additional parameters not considered in this study.

2. A data set of 30 well studied storms. This set includes the hurricanes of 1938 and 1944, which caused significant flooding in the NY-NJ region, as well as more recent storms for which more abundant data are available. This data set includes track coordinates, central pressure, and wind field parameters taken every 6 hours (sometimes every 3 hours near landfall). Some of the data for the older storms have been derived from reanalysis and interpolation from regional weather records, reports from "ships of opportunity," and other data sources identified by OWI. The data sources used and process followed are documented in the OWI report. The wind field parameters are defined in terms of a single or double-exponential representation (as appropriate). The double-exponential representation has the following six parameters: two pressure deficits (which add to the total ΔP), two radii R_1 and R_2, and two Holland B parameters. Sensitivity studies performed as part of this study indicated that the double-exponential storms could be represented (for the purposes of surge response along the NY-NJ coast) by means of "equivalent" single-exponential representation with the same parameters described in Section 1. The analysis conducted in this study considered only these equivalent single-exponential representations.

This study considered only hurricanes with central pressures of 980 millibars (mb) or lower (roughly corresponding to Category 2 and greater on the Saffir-Simpson Hurricane Wind Scale) at or near landfall. Based on experience with prior FEMA analyses and other recent studies, it is clear the weaker hurricanes and tropical storms make small contributions to surge hazards at frequencies of occurrence relevant to the purposes of mapping FEMA coastal flood hazard areas. In addition, the contribution of the weaker cyclonic storms to the 10-percent-annual-chance (10-year) surge elevations is much smaller than the contribution from extratropical storms.

[7] The limits of this screening are not important, provided that they are broader than the kernel size used in Chouinard's statistical analysis. This will become clear in Section 3.

2.3 PERIOD OF RECORD

The selection of the time period to use as input for the statistical calculations is one of the most important decisions in an analysis of this kind. The two data sets described above extend back to 1900 and 1938, respectively. In addition, the National Oceanic and Atmospheric Administration (NOAA) HURDAT (or the Atlantic Hurricane Database) database contains results from the re-analysis of data extending back to 1850[8].

The problem of selecting the period of record may be stated as follows. On the one hand, it is helpful to use as much of the available data as possible, in order to have the lowest possible statistical uncertainty in the resulting probabilistic tropical cyclone model. On the other hand, it is helpful to exclude older data that are incomplete or may contain significant biases, in order to have a probabilistic model that provides a complete representation of the storm environment.

Although coastal and inland weather measurements improved steadily in quality and geographical coverage over the 20th Century, measurements were sparse and erratic until relatively recently. The older offshore data often depended on unplanned encounters by ships whose position relative to the storm was difficult to establish. This situation changed dramatically during World War II with the initiation of aircraft missions specifically designed to measure storm parameters. Since that time the quality of both offshore and onshore data has risen steadily. Aircraft instrumentation and navigation have increased in a more or less continuous fashion since World War II. Satellite observations were added during the 1960s, and these too have become increasingly more sophisticated and useful. More instrument systems have been introduced in recent decades. Ocean data buoys with meteorological and oceanographic sensors have been deployed since the 1970s. A variety of Doppler radar installations have come online during the 1990s. Within the last few years, mobile meteorological stations have been added to increase the spatial density of storm measurements. Another important development is the National Centers for Environmental Prediction /National Center for Atmospheric Research (NCEP/NCAR) reanalysis project, which has assimilated data obtained since 1948 from the land surface, ships, aircraft, satellite, and other sources. This assimilation is performed in a consistent manner, producing estimates of atmospheric conditions with improved temporal and spatial resolution.

Superimposed on this evolution in the observing system, natural large-scale atmospheric cycles, with periods of several years to decades, may affect the rate and intensity of hurricanes (e.g., Gray, 1984; Webster et al., 2005; Bell and Chelliah, 2006; Resio and Orelup, 2006).

The year 1948 was chosen as the beginning of the period of record because this is the first year covered by the NCEP/NCAR re-analysis. In general, the choice of beginning year depends on the storm-history in the region and the evolution of the observation and re-analysis efforts. The year 2009 was used as the ending year because the data-collection task was completed in early 2010. In particular, this report does not consider Hurricanes Irene or Sandy, which occurred after completion of the work reported here.

Climate change and global warming are not considered in this study, largely because no significant changes in the storm climatology are anticipated during the period when the resulting

[8] This tabulation has a number of drawbacks. In particular, it lacks central-pressure data for many storms and it does not contain the storm radius R_p.

FEMA flood hazard maps will be in use. In addition, there is still considerable uncertainty about the effects of global warming on hurricane frequency and intensity (e.g., Holland and Webster, 2007; Gualdi et al., 2008). The climate fluctuations and observed trends discussed above may also contain climate-change effects, but it is difficult to precisely identify these effects at present. For these technical reasons, climate change factors are considered to be outside the scope of these studies. It is also important to note that, although extreme-event results of the type obtained in probabilistic surge studies are often referred to as *n-year* values, the long time periods implied by this terminology are irrelevant. The purpose of these studies is the characterization of low-probability flooding events during time periods that extend a few years from the present.

2.4 SELECTED STORMS FOR STATISTICAL ANALYSIS

Tables 2-1[9] lists the storms for which track and intensity information was available and Table 2-2 provides the storms for which detailed information was available (Well-Studied storms)[10] for storms that occurred within the geographical and temporal windows described above (both landfalling and bypassing), and their associated characteristics. These storms were used as data for the statistical analysis presented in the next section. These lists are not mutually exclusive.

[9] The values shown in Table 2-1 correspond to the closest approach to a point roughly half-way up the New Jersey coast (this location is shown as point 3 in Figure 3-1).

[10] These are generally more recent storms, for which more detailed information is available about wind and pressure fields. See Oceanweather (2010) for additional details.

Table 2-1. List of Storms for Which Track and Intensity Information Is Available

Name	Year	ΔP[11] (mb)	Distance (km)	Heading (deg)
Able	1950	60	315	45
Dog	1950	38	287	31
How	1951	54	387	55
1952_01	1952	22	227	28
Barbara	1953	38	150	44
Carol	1953	40	353	25
Florence	1953	12	458	61
Carol	1954	46	83	19
Edna	1954	49	177	28
Ione	1955	44	309	66
Flossy	1956	16	225	55
Daisy	1958	42	211	42
Helene	1958	58	431	63
Cindy	1959	17	122	49
Donna	1960	50	67	26
Esther	1961	45	208	24
Gerda	1961	24	488	34
Alma	1962	27	238	38
Dora	1964	24	297	52
Gladys	1964	37	376	42
1965_01	1965	10	293	69
Alma	1966	19	181	32
Gladys	1968	32	361	61
Anna	1969	17	352	43
Camille	1969	9	323	101
Gerda	1969	31	266	38
1970_04	1970	13	333	54
Arlene	1971	20	316	56
Beth	1971	28	467	43
Heidi	1971	21	412	11
Agnes	1972	27	64	-7
Carrie	1972	27	277	14
Alfa	1973	14	365	19
Dolly	1974	15	376	39
Belle	1976	40	48	12
Bob	1979	3	330	113

[11] Only storms with ΔP>33 mb were considered in the analysis, as will be discussed in Section 3.

Name	Year	ΔP[11] (mb)	Distance (km)	Heading (deg)
Charley	1980	5	433	141
Dennis	1981	23	397	69
Diana	1984	22	307	55
Danny	1985	5	183	64
Gloria	1985	58	22	20
Henri	1985	11	60	26
Andrew	1986	11	342	44
Charley	1986	23	146	55
Alberto	1988	8	191	44
Lili	1990	17	419	42
Bob	1991	62	129	26
Emily	1993	53	283	66
Allison	1995	20	271	55
Felix	1995	42	402	62
Edouard	1996	56	400	4
Josephine	1996	28	151	33
Un-named 1997	1997	8	277	36
Danny	1997	24	236	53
Bonnie	1998	24	272	55
Earl	1998	13	297	64
Floyd	1999	36	3	28
Irene	1999	51	399	56
Helene	2000	11	240	65
Allison	2001	13	81	51
Arthur	2002	12	476	72
Gustav	2002	32	328	55
Alex	2004	39	376	72
Bonnie	2004	6	103	30
Charley	2004	8	58	48
Gaston	2004	18	122	56
Hermine	2004	9	238	2
Ivan	2004	14	231	113
Jeanne	2004	16	118	100
Cindy	2005	9	65	80
Ophelia	2005	19	260	36
2005_22	2005	10	34	0
Alberto	2006	20	307	53
Beryl	2006	17	158	38
Barry	2007	18	109	27

Name	Year	ΔP[11] (mb)	Distance (km)	Heading (deg)
Gabrielle	2007	9	296	74
Noel	2007	45	394	21
Cristobal	2008	15	380	60
Kyle	2008	27	487	23
2009_01	2009	7	380	63

Table 2-2. List of Well-Studied Storms

Storm Name	Year	Max. Wind Speed (kt)	Minimum Sea Level Pressure (mb)
1938_04	1938	120	937
1944_07	1944	105	953
1948_03	1948	80	980
Baker	1952	100	962
Barbara	1953	90	970
Carol	1953	90	971
Carol	1954	100	962
Edna	1954	110	947
Hazel	1954	75	984
Connie	1955	85	976
Daisy	1958	90	969
Donna	1960	95	963
Esther	1961	90	969
Doria	1967	85	976
Gerda	1969	85	975
Agnes	1972	80	977
Belle	1976	85	975
Ella	1978	100	961
Gloria	1985	110	951
Bertha	1990	85	973
Bob	1991	105	952
Emily	1993	95	966
Edouard	1996	100	962
Hortense	1996	100	960
Floyd	1999	75	982
Gustav	2002	95	965
Isabel	2003	75	984
Alex	2004	105	957
Noel	2007	95	967
Bill	2009	100	962

SECTION THREE PROBABILISTIC MODEL OF STORM FREQUENCY AND CHARACTERISTICS (STORM CLIMATOLOGY)

3.1 INTRODUCTION

This section describes the development of a probabilistic model for the occurrence and storm characteristics of hurricanes affecting the NY-NJ Coast.

The occurrence of hurricanes in the neighborhood of a specific point is characterized by terms of the omni-directional rate $\lambda(\mathbf{x})$ or the directional rate $\lambda(\mathbf{x},\theta)$ [12] using a Poisson line-process model (see Chouinard and Liu, 1997, and FEMA, 2008, for details).

Because hurricanes are seen to weaken rapidly as they approach the study region, it was decided not to assume a priori that the storm properties are constant throughout the region. To this effect, seven points along the coast were selected (see Figure 3-1), and statistics were calculated with reference to these points. In addition, a finer grid (with 0.1-degree spacing) was used to investigate the variation of storm rates along the coast. The use of this grid is illustrated in the map shown in Figure 3-4.

3.2 CALCULATION OF STORM RATES FOR THE LANDFALLING STORMS

3.2.1 Methodology and Optimal Kernel Sizes

This study utilized the methodology of Chouinard and Liu (1997; see also Chouinard, 1992) to calculate the rate of storms in the vicinity of the reference point. This methodology is endorsed for Atlantic and Gulf of Mexico applications by the FEMA (2012) Gidelines for JPM-OS. The geometry of storm tracks as they pass near a specific site is idealized as a Poisson line process. The key parameter of this model is the directional rate $\lambda(\theta)$, which has units of storms/year/kilometer (km)/degree[13]. If direction is neglected, the key parameter is the omni-directional rate λ, which has units of storms/year/km. This study calculated both rates.

The passage of each storm near a given site (such as the Reference Point) is characterized by the associated minimum distance d and storm heading θ of the storm relative to the site (see Figure 1-1). To calculate the rate at a site, Chouinard and Liu (1997) propose a *kernel* estimate, where the rate is proportional to a weighted count of the observed data in the storm catalog, with weights that depend on the distance *d* from the storm to the site and the deviation of the storm track direction from the direction of interest. Storms that pass farther from the site or that have directions different from the direction of interest receive lower weight. The resulting expressions for the directional rate $\lambda(\theta)$ and the omni-directional rate λ, respectively, are as follows:

$$\lambda(\theta) = \frac{1}{T} \sum_{i \text{ (all storms)}} k(d_i)k(\theta_i - \theta) \qquad (3\text{-}1)$$

[12] Because this report considers a single site, namely the Reference Point, the argument $\mathbf{x}$ will be eliminated in the presentation that follows.

[13] Degree is used here as an angular measure.

$$\lambda = \frac{1}{T} \sum_{\text{(all storms)}} k(d_i) \qquad (3\text{-}2)$$

where the summation extends over all storms in the catalog, T is the period of record (in years), and the kernel functions are taken as normal-distribution shapes, as follows:

$$k(d_i) = \frac{1}{\sqrt{2\pi}h_d} \exp\left[-\frac{1}{2}\left(\frac{d_i}{h_d}\right)^2\right] \qquad (3\text{-}3)$$

and

$$k(\theta_i - \theta) = \frac{1}{\sqrt{2\pi}h_\theta} \exp\left[-\frac{1}{2}\left(\frac{\theta_i - \theta}{h_\theta}\right)^2\right] \qquad (3\text{-}4)$$

An important step in this procedure is the selection of the kernel widths h_d and h_θ. A small kernel width introduces too much statistical uncertainty, as the calculated rate effectively depends on data from a few storms. A large kernel width reduces the statistical uncertainty by considering storms occurring over a wider area, but may introduce too much spatial bias (i.e., it may mix data that are not homogeneous and thus fails to resolve spatial variability in the data). The aim becomes finding the optimal tradeoff between statistical precision and spatial resolution.

Chouinard and Liu (1997) utilize a technique known as *least-squares cross-validation* to determine the optimal kernel size for the estimation of rates. To calculate the optimal kernel width h_d for the omni-directional rate, the data are partitioned at random into two samples (the *estimation sample* and the *validation sample*) using a randomization scheme in which each storm is assigned to the estimation sample with probability p and to the validation sample with probability 1-p. The estimation sample is used to estimate the predicted rate at all grid points using Equations 3-12 and 3-23. The validation sample is then used to calculate the observed rate[14]. The two rates are then adjusted for the size of the two samples (i.e., for the effect of p), the difference between the two rates is squared and summed over all grid points, and the result is summed over many random partitions of the sample. The resulting quantity is the *cross-validated square error* (CVSE); the optimal choice of kernel width h_d is the one that yields the lowest CVSE. Figure 3-2 shows the values of CVSE as a function of kernel size for the calculation of directional rates. Although the data results suggest a somewhat larger value, a value of 200 km was selected in consideration of the confined nature of the New York Bight. This slight deviation from the calculated optimal value is a reasonable choice and is also the

[14] The observed rate is calculated by counting the number of storms in the validation sample that are within 40 km of the site and then dividing the result by 80 km and by the number of years in the storm catalog. Also, the probability p is set to 0.9 to avoid a large change to the size of the estimation sample. The resulting optimal kernel size is not sensitive to these choices, as long as they are within reasonable bounds (Chouinard and Liu, 1997). Similarly, the results for directional rates are not sensitive to the choice of angular interval to consider in the calculation of observed directional rates.

default kernel size recommended by FEMA (2012). This value, though smaller than the optimal value in Figure 3-2, is greater than the optimal value of 140 km obtained by Chouinard and Liu (1997) for the Gulf of Mexico.

A similar procedure is followed for determining the optimal combination of kernel widths h_d and h_θ for the calculation of directional rates. Results are shown in Figure 3-3, which indicates optimal kernel sizes of 60 km and 9°, respectively. These results are also comparable to those obtained by Chouinard and Liu (1997).

It is useful to compare this approach to the conventional approach, where a storm is counted in the calculation of rates if it makes landfall within a selected portion of the coast or a certain distance from the reference point[15]. The capture zone approach is equivalent to using a "boxcar" kernel of an arbitrary width. If two storms make landfall near the edge of the capture zone but only one of them is within the zone, one will receive a weight of 1/width and the other one will receive a weight of 0 (zero). In this case, because the total number of storms is small, a small change in the size of the capture zone will lead to a large change in the calculated rate. In contrast, the Chouinard and Liu (1997) approach will give these two storms nearly identical weights. The two main differences between the Chouinard and Liu (1997) approach and the capture zone approach are as follows: the smooth versus boxcar kernels, and the objective versus arbitrary procedures to determine kernel size.

3.2.2 Results for Rate and for the Distribution of Heading

Calculation of the directional rate for the seven points shown in Figure 3-1, using kernel sizes of 64 km and 9°, yields the values shown in Figure 3-5. These values can be grouped into New Jersey (sites 1-4) and Long Island (sites 5-7) and their associated rate functions can be approximated by normal distributions with mean values of 22 and 23 degrees, respectively, and a standard deviation of 10 km, as shown in Figure 3-5. Dividing the directional rate by the omni-directional rate yields the probability distribution of the storm heading θ.

3.3 CALCULATION OF STORM CHARACTERISTICS FOR THE LANDFALLING STORMS

3.3.1 Methodology and Optimal Kernel Size for ΔP

The methodology for determining the probability distribution of ΔP for hurricanes in the vicinity of the reference point is based on the work of Chouinard et al. (1997; see also Chouinard, 1992), and is in many ways similar to the methodology used earlier to estimate the rate of storms. The duration *T* of the period of record does not enter directly in this part of the calculation because the goal is to obtain the probability distribution of ΔP given that one storm has occurred.

[15] This discussion of the kernel and capture-zone approaches also applies to the approach for calculating the distribution of ΔP.

For this calculation, we used the same 1948-2009 data utilized above for the calculation of rates (Table 2-1)[16], augmented by the corresponding values obtained for the 1938 and 1944 hurricanes.

The analysis considered only storms with $\Delta P > 33\text{mb}$ and adopted a truncated Weibull distribution shape based on experience from earlier studies performed by Risk Engineering (2005). For this distribution shape, the complementary cumulative distribution of ΔP in the vicinity of the reference point is of the form

$$P[\Delta P > x] = \exp[-(x/u)^k + (\Delta P_0/u)^k] \qquad x > \Delta P_0 \qquad (3\text{-}5)$$

where u is a scale parameter, k is a shape parameter, and $\Delta P_0 = 33\text{mb}$ is the lower limit of the data being considered.

In addition, the constraint that the probability density function of ΔP must be a monotonically decreasing function over the $\Delta P > 33\text{mb}$ range is introduced. This constraint requires that more intense storms be less frequent than weaker ones, which is a physically reasonable constraint for storms in this ΔP range. This constraint improves the statistical stability of the results.

The distribution parameters u and k are estimated from all the storm data using the method of maximum weighted likelihood, where the weights depend on the distance between the track of storm i and the reference point, and subject to the monotonicity constraint described above. Specifically, the weighted log-likelihood is of the form

$$\ln(WL) = \sum_i w(d_i) \ln[f_{\Delta P}(\Delta p_i; u, k)] \qquad (3\text{-}6)$$

where d_i is the distance between the reference point and the track of storm i (associated with pressure deficit Δp_i at landfall), $w(d_i)$ is a Gaussian distance-dependent weight (which is given by Equation 3-3 introduced earlier[17], although the kernel size h_d is not necessarily the same as that used for the calculation of the storm rate), $f_{\Delta P}(\Delta p; u, k)$ is the Weibull probability density function[18], and the summation extends over all storms with $\Delta P > 33mb$ in the data set.

In a manner similar to what was done in for the calculation of optimal kernel size for rates, Chouinard et al. (1997) propose an approach for the selection of an optimal kernel size. This approach uses the cross-validated likelihood (CVL), which is calculated for multiple kernel sizes using simulated hurricane catalogs, and the optimal size is identified as the value associated with the minimum CVL. Figure 3-7 shows the values obtained for the cross-validated likelihood; based on these results, an optimal kernel size of 100 km was chosen.

[16] Note that only hurricanes with ΔP greater than 33 mb (central pressures less than or equal to 980 mb) are actually used in these calculations.

[17] The symbol w is utilized for the weight used to calculate the ΔP distribution (although the symbol k is utilized for the weight used to calculate the rates), in order to avoid confusion with the scale parameter k of the Weibull distribution.

[18] The Weibull probability density function is obtained by differentiating Equation 3-5 with respect to Δp (or with respect to x, according to the notation in Equation 3-5).

3.3.2 Results for the Probability Distribution of ΔP and Its Statistical Uncertainty

Once the kernel size is selected, the best-estimate values of the Weibull parameters *u* and *k* are obtained by maximizing Equation 3-6, subject to the monotonicity constraint described earlier. These best-estimate values of the parameters are not sufficient, however, because these parameters have significant uncertainty as a result of the small sample size. To quantify this uncertainty, a bootstrapping procedure (Efron, 1982) was utilized. In each cycle of the bootstrapping, a synthetic storm catalog with the same duration as the actual catalog is created by using a re-sampling scheme[19]. This catalog is then used to calculate a new set of parameter values (i.e., rate and Weibull parameters u and k), using the kernel size of 100 km determined earlier. This process is repeated 500 times, resulting in 500 values of the rate and 500 cumulative distributions of ΔP .

Figure 3-8 displays the summary statistics obtained from the cumulative distributions of ΔP for site 3 in Figure 3-1. Similar calculations were performed for other sites, obtaining nearly identical results. The statistical uncertainty (i.e., the uncertainty in the probability of exceeding a certain ΔP value at landfall, say 90 mb, given that a hurricane with $\Delta P > 33\text{mb}$ makes landfall near the site) is displayed by the distance between the 16- and 84-percentile curves. For low and moderate values of ΔP , these percentile curves are closely spaced, indicating low uncertainty. For higher values of ΔP , these percentile curves spread out gradually, indicating increasing uncertainty. The uncertainty is significant, but not unreasonably large, for ΔP in the 60-90 mb range, which is expected to control the results for the 1-percent-annual-chance exceedance probability. Also, the mean curve deviates from the 50-percentile or median curve (which is nearly identical to the best-estimate curve, not shown), as a result of skewness.

The resulting mean distribution of ΔP in Figure 3-8 is an average of Weibull distributions and does not necessarily follow a Weibull distribution. It was found, however, that a Weibull distribution with U=41.2 mb and k=2.05 provides a good approximation to the mean distribution of ΔP , for the range of ΔP of interest to this study. This distribution is used in all the analyses that follow. The rationale for using the mean distribution for ΔP , rather than the best-estimate distribution that one obtains by applying the Chouinard et al. procedure to the historical hurricane catalog, is based on the decomposition axiom of decision theory[20] (see Patè-Cornell, 1990, or McGuire et al., 2005)[21].

[19] For each historical storm in the data set, a random number is drawn from a Poisson distribution with mean value of 1. This number is then used for the number of times that this particular historical storm will appear in the synthetic catalog. Thus, a historical storm may appear 0, 1, 2, or more times in any given synthetic catalog (although it is unlikely that the storm will appear two or more times in the same synthetic catalog). On average, each historical storm will appear once in each synthetic catalog.

[20] This axiom states that rational decisions depend only on the possible outcomes and their probabilities, without regard for details about which intermediate events may have led to a given outcome. For the purposes of this analysis the axiom implies that rational decisions should not be affected by the distinction between aleatory uncertainty (i.e., chance) and epistemic uncertainty (i.e., lack of knowledge about the probability of the chance event). All that matters is the outcome (i.e., flooding at a certain location) and the decision maker's mean estimate of its probability of occurrence.

[21] By applying the Chouinard et al. procedure to multiple synthetic hurricane catalogs and then using the mean value of the cumulative distributions obtained from these catalogs, this study is employing a natural extension of the Chouinard et al. procedure. This extension was used in the study and in several other FEMA studies.

3.3.3 Radius of the Exponential Pressure Profile (Radius of Maximum Winds)

For this calculation, and other calculations that follow, data from the well investigated storms listed in Table 2-2 were used. Specifically, the parameter values associated with the closest approach to site 3 in Figure 3-1 were used, and those snapshots that OWI flagged as having poor quality or poor fit to the data were excluded. The resulting 19 values are listed in Table 3-1.

Considerable attention has been given to establishing whether the radius of the exponential pressure profile R_p is statistically independent of the central pressure of a storm, going as far back as NOAA National Weather Service (NWS) Technical Report NWS-38, published in 1987. Because the data in Tables 3-1 and 2-2 are not sufficient for developing a project-specific relationship between R_p and ΔP, this study adopted the model obtained by Vickery and Wadhera (2008) for all open-water hurricane measurements, which is their recommended model for Atlantic landfalling hurricanes. In this model, R_p given ΔP has a lognormal distribution with median and standard deviation given by

$$\begin{aligned} median(R_p) &= \exp\left(3.015 - 6.291\times10^{-5}\Delta P^2 + 0.0337\psi\right) \\ \sigma_{\ln[R_p|\Delta P]} &= 0.441 \end{aligned} \qquad (3\text{-}7)$$

where R_p [22] is given in km and ψ is the latitude in degrees (this study used a value of 40 degrees). Vickery and Wadhera (2008) find a decreasing standard deviation for ΔP values above 87 mb, but this study adopted a constant standard deviation because there are few data above 87 mb in their data set (see their Figure 8), and these data are likely not independent. The effect of not adopting this decrease is expected to be small because the 1-percent-annual-chance and 0.2-percent-annual-chance results are dominated by storms with ΔP below 87 mb.

Figure 3-9 shows the Vickery and Wadhera median and logarithmic $\pm\sigma$ curves, as well as the ΔP - R_p values from Table 3-1. This figure indicates that the model for R_p given ΔP is consistent with the sparse data.

As shown in Figure 3-9, the data for landfalling storms are sparse and the correlation of the parameters is not strong. However, the decision on whether to consider these two parameters as correlated has important consequences. If there is no negative correlation, then future storms with large radii and high ΔP's—which tend to generate higher surges, and these high surges affect a wider extent of the coast—are more likely than they are under the common assumption of negative correlation between ΔP and R_p. Models with negative correlation have been used in a number of other studies, such as NWS-38, Wen and Banon (1991), Vickery et al. (2000); Toro et al. (2004), Resio (2007), and FEMA (2008).

Shen (2006) provides some insight into the relationship between Rp and ΔP. This paper examines the kinetic-energy balance within a hurricane and concludes that, given the same large-scale environmental conditions, hurricanes with smaller radii have higher potential intensity.

[22] Vickery and Wadhera (2008) give this equation in terms of RMW, but their Equation 2 makes it clear that they are using R_p.

Shen (2006) also reports that this conclusion is not sensitive to changes in the parameters of his model. This result provides additional support for models with negative correlation.

An important consideration is that the large scatter observed in Figure 3-9 is not neglected and is carried through the JPM analysis. In particular, the JPM formulation considers that values or Rp from future storms may easily be larger by 60 percent than predicted by the median relation.

3.3.4 Holland B Parameter

As was the case for R_p, the data in Tables 2-1 and 2-2 are not sufficient to develop a project-specific relationship between Holland's B parameter and other storm characteristics, and it is tempting to adopt the model obtained by Vickery and Wadhera (2008) for their entire hurricane dataset. Comparisons of this model to the data in Table 3-1 indicated different trends, however. As a result, it was decided to model B as independent of ΔP and Rp. This project adopted the calculated mean value of 1.1 and standard deviation of 0.2.

3.3.5 Forward Velocity

Experience in many studies has shown that the hurricane parameter that has the least effect on the magnitude of a storm surge is the forward velocity V_f of the storm center. Still, this parameter must be characterized.

The data from Table 3-1 indicate that stronger storms move at faster speeds, as indicated in Figure 3-11. The resulting model has a mean and standard deviation given by

$$\begin{aligned} meam(V_f;\text{kt}) &= 6 + 0.4Max[\Delta P, 70](\text{mb}) \\ \sigma_{V_f|\Delta P} &= 7\text{kt} \end{aligned} \qquad (3\text{-}8)$$

The cap of 70 mb was introduced because the un-capped equation leads to unreasonably high velocities for stronger storms.

3.3.6 Variation of Storm Parameters Prior to Landfall

Storms moving along the Atlantic seaboard change substantially as they move from the Carolinas to the NY-NJ region. Figures 3-12 through 3-14 show the variation of ΔP, R_p, and V_f, respectively for the 30 storms in Table 2-2. Only V_f shows a systematic variation, which will be characterized by assuming that V_f varies linearly from 53 percent of the value in Equation 3-8 at 30 degrees latitude to 100 percent at 40 degrees latitude and greater.

Given the rapid motion of these storms, no pre-landfall filling is expected to occur.

3.4 MODEL FOR STORM TRACKS AND TEMPORAL VARIATION OF PARAMETERS

The numerical wind and wave calculations require as inputs a number of synthetic storms, with parameters at landfall taken from the probability distributions described earlier in this section. The process for generating these discrete parameter values at landfall is documented in the next section. For each synthetic storm, one must specify the track location and parameter values at each location along the track, beginning several days prior to landfall. More specifically, this

description of the storm contains hourly values of the coordinates of the storm center, ΔP (or central pressure), Rp, forward velocity, and Holland B.

The approach used to generate the storm tracks—given the values of $\Delta P, R_p, V_f, \theta, B$ at landfall, as well as the landfall location—is a purely deterministic approach, which is described below.

The geometry of the tracks is based on historical tracks for the region. The approach uses one or more master historical tracks (possibly with small modifications) as guides, but modifies the master track in a gradual manner to conform to the specified landfall location and heading[23]. The distance between successive points along the track is constant and is proportional to the forward velocity at landfall.

The forward speed varies linearly with latitude, as discussed earlier. Other storm characteristics are treated as constant.

3.5 SUMMARY

This section documents the development of the probabilistic model for the occurrence and characteristics of future hurricanes that may generate significant storm surge along the NY-NJ coast.

The storm population is partitioned into those that make landfall in New Jersey and those that make landfall in New York City and Long Island, and slightly different models are constructed for both. The variation in landfall rates is considered explicitly in the model. For each storm population, the following parameters were estimated or adopted from the literature: annual occurrence rate, probability distribution of pressure deficit ΔP, conditional probability distribution of storm size (as measured by Rp) given ΔP, probability distribution of the Holland B parameter, probability distribution of forward velocity, and probability distribution of storm heading θ. These parameters will be utilized in Section 4 to generate a set of representative synthetic storms, using a JPM-OS formulation.

Other characteristics of hurricanes are not included explicitly in this parameterization. The effect of these characteristics on the exceedance probabilities will be included in an approximate manner by means of a random error term.

Table 3-1. Data from Well-studied Storms Used for the Analysis of R_p, Holland B, and Forward Velocity

Name	Year	ΔP (mb)	R_p (nmi)	B	V_f (kt)
1938_04	1938	71.8	38	0.85	44.0
1944_07	1944	58.3	38	1.05	30
Barbara	1953	37.3	40	1.2	17
Carol_1953	1953	42.7	60	1.2	17
Carol_1954	1954	52.3	38	1	31
Edna	1954	64.6	22	0.9	25
Daisy	1958	44.5	20	1.28	20

[23] One can think of this approach as interpolating between the geometry of the master track and the landfall location and heading.

Name	Year	ΔP (mb)	R_p (nmi)	B	V_f (kt)
Donna	1960	48.7	75	1.3	30
Esther	1961	45.3	70	1.5	15
Doria	1967	32.5	22	1.05	11
Gerda	1969	32.8	37	1.2	30
Agnes	1972	26.3	120	1.1	20
Belle	1976	44.4	35	1.1	22
Gloria	1985	57.4	45	0.8	36
Bob	1991	63.4	28	0.95	27
Emily	1993	53.3	27	1.5	16
Floyd	1999	35.4	110	0.9	29
Gustav	2002	35.1	84	1.1	21
Alex	2004	39.3	20	1.24	16

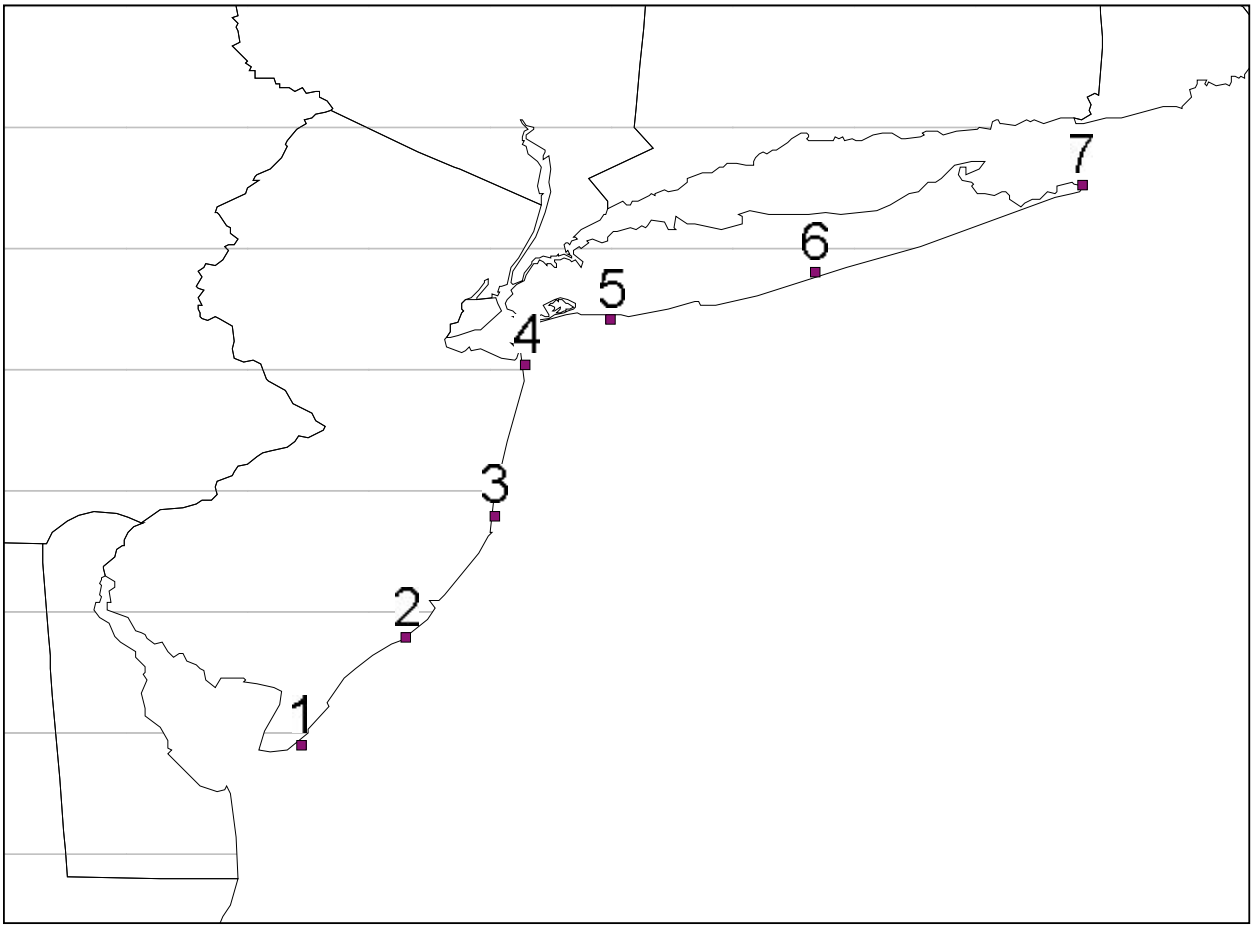

Figure 3-1. Sites considered for the analysis of storm statistics.

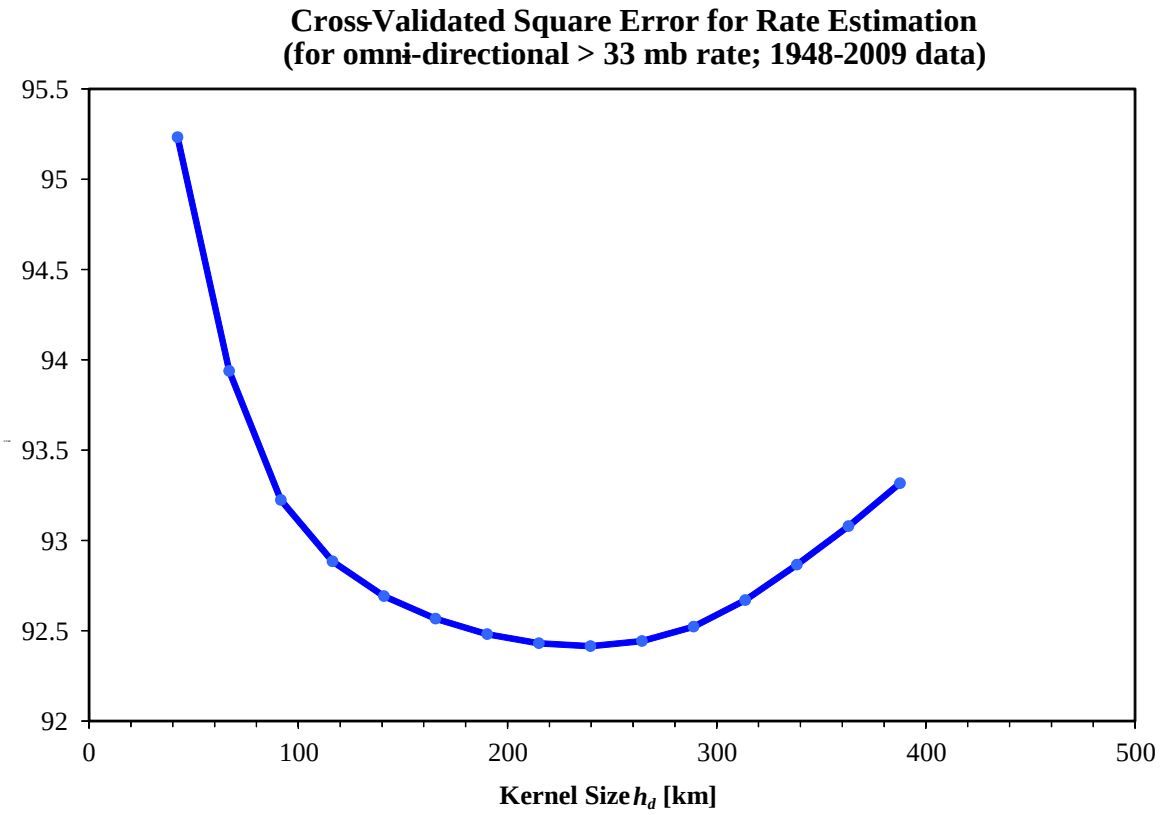

Figure 3-2. CVSE for the omni-directional storm rate for landfalling storms.

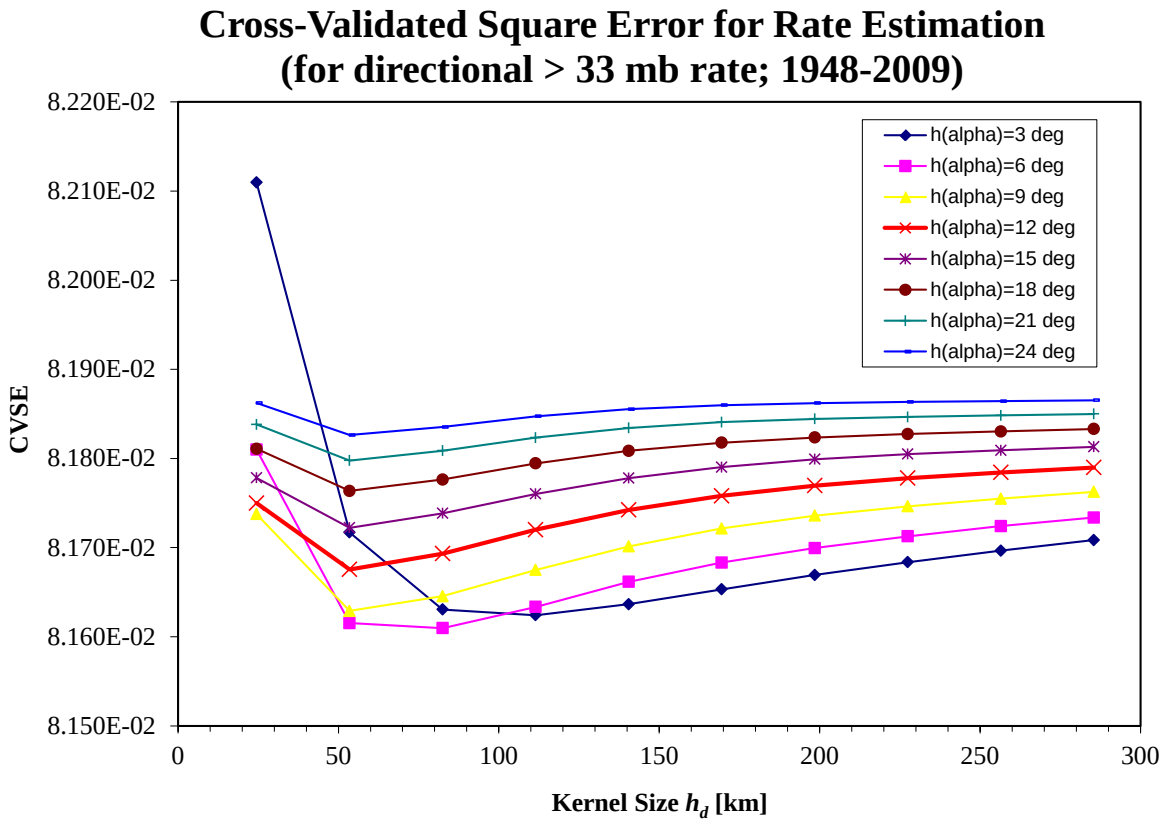

Figure 3-3. CVSE results for the directional storm rate for landfalling storms

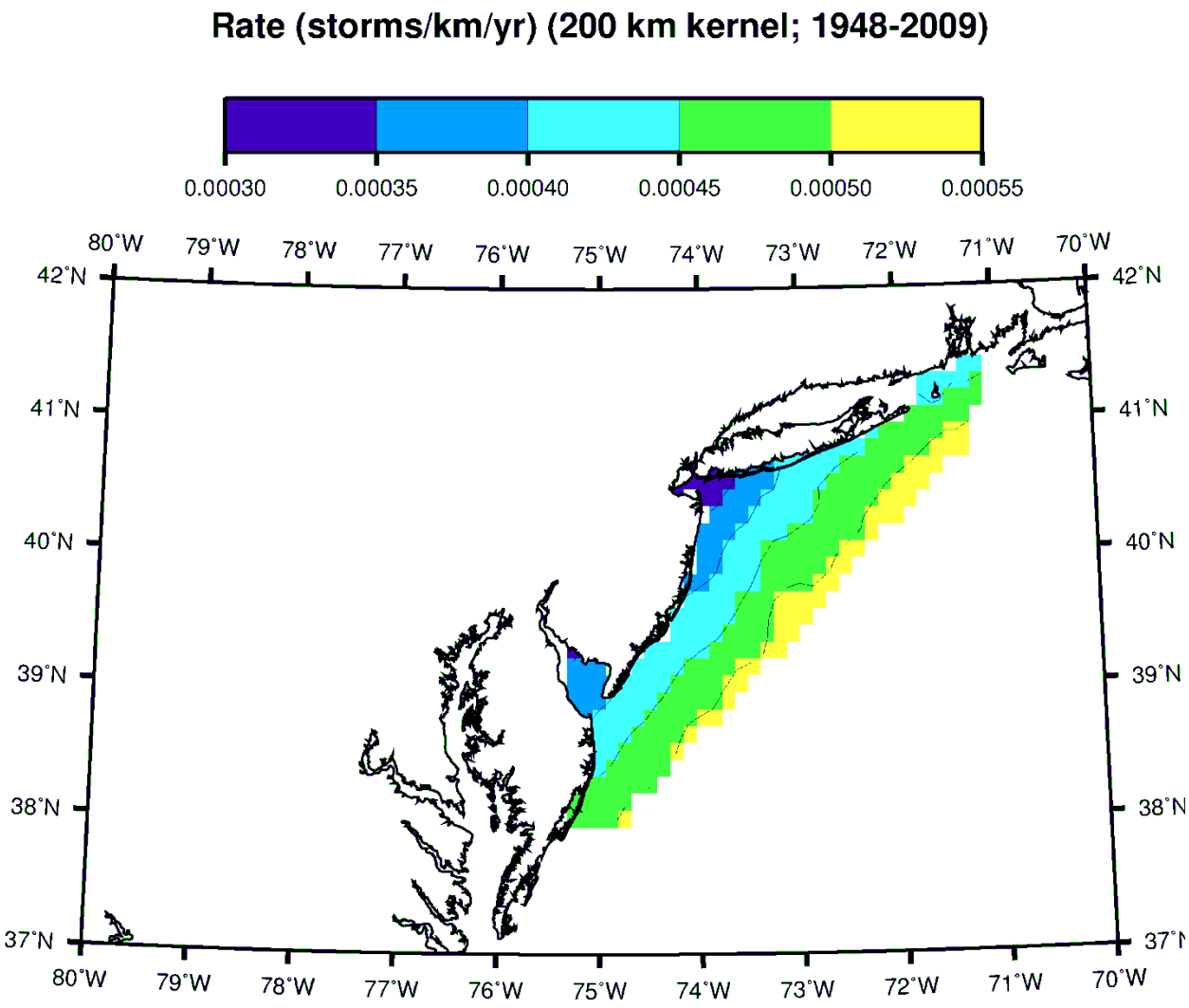

Figure 3-4. Variation in omni-directional rate.

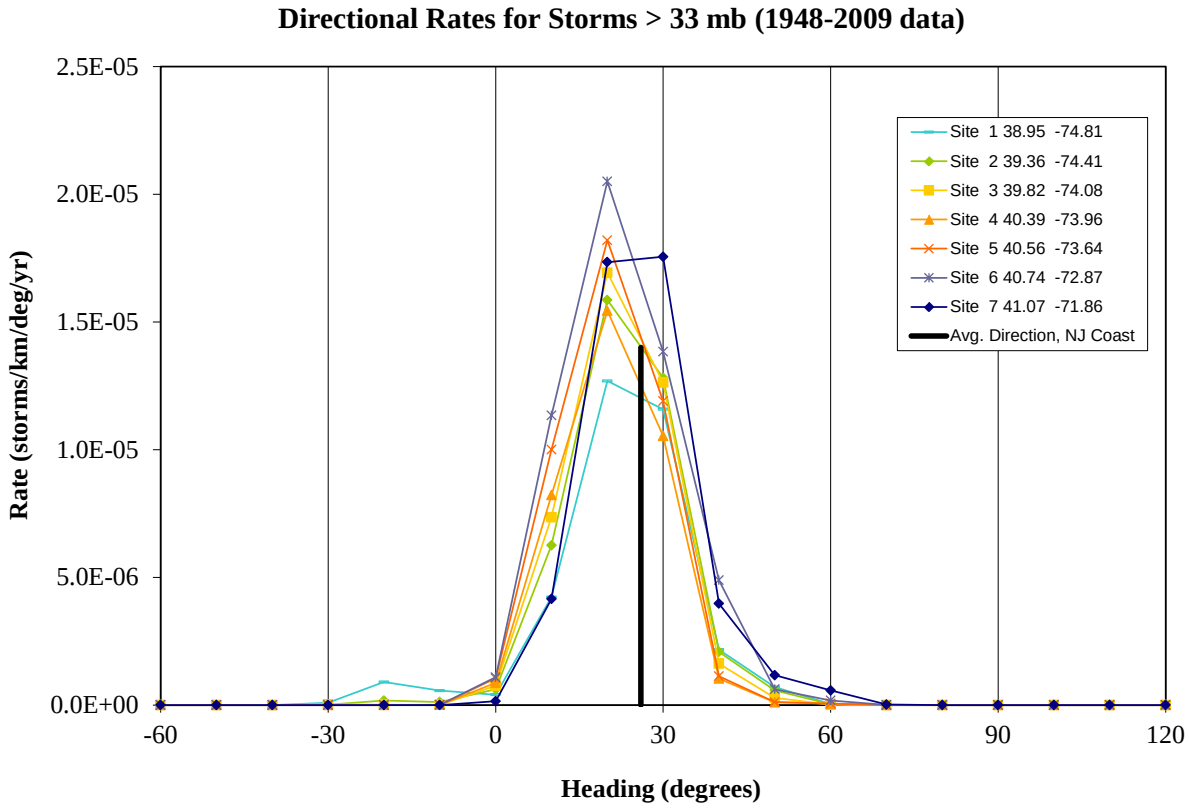

Figure 3-5. Directional rates and distribution fit of storm heading for landfalling storms.

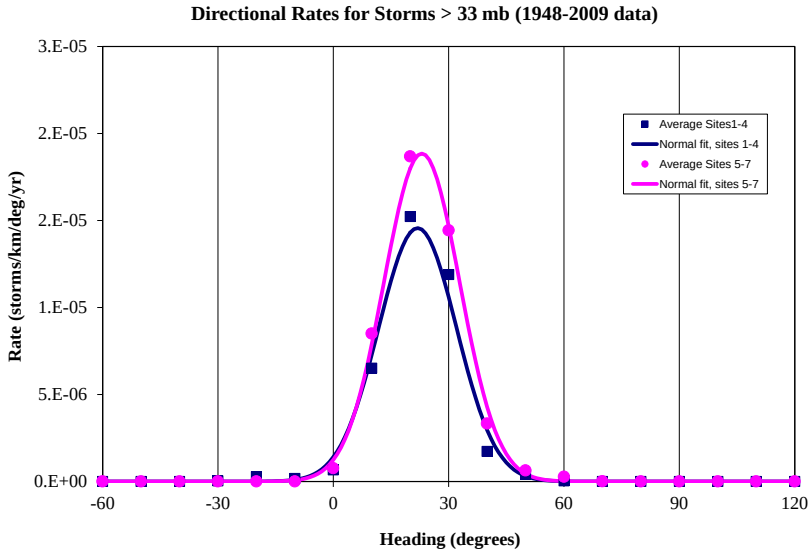

Figure 3-6. Directional rates and distribution fit for New Jersey (sites 1-4) and Long Island (sites 4-7), and associated normal-distribution fits.

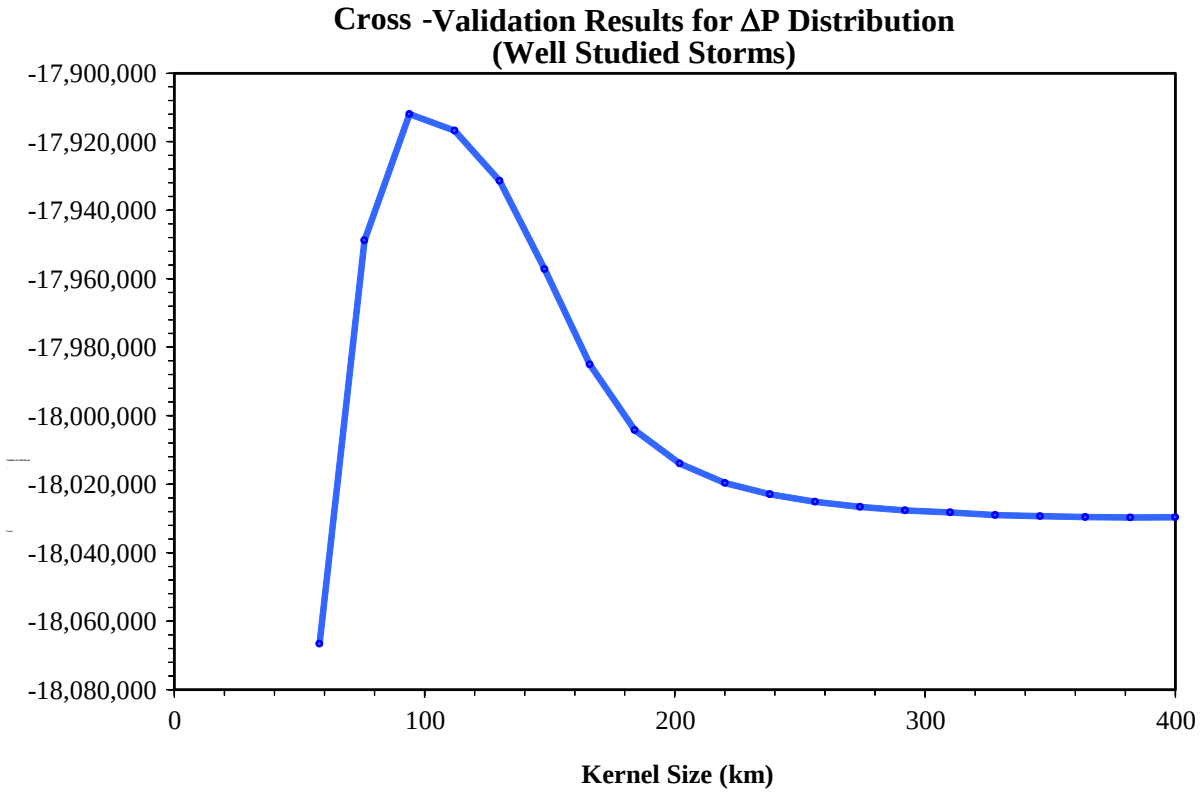

Figure 3-7. Selection of kernel size for the ΔP distribution obtained using CVL.

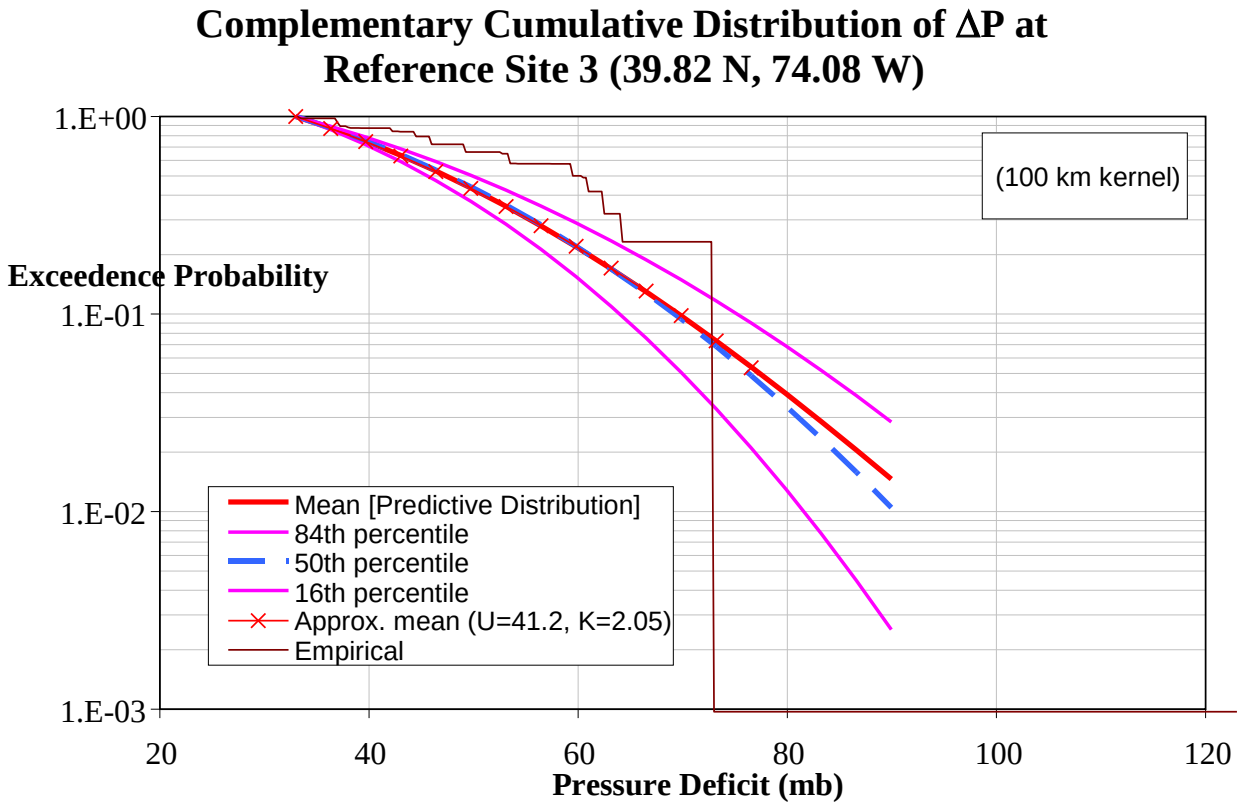

Figure 3-8. Complementary cumulative distribution function of ΔP at site 3 (see Figure 3-1).

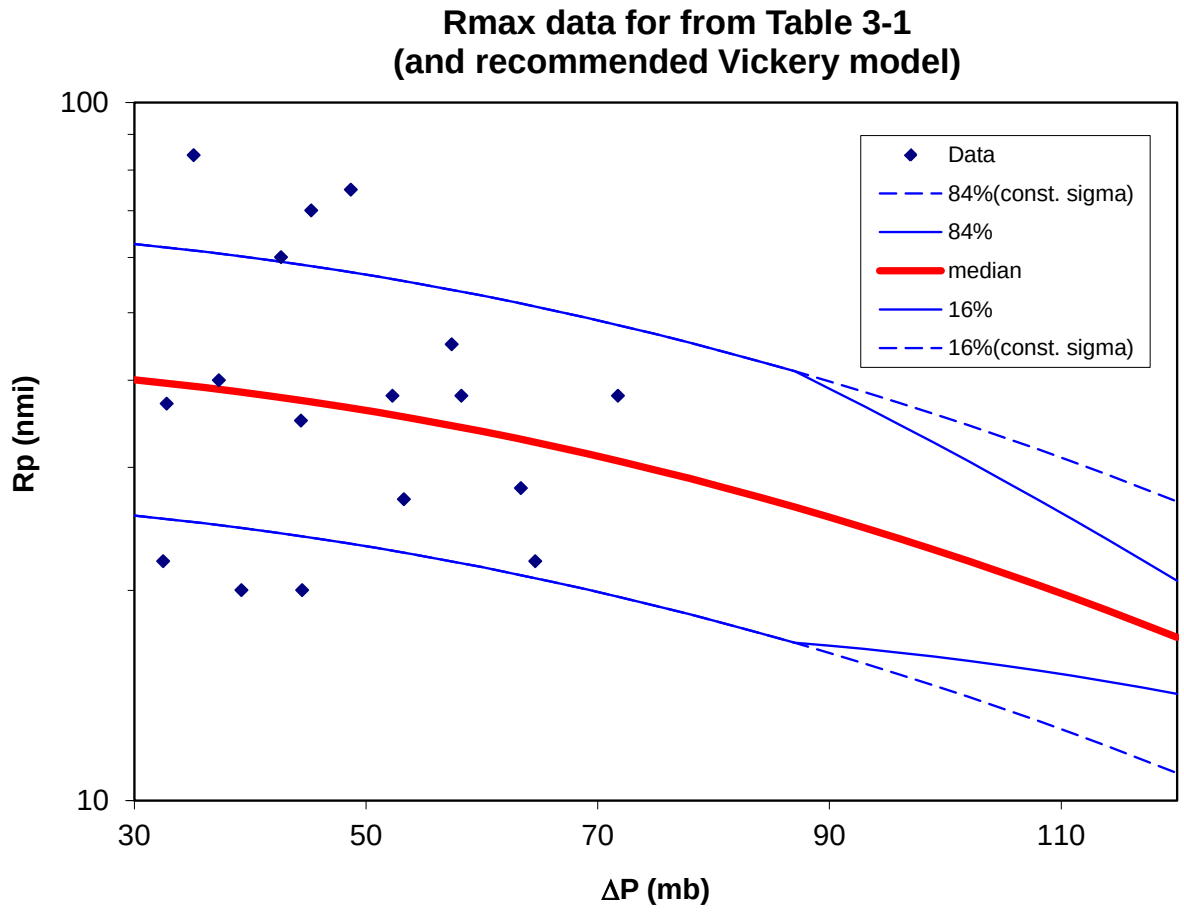

Figure 3-9. Data for R_p vs. ΔP for landfalling storms and recommended Vickery-Wadhera (2008) model. This project used the constant-sigma model, which has broader distribution tails for stronger storms.

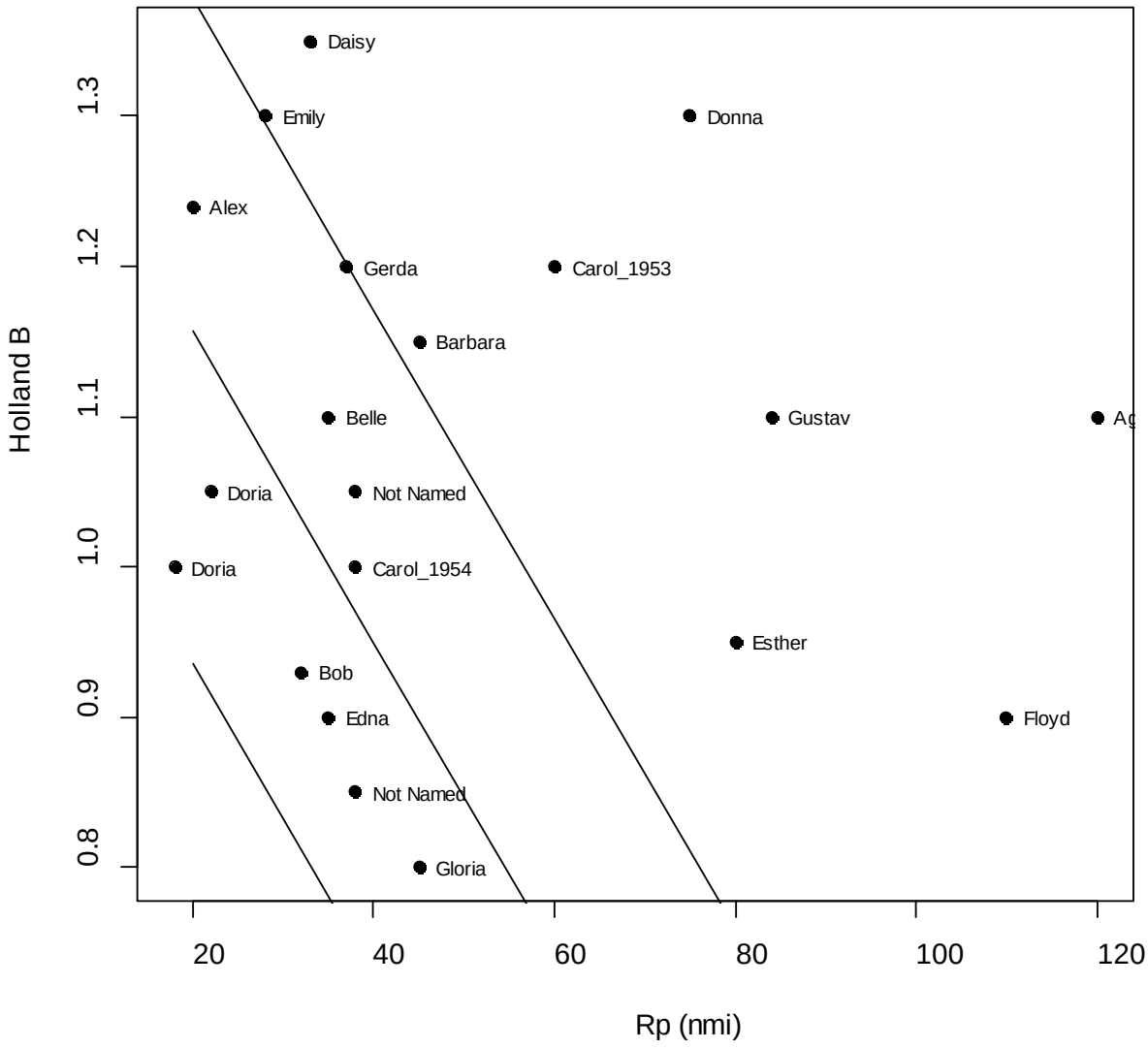

Figure 3-10. Comparison of the data on Holland B (text) to the relation (mean ± sigma) by Vickery and Wadhera (2008; lines). The central line denotes the mean relation; the outer lines denote the mean ± sigma relations.

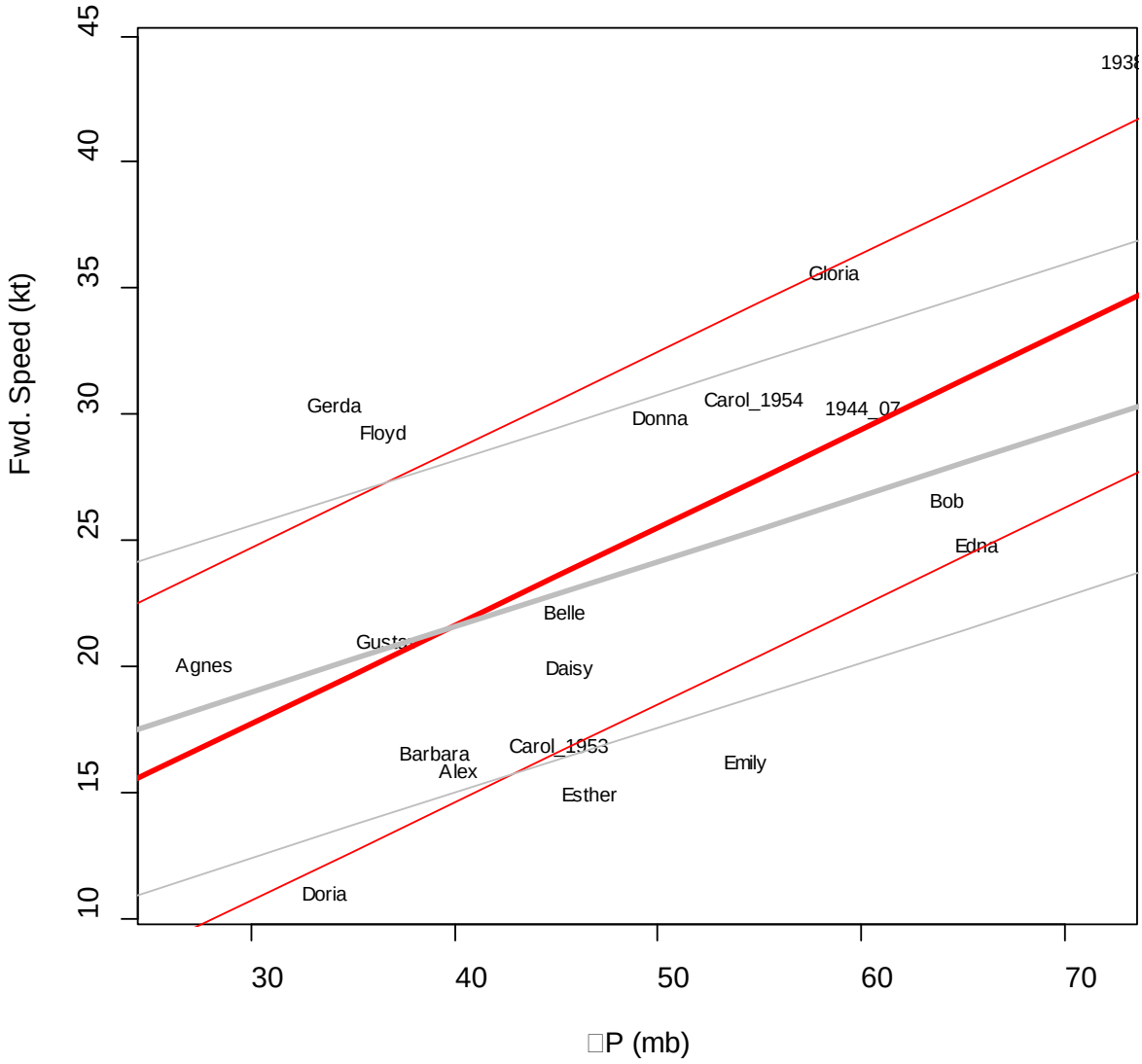

Figure 3-11. Data on forward speed and linear fit relation (mean and mean ± sigma) obtained in this project. The red lines (adopted) indicate the relation obtained using all the data in Table 3-1; the gray line indicates the relation obtained if the 1938 storm is removed.

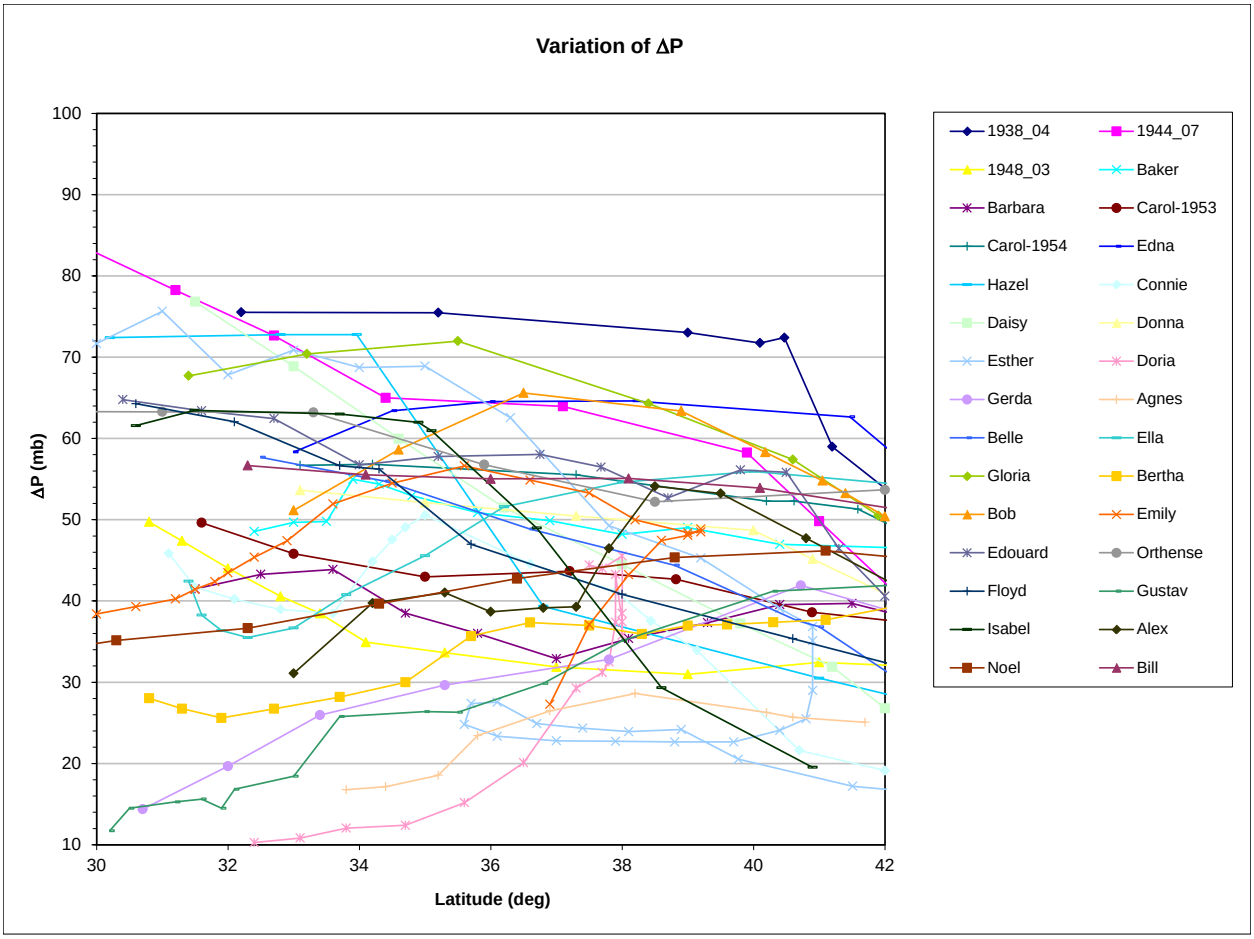

Figure 3-12. Variation of ΔP as a function of latitude. Note that the lower limit of 33 mb ΔP is not imposed in this figure.

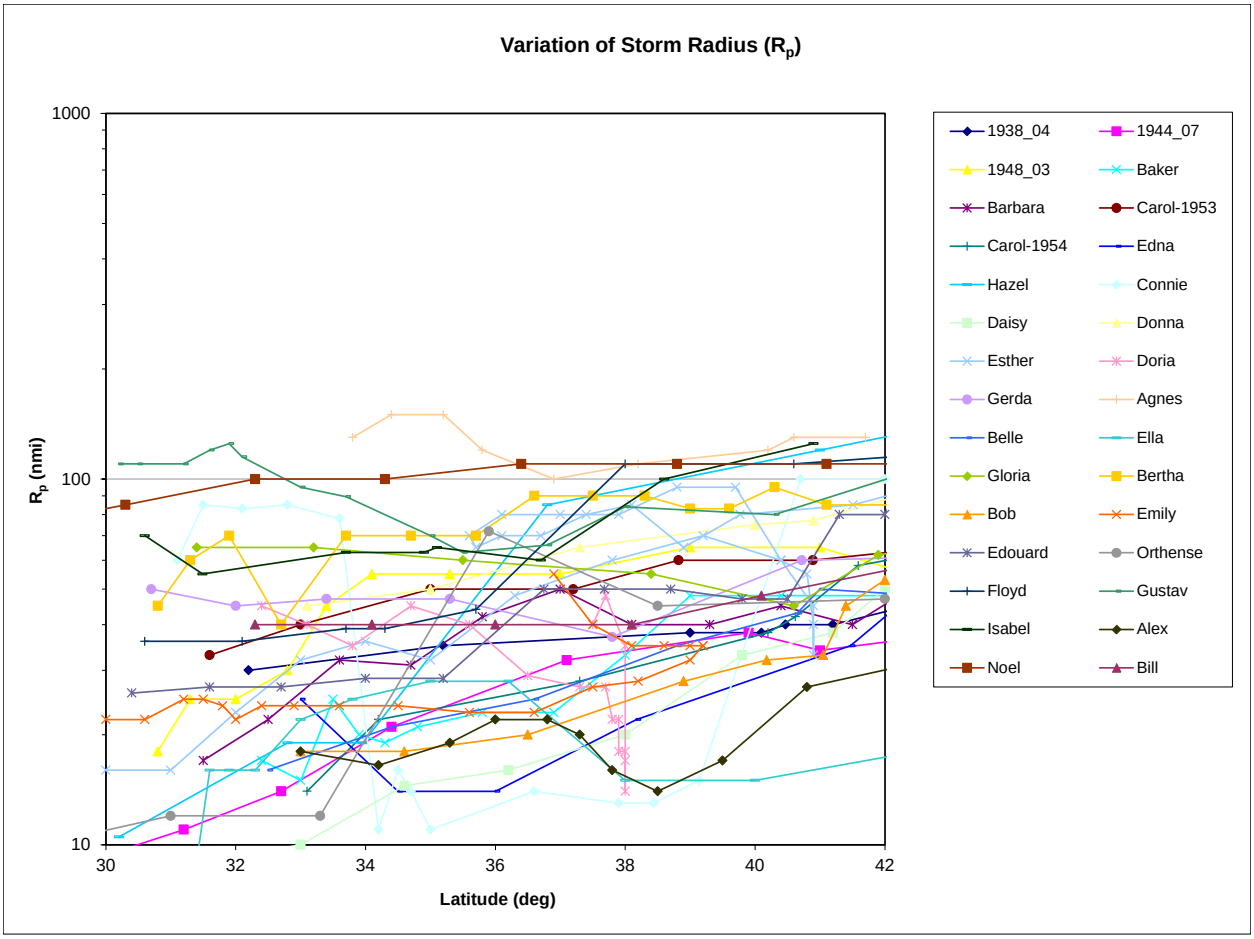

Figure 3-13. Variation of R_p as a function of latitude. Note that the lower limit of 33 mb ΔP is not imposed in this figure.

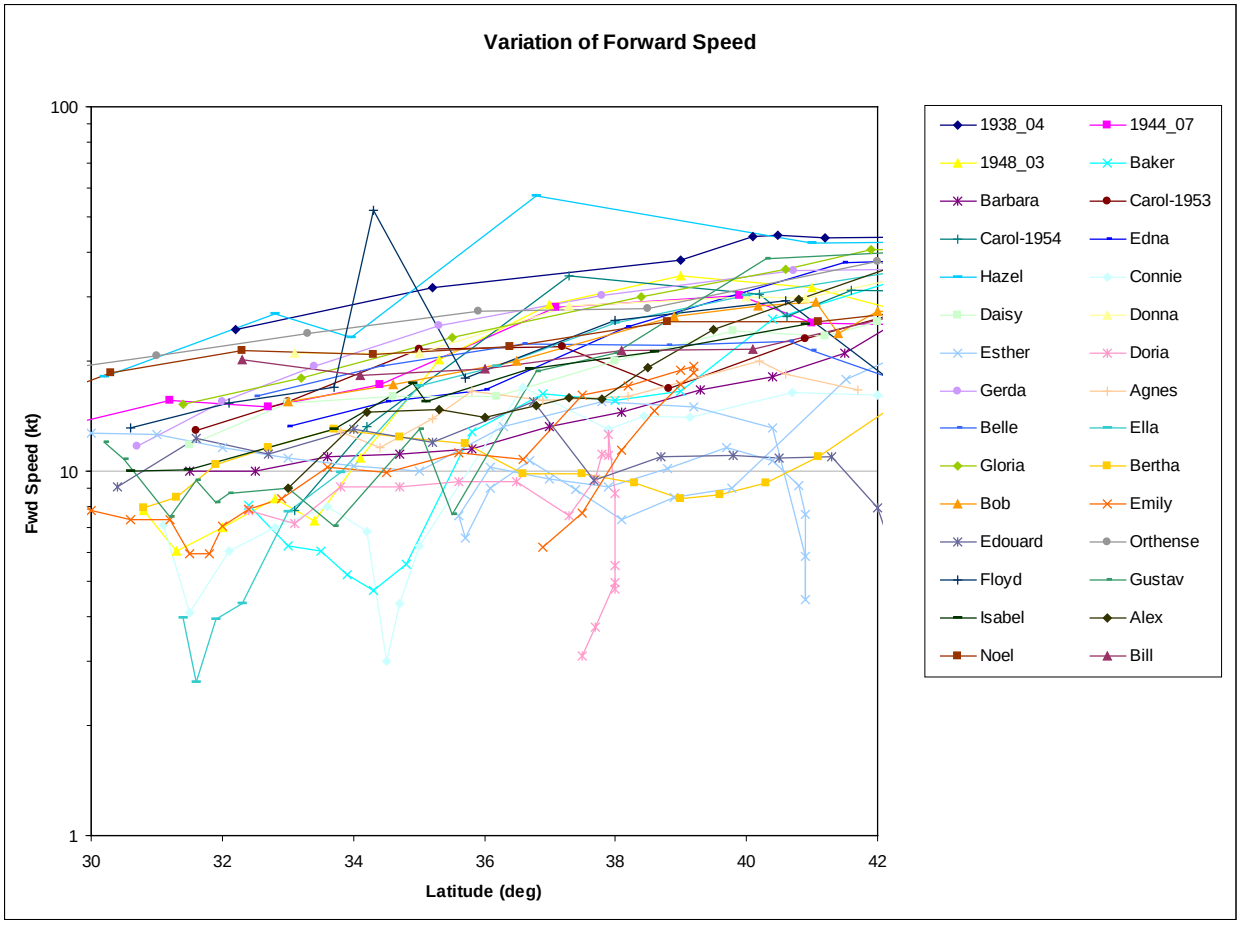

Figure 3-14. Variation of Forward Speed (V_f) as a function of latitude. Note that the lower limit of 33 mb ΔP is not imposed in this figure.

SECTION FOUR DEVELOPMENT AND IMPLEMENTATION OF JPM-OS APPROACH, INCLUDING THE DEVELOPMENT OF SYNTHETIC STORMS

4.1 INTRODUCTION

This section documents the development of a set of representative synthetic storms and their associated annual recurrence rates. These storms, together with their rates, provide a condensed representation of the population of possible future synthetic storms, for use in the calculation of surge inundation probabilities.

The section begins by describing the JPM method, including the rationale for the error terms that account for parameters and effects that are not explicitly represented in the JPM integral. This is followed by a general description of the Quadrature JPM-OS approach adopted in this study, and details of implementation.

The accuracy of the JPM-OS storm set for this study is verified by using ADCIRC (ADvanced CIRCulation Model for Oceanic, Coastal and Estuarine Waters) with a coarsely-spaced mesh to calculate surge elevations for the JPM-OS storm set and for a larger "reference set" obtained using standard JPM, and then comparing the 1-percent-annual-chance and 0.2-percent-annual-chance surge elevations calculated from both storm sets.

It is important to emphasize, however, that the coarse-mesh ADCIRC results are used only for the purposes of testing the JPM-OS formulation and for other diagnostic tests, and these results are not used in the coastal flood analysis. The advantage of using the coarse-mesh ADCIRC model in this context is that it is efficient and easy to run, while at the same time capturing the surge response related to storm characteristics.

This section also describes a Monte Carlo approach applied for the inclusion of astronomical tides in the storm simulations, and contains results from tests that demonstrate this approach does not introduce excessive sampling variability.

4.2 THE JPM

The JPM was developed for coastal storm surge studies by Myers (Myers, 1975; Ho and Meyers, 1975). JPM provides a mathematical framework for the calculation of surge exceedance probabilities in terms of the tropical cyclone climatology and surge effects. In particular, the JPM approach combines the following inputs:

- The annual rate of storms of interest λ. For this study, storms of interest are divided into four distinct populations, namely landfalling hurricanes, bypassing hurricanes, landfalling tropical storms, and bypassing tropical storms. Typically, it is also assumed that the occurrence of these storms in time represents a Poisson random process (Parzen, 1962)[24].
- The joint probability distribution $f_{\underline{X}}(\underline{x})$ of the storm characteristics for the storms of interest. These characteristics are defined very broadly at first, but they are narrowed later to make the approach practical.

[24] In practice, the Poisson assumption is not necessary. Weaker assumptions are sufficient when calculating the probabilities of rare events, as will be discussed below.

- The storm-generated surge[25] $\eta(\underline{X})$ at the site of interest, given the storm characteristics.

The combined effect of these three inputs is expressed by the multiple integral

$$P[\eta_{\max(1\,yr)} > \eta] = \lambda \int \ldots \int_{\underline{x}} f_{\underline{X}}(\underline{x}) P[\eta(\underline{x}) > \eta] d\underline{x} \qquad (4\text{-}1)$$

where $P[\eta(\underline{x}) > \eta]$ is the conditional probability that a storm of certain characteristics $\underline{x}$ will generate a flood elevation in excess of an arbitrary value η. This probability would be a Heaviside step function $H[\eta - \eta(\underline{X})]$[26] if vector $\underline{X}$ contained a complete characterization of the storm and if the numerical models for the calculation of surge given $\underline{X}$ were perfect, but these conditions cannot be satisfied in practice. The integral above considers all possible storm characteristics from the population of storms of interest and calculates the fraction of these storms that produce surges in excess of the value of interest η, using the total probability theorem (Benjamin and Cornell, 1970)[27].

The right hand side in Equation 4-1 actually represents the mean annual rate of storms that exceed η at the site, but it also provides a good approximation of the annual exceedance probability at the site of interest[28].

In this particular study, the right-hand side of Equation 4-1 will consist of four separate integrals, one for each storm population of interest. Equivalently, one can construct a composite joint probability distribution $f_{\underline{X}}(\underline{x})$ for the four populations and collapse the two integrals into one.

Equation 4-1 defines a smooth function of η that can be used to determine the flood levels associated with any annual probability of exceedance. Those of interest in this study are the 10%, 2%, 1%, and 0.2% annual probabilities. These are often referred to as the 10-, 50-, 100- and 500-year return periods, respectively. Unfortunately, the concept of return periods is often misunderstood, so the use of annual probabilities is preferred.

As noted by Resio (2007), some approximations are necessary in practice for the evaluation of Equation 4-1. First, it would be impossible to calculate the peak surge exactly, even if the storm's wind field as a function of time were known exactly. Accordingly, the actual elevation $\eta(\underline{X})$ is written in terms of the model-calculated elevation $\eta_m(\underline{X})$ as $\eta(\underline{X}) = \eta_m(\underline{X}) + \varepsilon_m$, where ε_m

[25] In this definition, the term surge represents the peak inundation, including the surge itself, wave setup, astronomical tide, etc.

[26] The Heaviside step function $H(z)$ is equal to 0 if z <0 and is equal to unity if z >0. Its value at z=0 is usually considered undefined.

[27] In this project, the rate λ varies along the coast. Therefore, λ should go inside the integral in Equation 4-1 because it depends on landfall location (one of the components of $\underline{x}$). The equation is kept in its original form here, as it is easier to understand.

[28] The derivation to show that the annual probability for a rare event is approximately equal to annual rate is usually made by assuming that event occurrences represent a Poisson process and then linearizing the resulting exponential. The same result may be obtained under weaker assumptions; it is sufficient to assume that the probability of two or more of these rare events in one year is much lower than the probability of one event. This condition is satisfied for hurricane-generated surges and for the exceedance probabilities of interest in this study (e.g., 0.01 per year).

is an epsilon term for model lack-of-skill, which will be treated as a random quantity independent of $\underline{X}$. If the model is unbiased, ε_m has a mean value of 0 (zero). Using the above representation, the actual conditional probability can be written as

$$P[\eta(\underline{X}) > \eta] = P[\eta_m(\underline{X}) + \varepsilon_m > \eta] \qquad (4\text{-}2)$$

In addition, it would be impossible to provide a complete characterization of the storm itself (i.e., the wind and pressure fields as a function of time). Thus, it is convenient to partition the vector of storm characteristics $\underline{X}$ into two parts, as follows: (1) a vector of principal quantities $\underline{X}_1 = (\Delta P, Rp, B, V_{f,}\text{landfall location}, \theta)$, whose probability distributions are represented explicitly and whose effects are also represented explicitly in the model calculations, and (2) a vector of secondary quantities $\underline{X}_2 = (R_{p2}, B_2, ...)$, whose distributions (relative to their base-case values) and effects are jointly represented in an approximate manner by random terms $(\varepsilon_{Rp2}, ...)$ (which have units of elevation)[29]. These secondary quantities are ignored or set to their base-case values in the model runs. Although these epsilons are conceptually different from the modeling error ε_m introduced earlier, they are combined operationally into one random quantity, $\varepsilon = \varepsilon_m + \varepsilon_{Rp2} + ...$.

Incorporating these simplifications, Equation 4-1 transforms into

$$P[\eta_{\max(1\,yr)} > \eta] = \lambda \int ... \int_{\underline{x}_1} f_{\underline{X}_1}(\underline{x}_1) P[\eta_m(\underline{x}_1) + \varepsilon > \eta]\, d\underline{x}_1 \qquad (4\text{-}3)$$

where $\underline{X}_1 = (\Delta P, Rp, B, V_{f,}\text{landfall location}, \theta)$. The subscript 1 [as in X_1] will be dropped in the remainder of this report for the sake of simplicity, resulting in

$$P[\eta_{\max(1\,yr)} > \eta] = \lambda \int ... \int_{\underline{x}} f_{\underline{X}}(\underline{x}) P[\eta_m(\underline{x}) + \varepsilon > \eta]\, d\underline{x} \qquad (4\text{-}4)$$

The quantification of the standard deviations for the various components of ε is discussed later in this section and also in Section 5.

4.3 THE QUADRATURE JPM-OS APPROACH

Evaluation of the JPM integral (Equation 4-4) using conventional numerical-integration approaches is impractical for the following two reasons: (1) each evaluation of the integrand

[29] The Holland B parameter receives special treatment in this study, for two reasons. First, the random variation of B is treated explicitly (i.e., B is considered part of X_1) for the so-called reference storms, but then it is shown that the effect of this random variation can be treated as a secondary quantity (i.e., as part of the secondary quantities, X_2). Second, the deterministic dependence of B on R_p is considered explicitly in all runs.

involves evaluation of $\eta_m(\underline{x})$ for one value of $\underline{x}$ (i.e., one synthetic storm), which requires computationally intensive numerical calculations of wind, waves, surge, wave setup, etc.; and, (2) numerical evaluation of the five-dimensional (5D) integral in Equation 4-4 using conventional approaches requires that the integrand be evaluated a large number of times (this is the so-called curse of dimensionality). Typically this can translate to a requirement for carrying out thousands of storm surge simulations. When a computation-intensive hydrodynamic model such as ADCIRC is to be used, this becomes prohibitive with respect to schedule and costs.

The approach used in this study approximates the integral in Equation 4-4 as a weighted summation, i.e.:

$$P[\eta_{\max(1\,yr)} > \eta] = \lambda \int \ldots \int_{\underline{x}} f_{\underline{X}}(\underline{x}) P[\eta_m(\underline{x}) + \varepsilon > \eta]\, d\underline{x} \approx \sum_{i=1}^{n} \lambda_i P[\eta_m(\underline{x}_i) + \varepsilon > \eta] \qquad (4\text{-}5)$$

where each $\underline{x}_i = (\Delta P_i, Rp_i, V_{f,i,}\text{landfall location}_i, \theta_i)$ may be interpreted as a synthetic storm with characteristics $\Delta P_i, Rp_i, V_{f,i,}\text{landfall location}_i, \theta_i$ at landfall, $\lambda_i = \lambda p_i$ may be interpreted as the annual occurrence rate for that storm, and $\eta_m(\underline{x}_i)$ may be interpreted as the numerical model's estimates of the surge elevation generated by that storm. For this approach to be practical, one must be able to specify the storm characteristics $\underline{x}_i$ and their rates λ_i so that the integral can be approximated with sufficient accuracy (for all η values of interest), using a reasonably small value of *n* (i.e., a reasonably small number of synthetic storms and corresponding numerical model runs).

The approach used to define the synthetic storms and their rates uses a combination of well-known and sophisticated numerical-integration techniques and may be summarized by the following three steps:

1. Discretize the distribution of ΔP into multiple broad slices.
2. Within each ΔP slice, discretize the joint probability distribution of ΔP, R_p, V_f, and θ using the multi-dimensional optimal-sampling procedure known as Bayesian Quadrature (see Toro et al., 2010a for details).
3. Discretize the distribution of landfall location by offsetting each of the synthetic storms defined in the previous two steps. The offset is equal to R_p and is measured perpendicular to the storm track. Following FEMA (2008), these landfall locations extend at least three R_p's to the south and one R_p to the north of the coastline of the study region[30].
4. Finally, one computes the probability p_i assigned to each synthetic storm as the product of the probabilities resulting from the three steps. Alternatively, one can compute the rate λ_i assigned to each synthetic storm as the product of the probabilities from the first two steps times the rate per unit length (at the landfall location) developed in Section 3 multiplied by the storm spacing.

[30]Slightly narrower criteria were used for the synthetic storms used in the JPM-OS validation tests.

The approach outlined above was applied separately to the landfalling and bypassing storms, with the modifications mentioned earlier.

4.4 DEVELOPMENT OF REFERENCE STORMS AND USE OF ADCIRC WITH A COARSE MESH

As was done in FEMA (2008), the accuracy of the JPM-OS scheme was checked by generating a larger set of reference storms using a conventional JPM approach, running ADCIRC with a coarse mesh for both the reference and JPM-OS sets of synthetic storms, calculating the 100-year and 500-year surge elevations at 49 target sites in the study region, and then comparing the results. These 49 sites were distributed throughout the study region, so that these comparisons cover the entire region. Figure 4-1 shows the location of these target sites.

4.4.1 Development of Reference Storm Set

Table 4-1 shows the discretization of storm parameters used to construct the reference storm set for the landfalling hurricanes. First, the distribution of ΔP is discretized into seven values using a 1D quadrature scheme. Because R_p depends on ΔP, seven separate conditional five-point discretizations of $R_p \mid \Delta P$ are constructed (one for each value of ΔP). Finally, three-point discretizations are constructed for forward speed, heading, and Holland B. These discretizations result in 7*5*3*3*3=945 combinations of storm parameters. These storms are then replicated along the coast, using a perpendicular spacing of R_p, resulting in 4,108 reference storms. Each one of these storms has an associated annual rate, which is equal to the product of the five associated probabilities in Table 4-1 multiplied by the annual rate per unit length (at the landfall location) times the track spacing. Figure 4-2 shows the tracks for the reference storms for the landfalling hurricanes.

These 4,108 synthetic reference storms were run through ADCIRC with a coarse mesh, and peak surge elevations were calculated at 49 target points throughout the study region (Figure 4-1). Surge elevations for the 1- and 0.2-percent-annual-chance recurrence intervals were then computed using these peak surge elevations and the annual rates for the associated synthetic storms. These results are discussed in Section 4.5.2 and used to confirm the adequacy of the JPM-OS storm set.

4.5 IMPLEMENTATION OF THE QUADRATURE JPM-OS APPROACH

4.5.1 Development of JPM-OS Storms

This study used the Quadrature JPM-OS approach to generate a set of synthetic storms that represent the joint probability distribution of the following: pressure deficit (ΔP), radius of maximum winds (R_p), forward velocity (V_f), Holland B, landfall location[31], and heading θ. This section documents the development of these synthetic storms. Sections 4.5.3 and 4.5.4 document the validation of these synthetic storms (using ADCIRC with a coarse mesh and the reference storms described earlier).

[31] For bypassing storms, the location where the storm crosses the bypass line is used instead of landfall location.

Table 4-2 shows the various slices of the ΔP distribution, their probabilities, and the number of nodes used in the Bayesian-Quadrature discretization for each slice. Table 4-3 shows the correlation distances used in the Bayesian-Quadrature procedure. These values were chosen based on the extensive sensitivity results presented in FEMA (2008) and Niedoroda et al. (2010), and then refined so that they preserve the marginal moments of the most important storm characteristics. Table 4-4 shows the discrete JPM-OS representation of the joint probability distribution of the storm characteristics, as obtained after the second of three steps outlined in Section 4.3. These storms are then replicated along the coast, using a spacing of R_p, resulting in 130 landfalling JPM-OS storms. Complete tracks are then generated for each storm using the approach described in Section 3.4. The resulting tracks are shown in Figure 4-3.

4.5.2 Coarse-mesh Test for the Verification of the JPM-OS Storm Set

The 130 synthetic JPM-OS storms were run through ADCIRC with the coarse mesh, and peak surge elevations were calculated at the 49 target points shown in Figure 4-1. Surge elevations for the 1- and 0.2-percent-annual-chance recurrence intervals were then computed by using these peak surge elevations and the annual rates for the associated synthetic storms. These levels were then compared to the 1- and 0.2-percent-annual-chance recurrence levels computed using the reference storm set. In both sets of surge-frequency calculations, no secondary factors (epsilons) were considered. This makes the verification more stringent, as the secondary factors make the integrand in Equation 4-1 smoother and easier to approximate by a summation.

Figure 4-4 illustrates these comparisons. Table 4-5 displays the summary statistics associated with these comparisons. The mean bias and the standard deviation meet the criteria established in Section 1.2, thereby confirming that the JPM-OS storm set provides an adequate representation of the joint probability distribution for pressure deficit (ΔP), radius of maximum winds (R_p), forward velocity (V_f), Holland B, landfall location, and heading θ.

The characteristics of the final JPM-OS storms at landfall are given in Table 4-5. The number of storms was increased slightly (to 159) because these storms were re-generated using a slightly finer spatial sampling.

4.6 TREATMENT OF ASTRONOMIC TIDE

4.6.1 Introduction

Astronomic tide can be an important contributor to the total water level during a coastal storm event. Although a particular surge height can be either higher or lower with tide than without tide, depending upon the relative phasing of the tide and the surge, the net effect of tide at the upper tail of the flood distribution is to increase the flood levels because more opportunities exist for generating high flood levels.

Unfortunately, tide and surge cannot be considered separately except in the case of a limiting approximation. If the tide is quite small, it can be handled as a "noise" term contributing a small random component to the total water level. In this limit, the computational effort to consider tide is not large, and can be handled entirely as a post-processing task after completion of the hydrodynamic simulations. This was the approach used in the Mississippi Study (FEMA, 2008), and was acceptable owing to the small amplitude of the tide relative to the much larger amplitude of the surge. The essential assumption was that simple linear superposition of the tide with the surge was sufficient in that case.

A difficulty arises for tides of more significant amplitude, as is the case in the NY-NJ region (e.g., the Battery tide gage has a Great Diurnal Range of 5.1 ft). The tide and surge are not physically independent. Instead, they interact so that the presence of one influences the behavior of the other. This non-linear interaction makes the general problem of the tide more difficult; linear superposition cannot be generally assumed, and more physically realistic methods are required. The next section briefly summarizes possible alternatives, followed by a description of the approach adopted for this study.

4.6.2 Candidate Methods

JPM: The most straightforward method would be to expand the JPM parameter space to include tide parameters as necessary to account for tide and surge behavior. For example, parameters related to tide amplitude and tide phase could be included. Hydrodynamic simulations would then be made for a larger number of storms occurring over a range of possible concurrent tide conditions. This approach would be costly, with a significant JPM implementation factor, since the number of storm simulations would become much greater and prohibitively expensive. A JPM-OS approach may be feasible, keeping the required number of simulations within reasonable bounds, but this approach was not implemented.

Regression: The approach adopted in earlier studies was summarized in the FEMA Coastal Storm Surge Model documentation (FEMA, 1988). It involves a rather complex set of secondary calculations to be performed following the basic JPM simulations. In brief, the idea is to perform linear superposition of the simulated JPM floods with tides of varying amplitudes and phases, producing a set of added surge and tide results. A number of additional hurricane simulations are then run with various tide amplitudes and phases. In these runs, the tides and the surge are computed together, so that the elevations represent the fully combined results, not just the simply added results.

At a given grid point within the study region, the combined results can be plotted against the added results, to obtain a regression expression relating one to the other, approximately. Both tides and storms must be chosen carefully for this exercise in order to cover the ranges of parameters of importance. The result is an approximation that can be thought of as a simple rule used to correct linear superposition to better match physical combination. The earlier FEMA experience recommends the use of different corrections for low and high tide. In addition, preliminary calculations performed for a South Carolina surge study suggested that these corrections may depend on the coordinates and characteristics of the grid point and on its location relative to the hurricane track. Given these complicated dependencies, it was decided not to use the regression approach.

Monte Carlo Simulation: A third approach has been used extensively by the State of Florida in its determinations of Coastal Construction Control Lines (Chiu and Dean, 2002). This work was published in a series of county-by-county reports by the Florida Department of Natural Resources (DNR), Bureau of Beaches and Shores. The idea is extremely simple and formed the basis of the procedure adopted in this study. The Florida DNR coastal setback work involves Monte Carlo simulation of many hundreds or thousands of storms using an inexpensive 1D surge model (locally calibrated against a 2D model)[32]. To account for the effects of tide, the 1D simulations are performed using local tide history as defined by choosing a random starting time

[32] See Chiu and Dean, 2002, for details on the 1D model and its calibration.

in the tide predictions for the hurricane season. Each simulation is performed with a random tide in this way, and the large number of simulations effectively reproduces a very long period of history, with tide and surge appropriately combined. From these calculations, the final total water levels are obtained directly, without need for additional tide analysis.

This latter procedure was investigated and applied in the ongoing South Carolina study and was also adopted in this study after proper validation. Simply defined, for each storm in the JPM-OS simulation set, choose a random starting time within the hurricane season, and simulate that storm with the corresponding tidal parameters as an ADCIRC boundary condition. The question to be investigated is whether the number of storms in the JPM-OS set is sufficient[33], so that the randomly chosen tides adequately sample the significant range of tidal effects and produce a stable estimate of the surge plus tide levels. The investigation conducted for this study is discussed in the following section.

4.6.3 Non-hydrodynamic Tests of Linear Superposition

A simple set of tests was performed to investigate the variability that might arise using this approach. The maximum variability in the statistics of the surge plus tide estimates should be revealed by simple linear superposition of the surge with random tides, with no consideration of hydrodynamic interactions. The first variant of this test was performed by assigning a random start time (during the hurricane season) to each JPM-OS storm, superimposing the surge and astronomic-tide hydrographs at each of the 49 locations, and then determining the peak combined surge. For the sake of simplicity, the astronomic tide was represented by the National Ocean Service predicted tide for the year 2008.

This process was repeated 500 times in order to observe the variation in the results as a consequence of the random-starting time assignments. These calculations were performed for three alternative values of the standard deviation of the secondary factors, but only the results obtained with a typical standard deviation (1.4 feet) are presented here.

Results for the 1- and 0.2-percent-annual-chance recurrence intervals are shown in Figures 4-6 and 4-7. These figures show the results for surge alone (red squares), the mean (blue circles with 1-standard deviation error bars) obtained from the 500 realizations of the randomized starting times, and the standard deviation among realizations (green triangles; keyed to the right Y axis).

The standard deviation represents the size of the typical error that one would make using one realization of the random starting time for each JPM-OS storm. This standard deviation has values of 0.15 to 0.3 foot for the 1-percent-annual frequency and 0.3 to 0.6 foot for the 0.2-percent-annual frequency. These values are sufficiently low, compared to other uncertainties in surge calculations.

If desired, one can reduce this error by running each storm with two random starting times (after halving the rate for each storm); this would reduce the above standard deviations by a factor of $2^{1/2}$=1.41.

[33] The number of JPM-OS storms (159) is much smaller than the number of storms considered in the Florida DNR work (hundreds or thousands). The results shown in Figures 4-6 and 4-7 indicate that stable results are obtained with this smaller number of storms.

4.6.4 Implementation

Implementation of this approach to the tide requires, first, the ability to characterize the tide along the NY-NJ coast at any given time. This capability already resides in the hydrodynamic model, subject to selection of a representative site and a starting time.

For the NY-NJ study area, the hurricane season is defined as covering the months of August and September for purposes of defining a storm starting time. Conditions outside of this time period will not differ significantly because this 2-month time period is the most active and because it includes multiple fortnightly cycles. Tidal conditions for the two-month period starting on August 1 can then be randomly sampled in order to define the subsequent tidal water levels over each storm's duration. It was decided to require different starting times for all storms, and each starting time was defined to the whole hour. Hurricane occurrence was assumed to be random and uniformly distributed over the time interval, so that 159 uniformly distributed, non-repeating start times were selected. After these times were generated, the storms were then paired at random to these starting times, so as to enforce complete time randomization among the storms. Table 4-7 displays the results. The second and third columns show which storm in the JPM-OS set was run with the start-time shown in columns 4-7 (year, month, day, hour). The second and third columns employ the two different naming conventions used in the project for the JPM-OS storms. The typical year of 2010 was used.

4.7 SUMMARY

This section documents the development of a JPM-OS set of synthetic storms and associated annual rates, based on the probabilistic hurricane model described in Section 3. These storms, and their rates, are representative of future hurricanes[34] that may generate significant storm surge affecting the inhabitants and infrastructure along the NY-NJ coast, based on present storm climatology.

In addition, this section introduces a Monte Carlo approach for the assignment of random starting times for the JPM-OS synthetic storms. These random starting times—together with the capability of the ADCIRC model to simulate astronomical tides—provide a straightforward mechanism for the inclusion of tides in the JPM-OS surge calculations, including nonlinear interactions. Tests presented here indicate that the sampling variability resulting from the use of one randomly assigned starting time to each JPM-OS storm is sufficiently small. This approach for the treatment of astronomical tides was preferred to approaches that treat tide as a secondary factor because it takes nonlinear-interaction effects into account.

[34] As discussed in Section 2.3, climate change is not being considered. Therefore, these future hurricanes are assumed to have rate and characteristics representative of the present climate regime.

Table 4-1. Discretized Distributions of Storm Parameters Used to Construct the Reference Storm Set of New Jersey Hurricanes

Δ**P(mb)**	37.3	46.7	56.7	67.1	77.3	85.3	89.1
P_o(mb)	976	966	956	946	936	928	924
Probability	0.33130	0.27986	0.19806	0.11550	0.05379	0.01885	0.00436

ΔP(mb)	**Values of R_p(nmi) for Given ΔP**				
37.3	11.01	21.35	38.82	70.60	136.86
46.7	10.48	20.32	36.95	67.20	130.27
56.7	9.82	19.04	34.63	62.97	122.06
67.1	9.06	17.56	31.92	58.05	112.54
77.3	8.26	16.01	29.12	52.95	102.64
85.3	7.61	14.75	26.83	48.78	94.57
89.1	7.29	14.14	25.71	46.75	90.62
Probability	0.011	0.222	0.534	0.222	0.011

ΔP(mb)			
37.3	5.8	10.4	15.1
46.7	8.3	13.0	17.7
56.7	11.0	15.7	20.4
67.1	13.9	18.6	23.2
77.3	14.7	19.3	24.0
85.3	14.7	19.3	24.0
89.1	14.7	19.3	24.0
Probability	0.248	0.505	0.248

Headings (direction to; degrees clockwise from North)			
	-0.8	19.1	33.3
Probability	0.248	0.505	0.248

Holland B			
	mean – 1.37 □	mean	mean – 1.37 □
Probability	0.248	0.505	0.248

Table 4-2. Discretization of ΔP into Slices in JPM-OS Scheme for Landfalling Hurricanes

Slice	1	2
ΔP range (mb)	33-55	55-90
Probability	0.70	0.30
Number of points in Bayesian Quadrature	15	20

Table 4-3. Correlation Distances in JPM-OS Scheme for Landfalling Hurricanes

Correlation Distance (std normal units)				
ΔP (within slice)	R_p	V_f	Heading	B
2	2.5	4.5	4.5	3

Table 4-4. JPM-OS Representation of Joint Probability Distribution of Storm Characteristics for New Jersey Hurricanes

Probability	ΔP (mb)	R_p(nmi)	V_f (m/s)	Theta[35] (deg)	B
0.0468884	48.57	59.79	10.06	17.54	0.86
0.0468891	48.57	59.79	10.06	17.54	1.34
0.0524639	37.45	19.94	10.06	17.54	1.10
0.0357355	33.95	39.42	6.64	7.66	1.10
0.052464	37.45	75.51	10.06	17.54	1.10
0.0468884	48.57	22.33	10.06	17.54	1.34
0.0464212	37.55	38.79	10.06	17.54	1.44
0.0357354	33.95	39.42	13.49	24.01	1.10
0.049479	41.70	37.99	5.21	24.03	1.10
0.0464212	37.55	38.78	10.06	17.54	0.76
0.049479	41.70	37.99	14.92	7.59	1.10
0.0408534	44.96	37.32	14.76	25.12	1.10
0.0444567	53.84	35.32	10.06	17.54	1.10
0.0468891	48.57	22.33	10.06	17.54	0.86
0.0408534	44.96	37.32	5.37	3.59	1.10
0.0148037	56.82	37.18	17.36	19.58	1.38
0.0146643	60.38	20.26	15.59	5.31	1.25
0.013352	81.26	51.76	15.77	18.47	1.13
0.024501	66.89	30.79	18.92	20.58	1.13
0.0174049	63.53	64.53	15.54	18.30	1.28
0.0153145	71.29	28.94	14.12	17.25	1.48
0.0153013	55.52	26.01	13.51	16.78	1.04
0.0123944	86.66	21.81	15.15	18.02	1.17
0.0159291	65.33	60.55	13.58	16.84	0.85
0.0146643	60.38	20.26	12.25	24.43	1.25
0.0170342	72.18	33.32	9.90	24.08	1.10
0.0170343	72.18	33.32	13.51	2.15	1.10
0.0118118	55.73	66.68	13.28	16.60	1.06
0.0113446	59.53	16.80	18.98	20.62	0.90
0.0145968	76.36	27.18	16.31	18.86	0.77
0.0187136	61.94	25.52	11.29	15.00	0.85
0.0196723	59.97	38.95	9.81	13.77	1.20
0.0161513	58.66	40.25	18.47	7.37	0.96
0.0172425	73.29	15.13	13.71	16.94	1.09
0.0161512	58.66	40.25	14.98	25.20	0.96

[35] The heading angles for the Long Island hurricanes are larger by one degree.

Table 4-5. Summary Statistics from Comparison of Results from JPM-OS and Reference Storms

Return Period	100 yrs.	500 yrs.
Mean Bias (ft.)	0.1	-0.4
Std. Dev. (ft.)	0.5	0.4
Min. OS1-Ref (ft.)	1.3	0.5
Max. OS1-Ref (ft.)	-1.0	-1.3

Table 4-6. Characteristics of JPM-OS Synthetic Storms at Landfall

Original Name[36]	Sequential Name	ΔP (mb)	R_p (nmi)	V_f (m/s)	theta (deg)	B	Land-fall Lon. (deg)	Land-fall Lat. (deg)	Prob.
NJa_0001_005	NJA_0001	59.97	38.95	9.811	13.77	1.204	-74.74	39.04	5.18E-04
NJa_0001_006	NJA_0002	59.97	38.95	9.811	13.77	1.204	-73.39	40.66	4.89E-04
NJa_0002_005	NJA_0003	61.94	25.52	11.29	15	0.847	-74.86	38.93	3.22E-04
NJa_0002_006	NJA_0004	61.94	25.52	11.29	15	0.847	-73.71	40.64	2.73E-04
NJa_0002_007	NJA_0005	61.94	25.52	11.29	15	0.847	-73.17	40.68	3.28E-04
NJa_0003_005	NJA_0006	55.73	66.68	13.28	16.6	1.056	-74.85	38.94	5.31E-04
NJa_0004_005	NJA_0007	55.52	26.01	13.51	16.78	1.041	-74.54	39.22	2.70E-04
NJa_0004_006	NJA_0008	55.52	26.01	13.51	16.78	1.041	-73.4	40.66	2.53E-04
NJa_0006_005	NJA_0009	73.29	15.13	13.71	16.94	1.094	-74.97	38.81	1.78E-04
NJa_0006_006	NJA_0010	73.29	15.13	13.71	16.94	1.094	-74.46	39.29	1.77E-04
NJa_0006_007	NJA_0011	73.29	15.13	13.71	16.94	1.094	-73.58	40.65	1.56E-04
NJa_0006_008	NJA_0012	73.29	15.13	13.71	16.94	1.094	-73.25	40.67	1.74E-04
NJa_0007_005	NJA_0013	71.29	28.94	14.12	17.25	1.48	-74.61	39.16	3.00E-04
NJa_0007_006	NJA_0014	71.29	28.94	14.12	17.25	1.48	-73.36	40.67	2.86E-04
NJa_0008_005	NJA_0015	37.55	38.79	10.06	17.54	1.436	-73.47	40.66	1.12E-03
NJa_0009_005	NJA_0016	48.57	59.79	10.06	17.54	1.336	-74.8	38.99	1.89E-03
NJa_0010_005	NJA_0017	48.57	22.33	10.06	17.54	1.336	-74.74	39.04	7.07E-04
NJa_0010_006	NJA_0018	48.57	22.33	10.06	17.54	1.336	-73.58	40.65	6.27E-04
NJa_0011_005	NJA_0019	53.84	35.32	10.06	17.54	1.1	-74.42	39.33	1.07E-03
NJa_0012_005	NJA_0020	37.45	75.51	10.06	17.54	1.1	-74.78	39	2.67E-03
NJa_0013_005	NJA_0021	37.45	19.94	10.06	17.54	1.1	-74.78	39	7.06E-04
NJa_0013_006	NJA_0022	37.45	19.94	10.06	17.54	1.1	-73.66	40.65	6.09E-04
NJa_0013_007	NJA_0023	37.45	19.94	10.06	17.54	1.1	-73.23	40.67	7.05E-04
NJa_0014_005	NJA_0024	48.57	22.33	10.06	17.54	0.864	-74.57	39.2	7.10E-04
NJa_0014_006	NJA_0025	48.57	22.33	10.06	17.54	0.864	-73.46	40.66	6.52E-04
NJa_0015_005	NJA_0026	37.55	38.78	10.06	17.54	0.764	-75.04	38.73	1.24E-03
NJa_0015_006	NJA_0027	37.55	38.78	10.06	17.54	0.764	-73.4	40.66	1.15E-03
NJa_0016_005	NJA_0028	48.57	59.79	10.06	17.54	0.864	-75.22	38.1	2.13E-03

[36] The prefix JPM-OS1_ was removed from the storm names in the first two columns of this table for the sake of formatting.

Original Name[36]	Sequential Name	ΔP (mb)	R_p (nmi)	V_f (m/s)	theta (deg)	B	Land-fall Lon. (deg)	Land-fall Lat. (deg)	Prob.
NJa_0017_005	NJA_0029	86.66	21.81	15.15	18.02	1.172	-75.02	38.75	1.86E-04
NJa_0017_006	NJA_0030	86.66	21.81	15.15	18.02	1.172	-74.25	39.48	1.85E-04
NJa_0017_007	NJA_0031	86.66	21.81	15.15	18.02	1.172	-73.26	40.67	1.80E-04
NJa_0019_005	NJA_0032	81.26	51.76	15.77	18.47	1.128	-73.49	40.66	4.26E-04
NJa_0020_005	NJA_0033	76.36	27.18	16.31	18.86	0.768	-74.49	39.26	2.69E-04
NJa_0020_006	NJA_0034	76.36	27.18	16.31	18.86	0.768	-73.26	40.67	2.64E-04
NJa_0021_005	NJA_0035	56.82	37.18	17.36	19.58	1.384	-73.42	40.66	3.48E-04
NJa_0022_005	NJA_0036	66.89	30.79	18.92	20.58	1.132	-73.5	40.66	4.65E-04
NJa_0023_005	NJA_0037	59.53	16.8	18.98	20.62	0.905	-74.8	38.98	1.29E-04
NJa_0023_006	NJA_0038	59.53	16.8	18.98	20.62	0.905	-73.59	40.65	1.14E-04
NJa_0023_007	NJA_0039	59.53	16.8	18.98	20.62	0.905	-73.22	40.68	1.29E-04
NJa_0024_005	NJA_0040	33.95	39.42	13.49	24.01	1.1	-74.38	39.36	9.59E-04
NJa_0025_005	NJA_0041	41.7	37.99	5.213	24.03	1.1	-74.65	39.12	1.27E-03
NJa_0026_005	NJA_0042	72.18	33.32	9.9	24.08	1.096	-73.47	40.66	3.53E-04
NJa_0027_005	NJA_0043	60.38	20.26	12.25	24.43	1.255	-74.67	39.11	2.01E-04
NJa_0027_006	NJA_0044	60.38	20.26	12.25	24.43	1.255	-73.25	40.67	1.99E-04
NJa_0028_005	NJA_0045	44.96	37.32	14.76	25.12	1.1	-74.28	39.46	1.04E-03
NJa_0029_005	NJA_0046	58.66	40.25	14.98	25.2	0.961	-74.27	39.47	4.44E-04
NJb_0001_005	NJB_0001	72.18	33.32	13.51	2.148	1.096	-75.17	38.19	1.90E-04
NJb_0001_006	NJB_0002	72.18	33.32	13.51	2.148	1.096	-74.84	38.94	1.70E-04
NJb_0001_007	NJB_0003	72.18	33.32	13.51	2.148	1.096	-74.54	39.22	1.71E-04
NJb_0001_008	NJB_0004	72.18	33.32	13.51	2.148	1.096	-74.23	39.5	1.72E-04
NJb_0001_009	NJB_0005	72.18	33.32	13.51	2.148	1.096	-73.87	40.5	1.41E-04
NJb_0001_010	NJB_0006	72.18	33.32	13.51	2.148	1.096	-73.57	40.65	1.52E-04
NJb_0001_011	NJB_0007	72.18	33.32	13.51	2.148	1.096	-73.27	40.67	1.68E-04
NJb_0002_005	NJB_0008	44.96	37.32	5.367	3.588	1.1	-75.17	38.2	5.11E-04
NJb_0002_006	NJB_0009	44.96	37.32	5.367	3.588	1.1	-74.77	39.01	4.57E-04
NJb_0002_007	NJB_0010	44.96	37.32	5.367	3.588	1.1	-74.42	39.33	4.61E-04
NJb_0002_008	NJB_0011	44.96	37.32	5.367	3.588	1.1	-74.01	40.14	4.06E-04
NJb_0002_009	NJB_0012	44.96	37.32	5.367	3.588	1.1	-73.63	40.65	3.98E-04
NJb_0002_010	NJB_0013	44.96	37.32	5.367	3.588	1.1	-73.3	40.67	4.46E-04
NJb_0003_005	NJB_0014	60.38	20.26	15.59	5.305	1.255	-75.24	38.07	1.01E-04
NJb_0003_006	NJB_0015	60.38	20.26	15.59	5.305	1.255	-74.98	38.8	9.02E-05
NJb_0003_007	NJB_0016	60.38	20.26	15.59	5.305	1.255	-74.77	39.01	8.91E-05
NJb_0003_008	NJB_0017	60.38	20.26	15.59	5.305	1.255	-74.57	39.19	8.95E-05
NJb_0003_009	NJB_0018	60.38	20.26	15.59	5.305	1.255	-74.37	39.37	8.99E-05
NJb_0003_010	NJB_0019	60.38	20.26	15.59	5.305	1.255	-74.15	39.71	8.69E-05
NJb_0003_011	NJB_0020	60.38	20.26	15.59	5.305	1.255	-73.85	40.54	7.35E-05
NJb_0003_012	NJB_0021	60.38	20.26	15.59	5.305	1.255	-73.66	40.65	7.69E-05

Original Name[36]	Sequential Name	ΔP (mb)	R_p (nmi)	V_f (m/s)	theta (deg)	B	Land-fall Lon. (deg)	Land-fall Lat. (deg)	Prob.
NJb_0003_013	NJB_0022	60.38	20.26	15.59	5.305	1.255	-73.47	40.66	8.20E-05
NJb_0003_014	NJB_0023	60.38	20.26	15.59	5.305	1.255	-73.29	40.67	8.71E-05
NJb_0004_005	NJB_0024	58.66	40.25	18.47	7.374	0.961	-74.9	38.88	1.96E-04
NJb_0004_006	NJB_0025	58.66	40.25	18.47	7.374	0.961	-74.48	39.27	1.96E-04
NJb_0004_007	NJB_0026	58.66	40.25	18.47	7.374	0.961	-73.91	40.44	1.63E-04
NJb_0004_008	NJB_0027	58.66	40.25	18.47	7.374	0.961	-73.51	40.66	1.77E-04
NJb_0004_009	NJB_0028	58.66	40.25	18.47	7.374	0.961	-73.14	40.68	2.00E-04
NJb_0005_005	NJB_0029	41.7	37.99	14.92	7.594	1.1	-74.79	38.99	5.64E-04
NJb_0005_006	NJB_0030	41.7	37.99	14.92	7.594	1.1	-74.39	39.35	5.69E-04
NJb_0005_007	NJB_0031	41.7	37.99	14.92	7.594	1.1	-73.81	40.61	4.62E-04
NJb_0005_008	NJB_0032	41.7	37.99	14.92	7.594	1.1	-73.46	40.66	5.21E-04
NJb_0006_005	NJB_0033	33.95	39.42	6.644	7.657	1.1	-75.17	38.2	4.72E-04
NJb_0006_006	NJB_0034	33.95	39.42	6.644	7.657	1.1	-74.66	39.11	4.24E-04
NJb_0006_007	NJB_0035	33.95	39.42	6.644	7.657	1.1	-74.24	39.49	4.28E-04
NJb_0006_008	NJB_0036	33.95	39.42	6.644	7.657	1.1	-73.66	40.65	3.64E-04
NJb_0006_009	NJB_0037	33.95	39.42	6.644	7.657	1.1	-73.3	40.67	4.11E-04
LI_0001_005	LI_0001	48.57	59.79	10.06	23	0.864	-72.67	40.78	2.25E-03
LI_0002_005	LI_0002	48.57	59.79	10.06	23	1.336	-72.72	40.77	2.24E-03
LI_0003_005	LI_0003	37.45	19.94	10.06	23	1.1	-73.09	40.69	8.08E-04
LI_0003_006	LI_0004	37.45	19.94	10.06	23	1.1	-72.54	40.8	8.51E-04
LI_0003_007	LI_0005	37.45	19.94	10.06	23	1.1	-71.92	41.04	9.08E-04
LI_0003_008	LI_0006	37.45	19.94	10.06	23	1.1	-71.21	41.42	8.40E-04
LI_0004_005	LI_0007	33.95	39.42	6.644	11.03	1.1	-72.57	40.8	1.14E-03
LI_0004_006	LI_0008	33.95	39.42	6.644	11.03	1.1	-71.51	41.37	1.12E-03
LI_0006_005	LI_0009	48.57	22.33	10.06	23	1.336	-73.02	40.71	8.14E-04
LI_0006_006	LI_0010	48.57	22.33	10.06	23	1.336	-72.41	40.83	8.62E-04
LI_0006_007	LI_0011	48.57	22.33	10.06	23	1.336	-71.55	41.36	8.31E-04
LI_0007_005	LI_0012	37.55	38.79	10.06	23	1.436	-72.65	40.78	1.45E-03
LI_0007_006	LI_0013	37.55	38.79	10.06	23	1.436	-71.34	41.4	1.44E-03
LI_0008_005	LI_0014	33.95	39.42	13.49	34.97	1.1	-71.46	41.38	1.12E-03
LI_0009_005	LI_0015	41.7	37.99	5.213	35.04	1.1	-72.98	40.71	1.47E-03
LI_0009_006	LI_0016	41.7	37.99	5.213	35.04	1.1	-71.26	41.41	1.51E-03
LI_0010_005	LI_0017	37.55	38.78	10.06	23	0.764	-72.7	40.77	1.44E-03
LI_0010_006	LI_0018	37.55	38.78	10.06	23	0.764	-71.39	41.39	1.44E-03
LI_0011_005	LI_0019	41.7	37.99	14.92	10.96	1.1	-72.66	40.78	1.51E-03
LI_0011_006	LI_0020	41.7	37.99	14.92	10.96	1.1	-71.64	41.35	1.49E-03
LI_0012_005	LI_0021	44.96	37.32	14.76	39.44	1.1	-72.99	40.71	1.19E-03
LI_0012_006	LI_0022	44.96	37.32	14.76	39.44	1.1	-71.08	41.44	1.23E-03
LI_0013_005	LI_0023	53.84	35.32	10.06	23	1.1	-72.75	40.76	1.25E-03

Original Name[36]	Sequential Name	ΔP (mb)	R_p (nmi)	V_f (m/s)	theta (deg)	B	Land-fall Lon. (deg)	Land-fall Lat. (deg)	Prob.
LI_0013_006	LI_0024	53.84	35.32	10.06	23	1.1	-71.54	41.36	1.25E-03
LI_0014_005	LI_0025	48.57	22.33	10.06	23	0.864	-72.74	40.76	8.36E-04
LI_0014_006	LI_0026	48.57	22.33	10.06	23	0.864	-72.08	40.97	8.90E-04
LI_0014_007	LI_0027	48.57	22.33	10.06	23	0.864	-71.28	41.41	8.39E-04
LI_0015_005	LI_0028	44.96	37.32	5.367	6.555	1.1	-73.12	40.68	1.17E-03
LI_0015_006	LI_0029	44.96	37.32	5.367	6.555	1.1	-72.25	40.89	1.28E-03
LI_0015_007	LI_0030	44.96	37.32	5.367	6.555	1.1	-71.32	41.4	1.22E-03
LI_0016_005	LI_0031	56.82	37.18	17.36	25.98	1.384	-73.06	40.7	4.26E-04
LI_0016_006	LI_0032	56.82	37.18	17.36	25.98	1.384	-71.9	41.05	4.78E-04
LI_0017_005	LI_0033	60.38	20.26	15.59	8.425	1.255	-73.11	40.69	2.29E-04
LI_0017_006	LI_0034	60.38	20.26	15.59	8.425	1.255	-72.63	40.79	2.40E-04
LI_0017_007	LI_0035	60.38	20.26	15.59	8.425	1.255	-72.15	40.94	2.51E-04
LI_0017_008	LI_0036	60.38	20.26	15.59	8.425	1.255	-71.6	41.36	2.36E-04
LI_0017_009	LI_0037	60.38	20.26	15.59	8.425	1.255	-71.12	41.43	2.39E-04
LI_0018_005	LI_0038	81.26	51.76	15.77	24.32	1.128	-71.64	41.35	5.47E-04
LI_0019_005	LI_0039	66.89	30.79	18.92	27.59	1.132	-72.56	40.8	6.12E-04
LI_0019_006	LI_0040	66.89	30.79	18.92	27.59	1.132	-71.35	41.39	6.03E-04
LI_0020_005	LI_0041	63.53	64.53	15.54	24.08	1.28	-72.06	40.98	9.58E-04
LI_0021_005	LI_0042	71.29	28.94	14.12	22.61	1.48	-72.43	40.83	3.64E-04
LI_0021_006	LI_0043	71.29	28.94	14.12	22.61	1.48	-71.4	41.39	3.54E-04
LI_0022_005	LI_0044	55.52	26.01	13.51	21.97	1.041	-72.52	40.81	3.24E-04
LI_0022_006	LI_0045	55.52	26.01	13.51	21.97	1.041	-71.58	41.36	3.16E-04
LI_0023_005	LI_0046	86.66	21.81	15.15	23.68	1.172	-72.92	40.73	2.12E-04
LI_0023_006	LI_0047	86.66	21.81	15.15	23.68	1.172	-72.3	40.87	2.25E-04
LI_0023_007	LI_0048	86.66	21.81	15.15	23.68	1.172	-71.45	41.38	2.15E-04
LI_0024_005	LI_0049	65.33	60.55	13.58	22.05	0.851	-72.57	40.8	7.82E-04
LI_0025_005	LI_0050	60.38	20.26	12.25	36.38	1.255	-72.99	40.71	2.32E-04
LI_0025_006	LI_0051	60.38	20.26	12.25	36.38	1.255	-72.25	40.89	2.49E-04
LI_0025_007	LI_0052	60.38	20.26	12.25	36.38	1.255	-71.13	41.43	2.39E-04
LI_0026_005	LI_0053	72.18	33.32	9.9	35.19	1.096	-72.5	40.81	4.64E-04
LI_0027_005	LI_0054	72.18	33.32	13.51	5.002	1.096	-72.86	40.74	4.48E-04
LI_0027_006	LI_0055	72.18	33.32	13.51	5.002	1.096	-72.09	40.96	4.82E-04
LI_0027_007	LI_0056	72.18	33.32	13.51	5.002	1.096	-71.28	41.41	4.55E-04
LI_0028_005	LI_0057	55.73	66.68	13.28	21.74	1.056	-72.43	40.83	6.47E-04
LI_0029_005	LI_0058	59.53	16.8	18.98	27.66	0.905	-72.96	40.72	1.49E-04
LI_0029_006	LI_0059	59.53	16.8	18.98	27.66	0.905	-72.46	40.82	1.56E-04
LI_0029_007	LI_0060	59.53	16.8	18.98	27.66	0.905	-71.86	41.06	1.66E-04
LI_0029_008	LI_0061	59.53	16.8	18.98	27.66	0.905	-71.17	41.42	1.53E-04
LI_0030_005	LI_0062	76.36	27.18	16.31	24.88	0.768	-72.81	40.75	3.15E-04

Original Name[36]	Sequential Name	ΔP (mb)	R_p (nmi)	V_f (m/s)	theta (deg)	B	Land-fall Lon. (deg)	Land-fall Lat. (deg)	Prob.
LI_0030_006	LI_0063	76.36	27.18	16.31	24.88	0.768	-71.97	41.02	3.44E-04
LI_0031_005	LI_0064	61.94	25.52	11.29	19.66	0.847	-73.04	40.7	3.71E-04
LI_0031_006	LI_0065	61.94	25.52	11.29	19.66	0.847	-72.37	40.84	3.95E-04
LI_0031_007	LI_0066	61.94	25.52	11.29	19.66	0.847	-71.49	41.37	3.80E-04
LI_0032_005	LI_0067	59.97	38.95	9.811	18.13	1.204	-72.51	40.81	6.25E-04
LI_0032_006	LI_0068	59.97	38.95	9.811	18.13	1.204	-71.32	41.4	6.13E-04
LI_0033_005	LI_0069	58.66	40.25	18.47	10.71	0.961	-72.42	40.83	5.35E-04
LI_0033_006	LI_0070	58.66	40.25	18.47	10.71	0.961	-71.35	41.4	5.20E-04
LI_0034_005	LI_0071	73.29	15.13	13.71	22.18	1.094	-73	40.71	2.03E-04
LI_0034_006	LI_0072	73.29	15.13	13.71	22.18	1.094	-72.59	40.8	2.11E-04
LI_0034_007	LI_0073	73.29	15.13	13.71	22.18	1.094	-72.14	40.94	2.21E-04
LI_0034_008	LI_0074	73.29	15.13	13.71	22.18	1.094	-71.54	41.37	2.07E-04
LI_0034_009	LI_0075	73.29	15.13	13.71	22.18	1.094	-71.13	41.43	2.10E-04
LI_0035_005	LI_0076	58.66	40.25	14.98	39.92	0.961	-71.34	41.4	5.20E-04

Table 4-7. Random Starting Times for JPM-OS Storms

No.	Original Storm Name	Sequential Name	Year	Month	Day	Hour
1	JPM-OS1_NJb_0001_011	JPM-OS1_NJB_0007	2010	8	1	1
2	JPM-OS1_NJa_0012_005	JPM-OS1_NJA_0020	2010	8	1	10
3	JPM-OS1_NJa_0013_006	JPM-OS1_NJA_0022	2010	8	1	22
4	JPM-OS1_LI_0020_005	JPM-OS1_LI_0041	2010	8	2	5
5	JPM-OS1_NJb_0003_014	JPM-OS1_NJB_0023	2010	8	2	12
6	JPM-OS1_LI_0030_006	JPM-OS1_LI_0063	2010	8	2	21
7	JPM-OS1_NJb_0004_008	JPM-OS1_NJB_0027	2010	8	3	14
8	JPM-OS1_LI_0034_006	JPM-OS1_LI_0072	2010	8	3	20
9	JPM-OS1_LI_0009_005	JPM-OS1_LI_0015	2010	8	4	7
10	JPM-OS1_NJb_0002_009	JPM-OS1_NJB_0012	2010	8	4	11
11	JPM-OS1_LI_0015_006	JPM-OS1_LI_0029	2010	8	4	20
12	JPM-OS1_NJa_0015_006	JPM-OS1_NJA_0027	2010	8	5	10
13	JPM-OS1_LI_0008_005	JPM-OS1_LI_0014	2010	8	5	21
14	JPM-OS1_LI_0017_009	JPM-OS1_LI_0037	2010	8	6	5
15	JPM-OS1_NJb_0001_006	JPM-OS1_NJB_0002	2010	8	6	14
16	JPM-OS1_NJa_0019_005	JPM-OS1_NJA_0032	2010	8	6	22
17	JPM-OS1_NJa_0001_005	JPM-OS1_NJA_0001	2010	8	7	7
18	JPM-OS1_NJb_0001_008	JPM-OS1_NJB_0004	2010	8	7	14
19	JPM-OS1_LI_0017_008	JPM-OS1_LI_0036	2010	8	8	2
20	JPM-OS1_LI_0024_005	JPM-OS1_LI_0049	2010	8	8	9
21	JPM-OS1_LI_0003_005	JPM-OS1_LI_0003	2010	8	8	19
22	JPM-OS1_LI_0011_005	JPM-OS1_LI_0019	2010	8	9	5
23	JPM-OS1_NJa_0007_005	JPM-OS1_NJA_0013	2010	8	9	12
24	JPM-OS1_NJa_0014_006	JPM-OS1_NJA_0025	2010	8	9	21
25	JPM-OS1_NJa_0027_005	JPM-OS1_NJA_0043	2010	8	10	3

No.	Original Storm Name	Sequential Name	Year	Month	Day	Hour
26	JPM-OS1_LI_0019_005	JPM-OS1_LI_0039	2010	8	10	14
27	JPM-OS1_NJa_0006_007	JPM-OS1_NJA_0011	2010	8	10	22
28	JPM-OS1_NJb_0006_006	JPM-OS1_NJB_0034	2010	8	11	8
29	JPM-OS1_NJa_0023_007	JPM-OS1_NJA_0039	2010	8	11	15
30	JPM-OS1_NJb_0005_005	JPM-OS1_NJB_0029	2010	8	12	2
31	JPM-OS1_NJb_0006_007	JPM-OS1_NJB_0035	2010	8	12	9
32	JPM-OS1_NJa_0002_007	JPM-OS1_NJA_0005	2010	8	13	1
33	JPM-OS1_NJa_0020_005	JPM-OS1_NJA_0033	2010	8	13	9
34	JPM-OS1_LI_0006_005	JPM-OS1_LI_0009	2010	8	13	12
35	JPM-OS1_LI_0023_005	JPM-OS1_LI_0046	2010	8	14	1
36	JPM-OS1_NJa_0010_006	JPM-OS1_NJA_0018	2010	8	14	9
37	JPM-OS1_LI_0027_006	JPM-OS1_LI_0055	2010	8	14	20
38	JPM-OS1_LI_0034_007	JPM-OS1_LI_0073	2010	8	15	1
39	JPM-OS1_NJb_0006_009	JPM-OS1_NJB_0037	2010	8	15	11
40	JPM-OS1_LI_0029_005	JPM-OS1_LI_0058	2010	8	15	23
41	JPM-OS1_LI_0006_006	JPM-OS1_LI_0010	2010	8	16	9
42	JPM-OS1_NJb_0001_009	JPM-OS1_NJB_0005	2010	8	16	16
43	JPM-OS1_LI_0019_006	JPM-OS1_LI_0040	2010	8	16	23
44	JPM-OS1_NJb_0004_009	JPM-OS1_NJB_0028	2010	8	17	6
45	JPM-OS1_LI_0012_006	JPM-OS1_LI_0022	2010	8	17	17
46	JPM-OS1_LI_0033_006	JPM-OS1_LI_0070	2010	8	18	4
47	JPM-OS1_LI_0028_005	JPM-OS1_LI_0057	2010	8	18	14
48	JPM-OS1_NJb_0005_006	JPM-OS1_NJB_0030	2010	8	18	21
49	JPM-OS1_NJa_0023_006	JPM-OS1_NJA_0038	2010	8	19	7
50	JPM-OS1_NJa_0006_005	JPM-OS1_NJA_0009	2010	8	19	14
51	JPM-OS1_LI_0029_007	JPM-OS1_LI_0060	2010	8	20	2
52	JPM-OS1_LI_0026_005	JPM-OS1_LI_0053	2010	8	20	6
53	JPM-OS1_NJa_0014_005	JPM-OS1_NJA_0024	2010	8	20	18
54	JPM-OS1_LI_0021_005	JPM-OS1_LI_0042	2010	8	21	0
55	JPM-OS1_LI_0007_006	JPM-OS1_LI_0013	2010	8	21	11
56	JPM-OS1_NJa_0008_005	JPM-OS1_NJA_0015	2010	8	22	0
57	JPM-OS1_NJa_0006_008	JPM-OS1_NJA_0012	2010	8	22	8
58	JPM-OS1_NJb_0004_006	JPM-OS1_NJB_0025	2010	8	22	15
59	JPM-OS1_NJb_0003_010	JPM-OS1_NJB_0019	2010	8	23	4
60	JPM-OS1_LI_0025_006	JPM-OS1_LI_0051	2010	8	23	10
61	JPM-OS1_LI_0011_006	JPM-OS1_LI_0020	2010	8	23	21
62	JPM-OS1_LI_0016_005	JPM-OS1_LI_0031	2010	8	24	2
63	JPM-OS1_NJb_0004_007	JPM-OS1_NJB_0026	2010	8	24	11
64	JPM-OS1_NJa_0001_006	JPM-OS1_NJA_0002	2010	8	24	19
65	JPM-OS1_LI_0010_005	JPM-OS1_LI_0017	2010	8	25	7
66	JPM-OS1_LI_0034_005	JPM-OS1_LI_0071	2010	8	25	15
67	JPM-OS1_LI_0014_006	JPM-OS1_LI_0026	2010	8	26	6
68	JPM-OS1_LI_0035_005	JPM-OS1_LI_0076	2010	8	26	10
69	JPM-OS1_NJb_0003_013	JPM-OS1_NJB_0022	2010	8	26	23
70	JPM-OS1_LI_0032_005	JPM-OS1_LI_0067	2010	8	27	8
71	JPM-OS1_NJa_0004_005	JPM-OS1_NJA_0007	2010	8	27	15
72	JPM-OS1_NJa_0006_006	JPM-OS1_NJA_0010	2010	8	27	22

No.	Original Storm Name	Sequential Name	Year	Month	Day	Hour
73	JPM-OS1_NJa_0021_005	JPM-OS1_NJA_0035	2010	8	28	11
74	JPM-OS1_NJb_0002_006	JPM-OS1_NJB_0009	2010	8	28	20
75	JPM-OS1_LI_0013_006	JPM-OS1_LI_0024	2010	8	28	23
76	JPM-OS1_LI_0025_007	JPM-OS1_LI_0052	2010	8	29	15
77	JPM-OS1_LI_0014_007	JPM-OS1_LI_0027	2010	8	30	0
78	JPM-OS1_LI_0015_005	JPM-OS1_LI_0028	2010	8	30	4
79	JPM-OS1_NJa_0025_005	JPM-OS1_NJA_0041	2010	8	30	15
80	JPM-OS1_NJa_0013_007	JPM-OS1_NJA_0023	2010	8	31	2
81	JPM-OS1_LI_0022_005	JPM-OS1_LI_0044	2010	8	31	6
82	JPM-OS1_NJa_0017_007	JPM-OS1_NJA_0031	2010	8	31	21
83	JPM-OS1_NJb_0001_010	JPM-OS1_NJB_0006	2010	9	1	7
84	JPM-OS1_LI_0034_009	JPM-OS1_LI_0075	2010	9	1	9
85	JPM-OS1_NJb_0002_010	JPM-OS1_NJB_0013	2010	9	1	20
86	JPM-OS1_LI_0031_005	JPM-OS1_LI_0064	2010	9	2	4
87	JPM-OS1_LI_0017_006	JPM-OS1_LI_0034	2010	9	2	12
88	JPM-OS1_NJb_0003_006	JPM-OS1_NJB_0015	2010	9	2	21
89	JPM-OS1_NJa_0017_006	JPM-OS1_NJA_0030	2010	9	3	11
90	JPM-OS1_NJa_0029_005	JPM-OS1_NJA_0046	2010	9	3	22
91	JPM-OS1_LI_0015_007	JPM-OS1_LI_0030	2010	9	4	7
92	JPM-OS1_LI_0013_005	JPM-OS1_LI_0023	2010	9	4	17
93	JPM-OS1_NJb_0003_009	JPM-OS1_NJB_0018	2010	9	5	0
94	JPM-OS1_NJa_0023_005	JPM-OS1_NJA_0037	2010	9	5	8
95	JPM-OS1_NJa_0009_005	JPM-OS1_NJA_0016	2010	9	5	19
96	JPM-OS1_LI_0003_006	JPM-OS1_LI_0004	2010	9	6	1
97	JPM-OS1_LI_0016_006	JPM-OS1_LI_0032	2010	9	6	5
98	JPM-OS1_NJb_0001_007	JPM-OS1_NJB_0003	2010	9	6	14
99	JPM-OS1_NJa_0007_006	JPM-OS1_NJA_0014	2010	9	7	3
100	JPM-OS1_LI_0025_005	JPM-OS1_LI_0050	2010	9	7	10
101	JPM-OS1_NJa_0028_005	JPM-OS1_NJA_0045	2010	9	7	23
102	JPM-OS1_NJa_0017_005	JPM-OS1_NJA_0029	2010	9	8	8
103	JPM-OS1_NJb_0002_005	JPM-OS1_NJB_0008	2010	9	8	19
104	JPM-OS1_LI_0004_005	JPM-OS1_LI_0007	2010	9	9	5
105	JPM-OS1_NJb_0003_007	JPM-OS1_NJB_0016	2010	9	9	13
106	JPM-OS1_NJb_0003_005	JPM-OS1_NJB_0014	2010	9	9	16
107	JPM-OS1_NJb_0002_007	JPM-OS1_NJB_0010	2010	9	10	5
108	JPM-OS1_NJa_0002_006	JPM-OS1_NJA_0004	2010	9	10	18
109	JPM-OS1_NJb_0005_007	JPM-OS1_NJB_0031	2010	9	11	0
110	JPM-OS1_LI_0034_008	JPM-OS1_LI_0074	2010	9	11	7
111	JPM-OS1_LI_0003_008	JPM-OS1_LI_0006	2010	9	11	14
112	JPM-OS1_LI_0031_006	JPM-OS1_LI_0065	2010	9	12	1
113	JPM-OS1_LI_0001_005	JPM-OS1_LI_0001	2010	9	12	7
114	JPM-OS1_NJb_0005_008	JPM-OS1_NJB_0032	2010	9	12	23
115	JPM-OS1_NJa_0026_005	JPM-OS1_NJA_0042	2010	9	13	5
116	JPM-OS1_LI_0027_007	JPM-OS1_LI_0056	2010	9	13	14
117	JPM-OS1_NJa_0027_006	JPM-OS1_NJA_0044	2010	9	14	0
118	JPM-OS1_LI_0004_006	JPM-OS1_LI_0008	2010	9	14	4
119	JPM-OS1_LI_0003_007	JPM-OS1_LI_0005	2010	9	14	15

No.	Original Storm Name	Sequential Name	Year	Month	Day	Hour
120	JPM-OS1_LI_0032_006	JPM-OS1_LI_0068	2010	9	15	0
121	JPM-OS1_NJa_0022_005	JPM-OS1_NJA_0036	2010	9	15	13
122	JPM-OS1_NJa_0024_005	JPM-OS1_NJA_0040	2010	9	15	19
123	JPM-OS1_LI_0027_005	JPM-OS1_LI_0054	2010	9	16	5
124	JPM-OS1_NJa_0020_006	JPM-OS1_NJA_0034	2010	9	16	15
125	JPM-OS1_NJb_0004_005	JPM-OS1_NJB_0024	2010	9	17	2
126	JPM-OS1_NJa_0003_005	JPM-OS1_NJA_0006	2010	9	17	11
127	JPM-OS1_LI_0029_006	JPM-OS1_LI_0059	2010	9	17	16
128	JPM-OS1_NJa_0011_005	JPM-OS1_NJA_0019	2010	9	18	3
129	JPM-OS1_NJb_0002_008	JPM-OS1_NJB_0011	2010	9	18	7
130	JPM-OS1_LI_0021_006	JPM-OS1_LI_0043	2010	9	18	21
131	JPM-OS1_NJa_0002_005	JPM-OS1_NJA_0003	2010	9	19	7
132	JPM-OS1_NJa_0015_005	JPM-OS1_NJA_0026	2010	9	19	17
133	JPM-OS1_NJa_0013_005	JPM-OS1_NJA_0021	2010	9	19	20
134	JPM-OS1_LI_0014_005	JPM-OS1_LI_0025	2010	9	20	10
135	JPM-OS1_LI_0017_007	JPM-OS1_LI_0035	2010	9	20	15
136	JPM-OS1_LI_0007_005	JPM-OS1_LI_0012	2010	9	21	2
137	JPM-OS1_NJb_0003_011	JPM-OS1_NJB_0020	2010	9	21	15
138	JPM-OS1_LI_0018_005	JPM-OS1_LI_0038	2010	9	21	22
139	JPM-OS1_LI_0033_005	JPM-OS1_LI_0069	2010	9	22	7
140	JPM-OS1_NJb_0003_008	JPM-OS1_NJB_0017	2010	9	22	14
141	JPM-OS1_NJa_0004_006	JPM-OS1_NJA_0008	2010	9	23	4
142	JPM-OS1_LI_0022_006	JPM-OS1_LI_0045	2010	9	23	5
143	JPM-OS1_LI_0010_006	JPM-OS1_LI_0018	2010	9	23	21
144	JPM-OS1_LI_0009_006	JPM-OS1_LI_0016	2010	9	24	3
145	JPM-OS1_NJb_0001_005	JPM-OS1_NJB_0001	2010	9	24	14
146	JPM-OS1_LI_0023_007	JPM-OS1_LI_0048	2010	9	24	23
147	JPM-OS1_NJa_0016_005	JPM-OS1_NJA_0028	2010	9	25	3
148	JPM-OS1_NJa_0010_005	JPM-OS1_NJA_0017	2010	9	25	19
149	JPM-OS1_NJb_0006_005	JPM-OS1_NJB_0033	2010	9	25	22
150	JPM-OS1_LI_0012_005	JPM-OS1_LI_0021	2010	9	26	8
151	JPM-OS1_LI_0023_006	JPM-OS1_LI_0047	2010	9	26	16
152	JPM-OS1_LI_0002_005	JPM-OS1_LI_0002	2010	9	27	6
153	JPM-OS1_NJb_0006_008	JPM-OS1_NJB_0036	2010	9	27	11
154	JPM-OS1_LI_0031_007	JPM-OS1_LI_0066	2010	9	28	0
155	JPM-OS1_LI_0006_007	JPM-OS1_LI_0011	2010	9	28	7
156	JPM-OS1_LI_0017_005	JPM-OS1_LI_0033	2010	9	28	13
157	JPM-OS1_NJb_0003_012	JPM-OS1_NJB_0021	2010	9	28	22
158	JPM-OS1_LI_0030_005	JPM-OS1_LI_0062	2010	9	29	6
159	JPM-OS1_LI_0029_008	JPM-OS1_LI_0061	2010	9	29	15

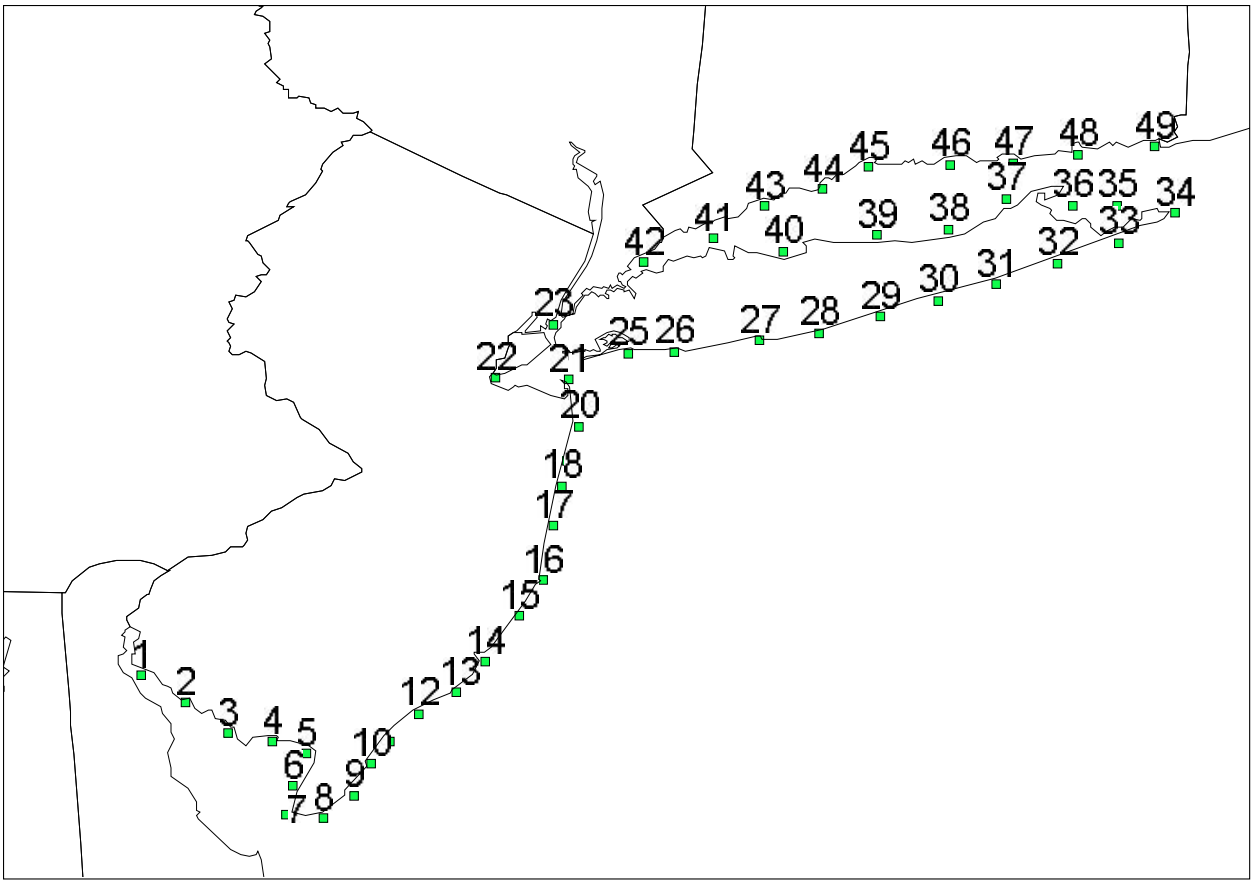

Figure 4-1. Map of target sites used in the JPM-OS Validation.

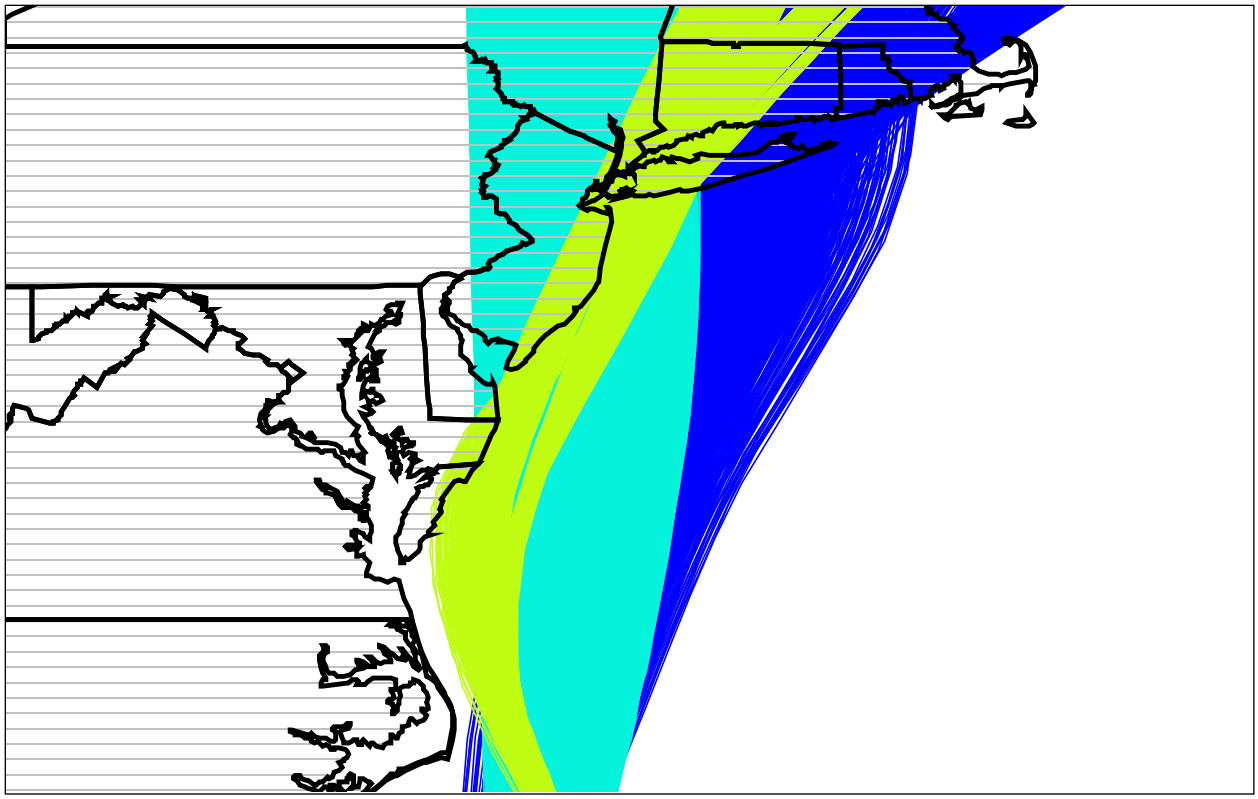

Figure 4-2. Map showing the tracks of the Reference landfalling hurricanes

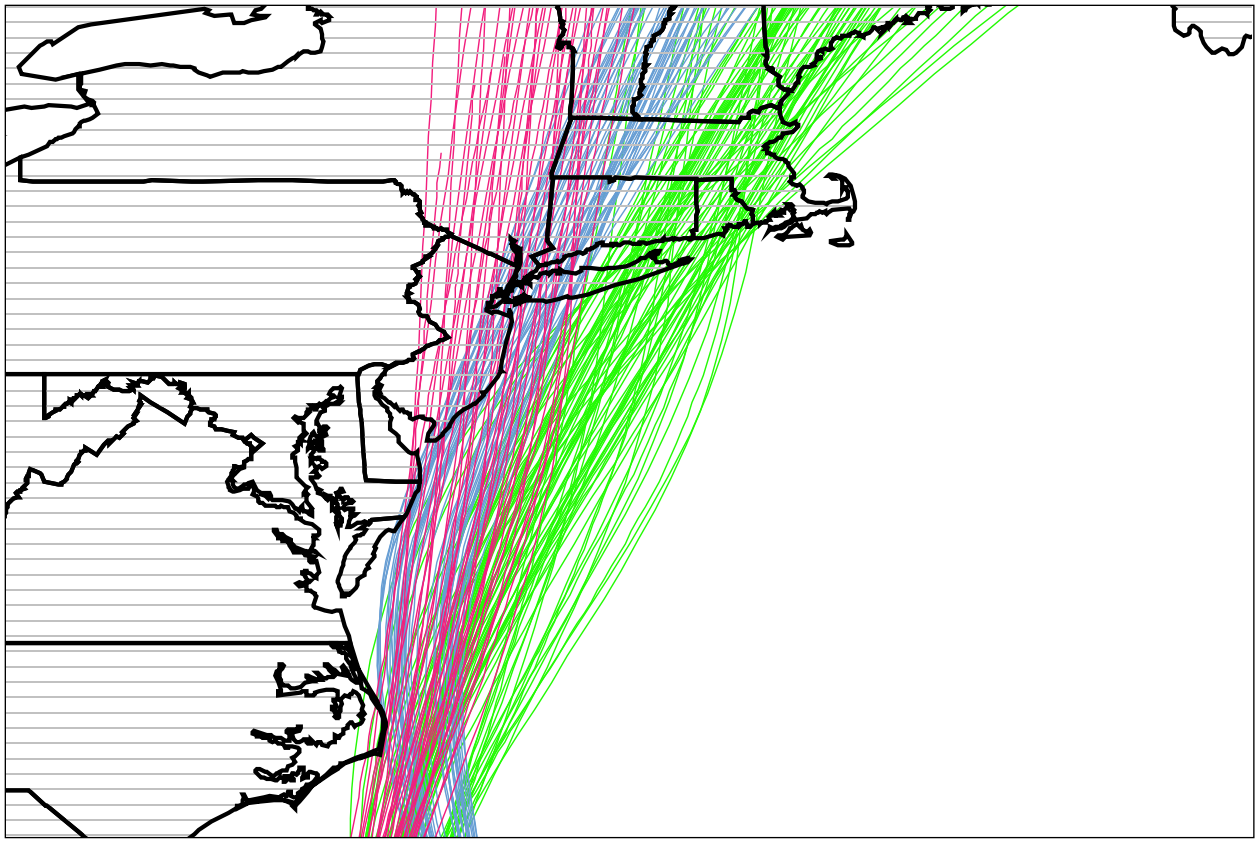

Figure 4-3. Map of tracks for JPM-OS landfalling storms.

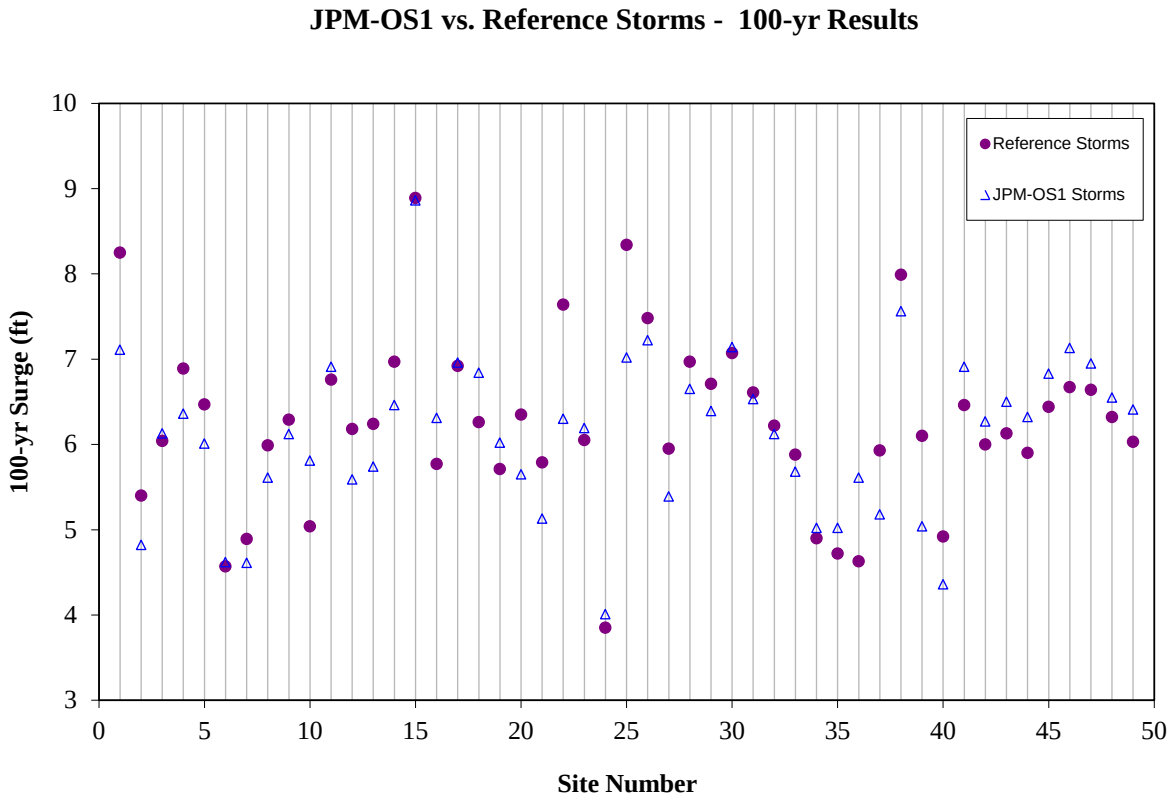

Figure 4-4. Comparison of 100-year surge elevations calculated with ADCIRC with a coarse mesh for JPM-OS1 and Reference Storm sets. The JPM-OS results include a secondary factor for the effect of B, using a standard deviation equal to 34% of the calculated η.

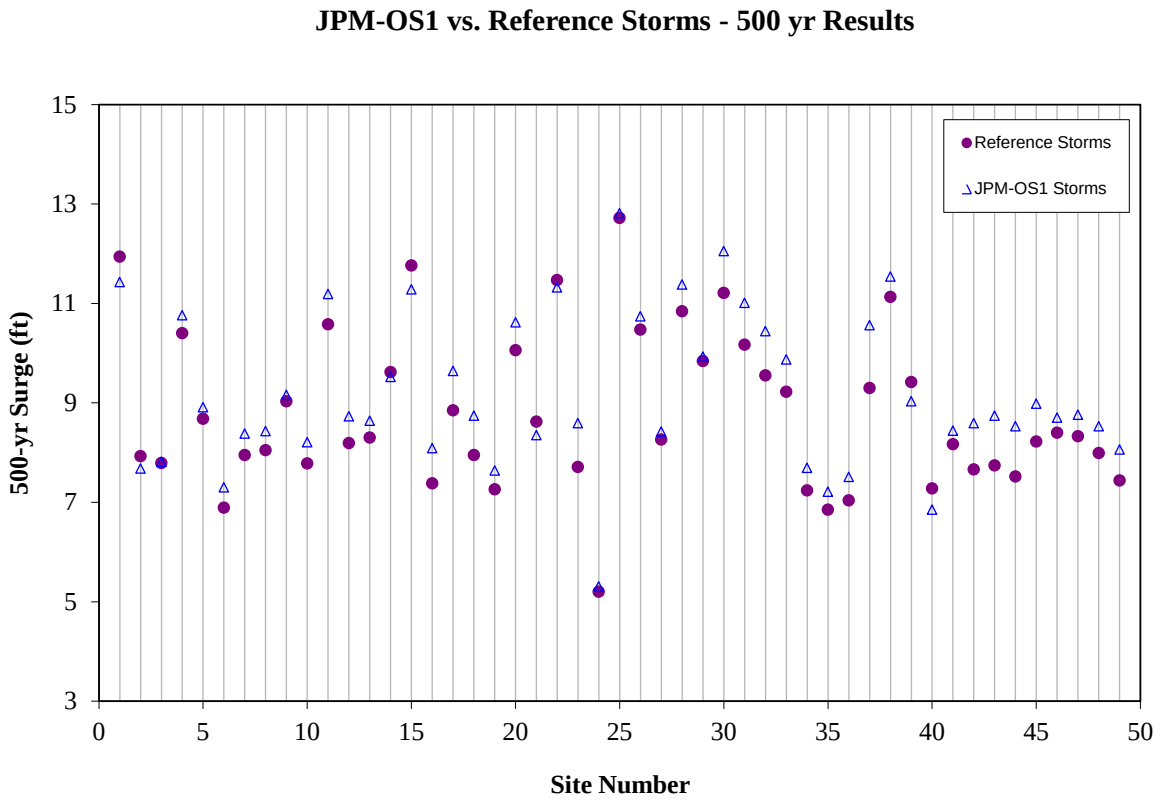

Figure 4-5. Comparison of 500-year surge elevations calculated with ADCIRC with a coarse mesh for JPM-OS1 and Reference Storm sets. The JPM-OS results include a secondary factor for the effect of B, using a standard deviation equal to 34% of the calculated η.

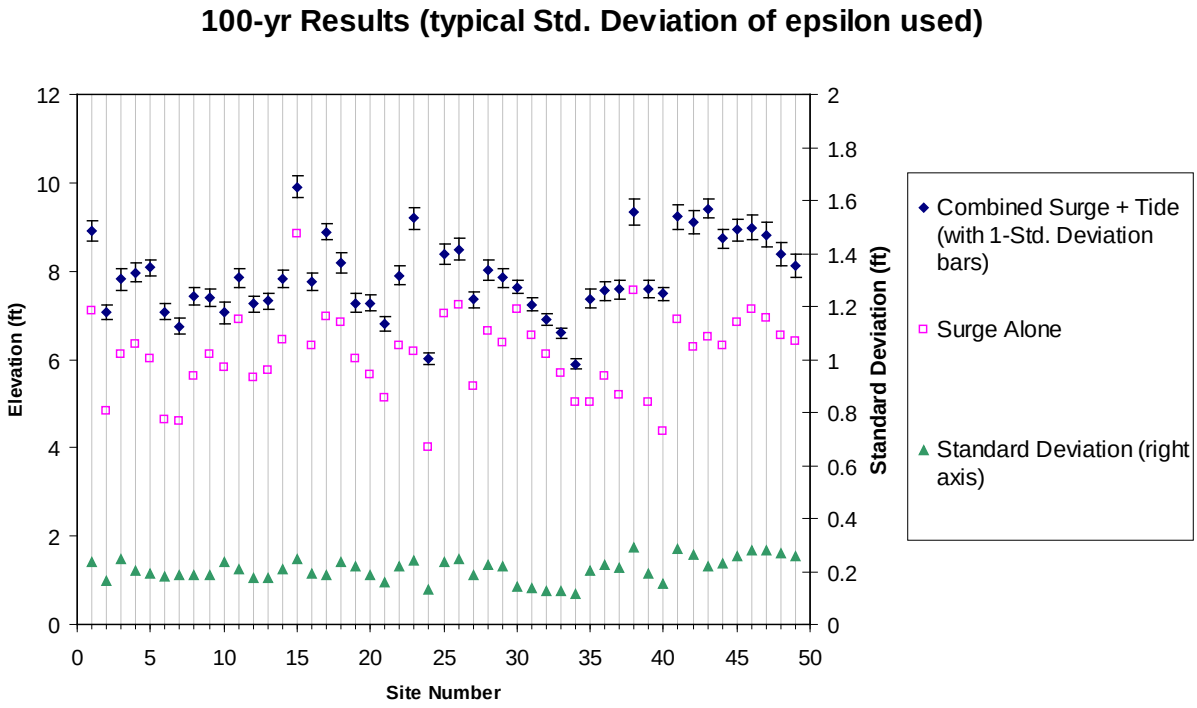

Figure 4-6. Results from Random-tide Tests for 1%-Annual Exceedance Frequency.

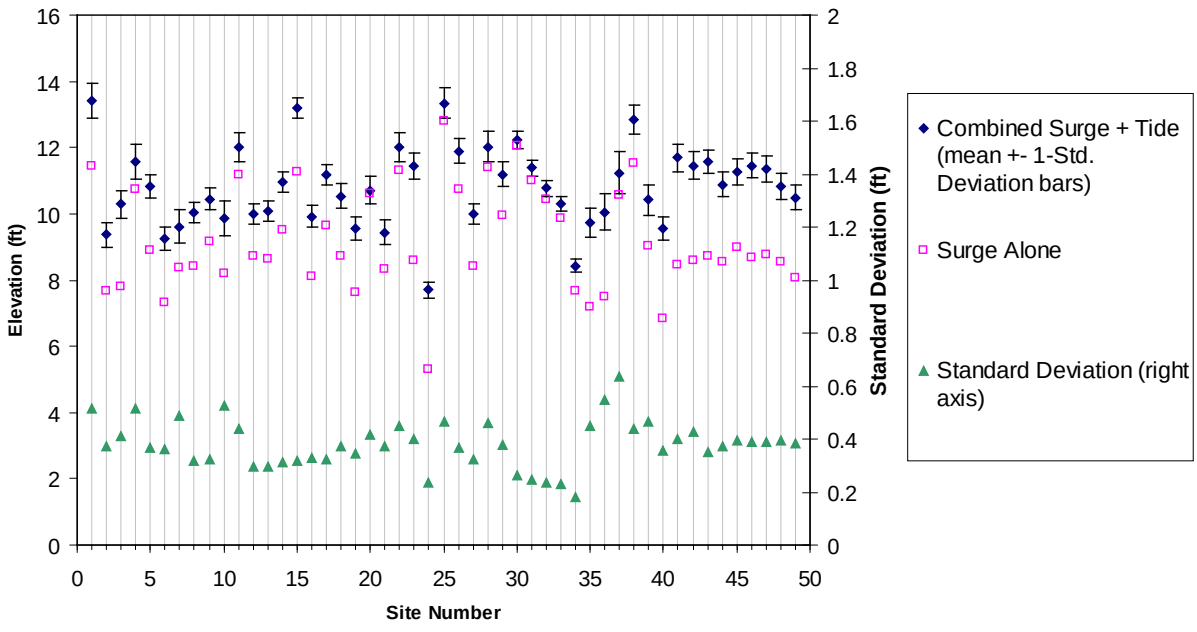

Figure 4-7. Results from Random-tide Tests for 0.2% Annual Exceedance Frequency.

SECTION FIVE METHODOLOGY ISSUES AND SENSITIVITY STUDIES RELATED TO THE ANALYSIS OF EXTRATROPICAL STORMS

5.1 INTRODUCTION AND BACKGROUND

In current practice, the occurrence and surge effects of extratropical storms are not modeled with the JPM-OS approach described in Section 4 of this report. Instead, they are modeled using the historical (sometimes called "points-over-threshold") method or the EST (Empirical Simulation Technique) method (Borgman et al., 1992). The NY-NJ study used the historical method combined with distribution fitting at each grid point.

The NY-NJ surge study selected the top 30 extratropical storms that affected the region during the past 60 years. The selection of these storms and time period is further discussed in a separate report (RAMPP, 2014a).. OWI developed the wind and pressure fields for these extratropical storms, which were then simulated using the ADCIRC hydrodynamics model as part of the final storm set for the study.

Given the time period and number of storms, direct use of the observed "empirical distributions" of hindcast surges (using the "plotting position" or similar approaches) carries significant statistical uncertainty as a result of sampling error. One way to produce more stable results is to fit a probability distribution to the hindcast surge at each grid point. RAMPP investigated a number of distribution shapes and fitting approaches and selected the generalized extreme value (GEV) distribution and the L-Moment approach. These approaches are routinely used in hydrology for fitting extreme values. The effect of astronomic tide was introduced by specifying random starting times, as was detailed in Section 4 for the tropical events.

This Section documents the results of several sensitivity analyses performed in order to investigate the statistical properties of the technique described above, as well as a technique for fitting distributions to upland grid points that may be affected by a few of the storms.

5.2 STATISTICAL PROPERTIES OF GEV DISTRIBUTION FIT TO 30 STORMS

A test was conducted to examine the bias (if any) and statistical uncertainty of the GEV fit using the L-Moment approach when using a sample size of 30 storms. The approach for these calculations is as follows[37]:

1. Take one GEV distribution as given (i.e., the initial or "true" distribution).
2. Generate 100 samples of 30 storms from that distribution.
3. Fit a GEV distribution to each sample using the L-Moment approach.
4. Examine the results to investigate bias and uncertainty.

Figure 5-1 shows the 100 cumulative curves obtained. Note that, even though all synthetic catalogs come from the "true" distribution, there is significant scatter among the curve fits because the number of storms in each catalog is small. Figure 5-2 displays the associated summary statistics (i.e., mean, median, 15th percentile, and 85th percentile), as well as the initial

[37] This technique is known as parametric bootstrapping.

or "true" model. The mean curve is nearly identical to the initial model, indicating that the procedure is essentially unbiased. The range between the 15th and 85th percentile indicates the statistical uncertainty. The uncertainty in the positive direction (i.e., the potential for over-estimating the hazard) is moderate for all exceedance frequencies of interest. The potential for under-estimation is larger, but this is not too serious in practice because the hurricanes would control in those cases, preventing gross under-estimation of the hazard.

5.3 GEV FIT FOR UPLAND POINTS AND ITS STATISTICAL PROPERTIES

Points located away from the shore (upland points) may not be affected by all 30 storms. Fitting distributions at these locations becomes even more uncertain because there are fewer than 30 storms to fit. To overcome this difficulty, one can "borrow" the hindcast surge from the nearest point along the coast or water body that has results from all the storms and fit a GEV to these data (which becomes a "reference point" for the more upland point). Figure 5-3 illustrates the approach.

To investigate this approach, we consider surge results along multiple transects spread throughout the NY-NJ region, such as the ones illustrated in Figure 5-4. Each transect begins at the coast or at a wet location in a river or other inter-tidal water body. Figure 5-5 shows a scatter diagram between results at upland points and at the first point in the corresponding transect. Figure 5-6 shows similar results, but using the closest site shown in Figure 4-1 as the as reference point. The associated mean-square errors are 0.09 and 0.18 m, respectively. This indicates that, for storms that affect both the inland and the wet point, there is a strong correlation between the surge values in both (even when the reference point is not optimally located).

We also use the observed scatter of 0.18 m to investigate the additional uncertainty introduced by using these "borrowed" surge elevations performing the following calculation:

1. Take one GEV distribution as given (i.e., the initial or "true" distribution).
2. Generate 100 samples of 30 storms from that distribution. In this case, only the "virtual" data are randomized, using a standard deviation of 0.18 m.
3. Fit a GEV distribution to each sample using the L-Moment approach.
4. Examine the results to investigate bias and uncertainty.

Figure 5-7 and Figure 5-8 show the results for locations with ground-elevations of 1.5 and 3.0 m. In both cases, the bias (as represented by the difference between the initial model and the mean) and scatter (as represented by the difference between the 15 and 85 percentiles)[38] are small, indicating that the procedure for upland points is robust.

[38] This scatter represents additional scatter, associated with the borrowing of data, besides the scatter observed in Figure 5-2.

5.4 INCORPORATION OF ASTRONOMIC TIDE AND RESULTING STATISTICAL UNCERTAINTY

The effect of astronomic tide was introduced by specifying random starting times, as was done in Section 4.6 for tropical events. A concern arose that the number of extratropical storms (30) is smaller than the number of JPM-OS storms (159), which leads to additional statistical uncertainty. On the other hand, extratropical storms have longer durations, which makes the combined surge plus tide levels less sensitive to the semi-diurnal phasing of the tide.

This statistical uncertainty is investigated using the same approach that was used in Section 4.6.3 for tropical events. Figure 5-9 and Figure 5-10 show the results for the 10- and 1-percent–annual-chance recurrence intervals. Typical values of the standard deviations obtained are 0.3 feet for the 10-percent-annual-chance levels and 1 foot for the 1-percent-annual-chance (two of 49 test sites exhibiting standard deviations as high as 1.9 feet at the 1-percent-annual-chance levels).

In light of the latter results, it was decided to run two realizations of each extratropical storm with two random starting times (reducing the associated annual rate for each storm from 1/59 to 1/118). If the two random starting times for each storm are drawn independently, this implies an anticipated reduction by a factor of $2^{1/2} = 1.41$ in the standard deviation (and possibly more for the two outlier sites. If the starting times are drawn in an antithetical manner (e.g., with lag times equal to ½ the fortnightly period), the reduction may be even greater because negative correlation is introduced, thereby reducing the variances.

Another consideration regarding the results for 1-percent-annual-chance exceedance frequency is that both tropical and extratropical storms are important contributors to these results. As a result, the errors in the combined results are smaller than the errors at the 1-percent-annual-chance level for either of the two contributors.

5.5 SUMMARY

This Section has investigated some of the statistical issues that arose in the analysis of extratropical storms for the NY-NJ study. Results indicate that the approaches used have good statistical properties, which lead to reliable results.

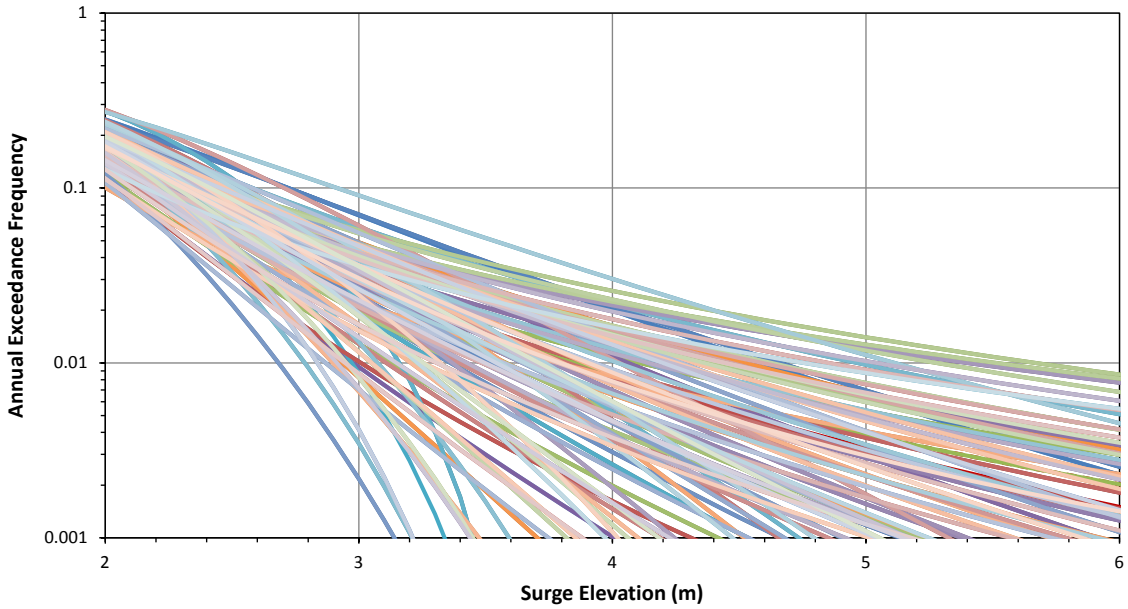

Figure 5-1. Cumulative curves obtained by fitting GEV distributions to data from 100 synthetic storm catalogs obtained using bootstrapping.

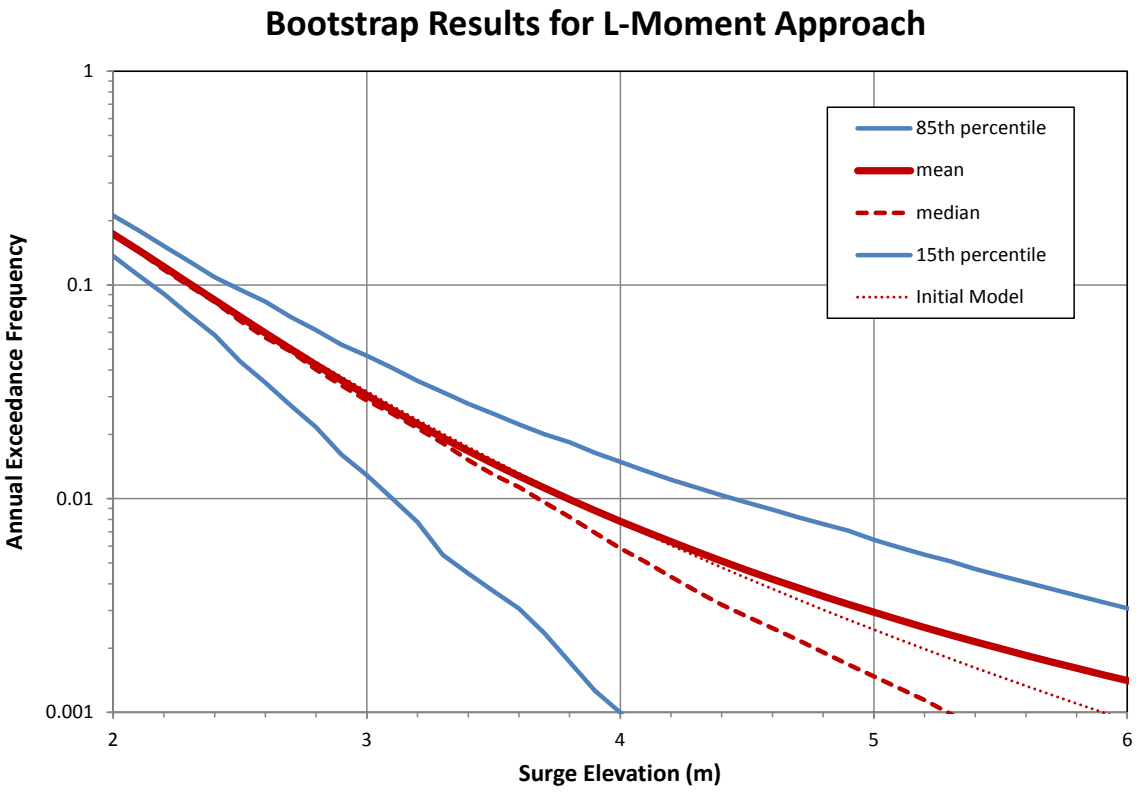

Figure 5-2. Summary statistics from the 100 GEV fits.

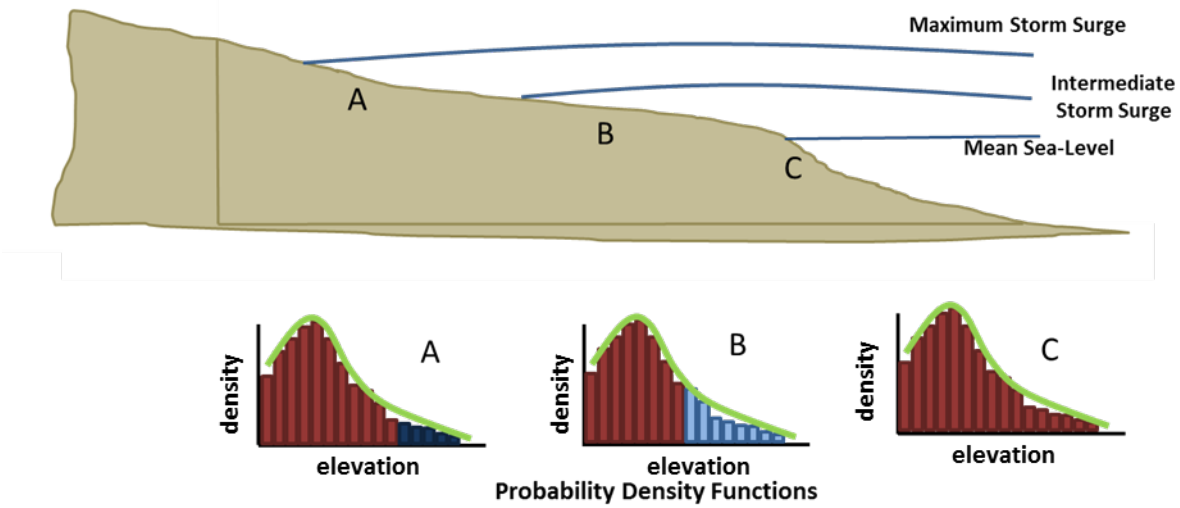

Figure 5-3. Illustration of the approach used to fit extreme-value distributions to upland locations. The red color indicates the data from node C, which are also used to characterize the lower portion of the distribution at upland locations A and B.

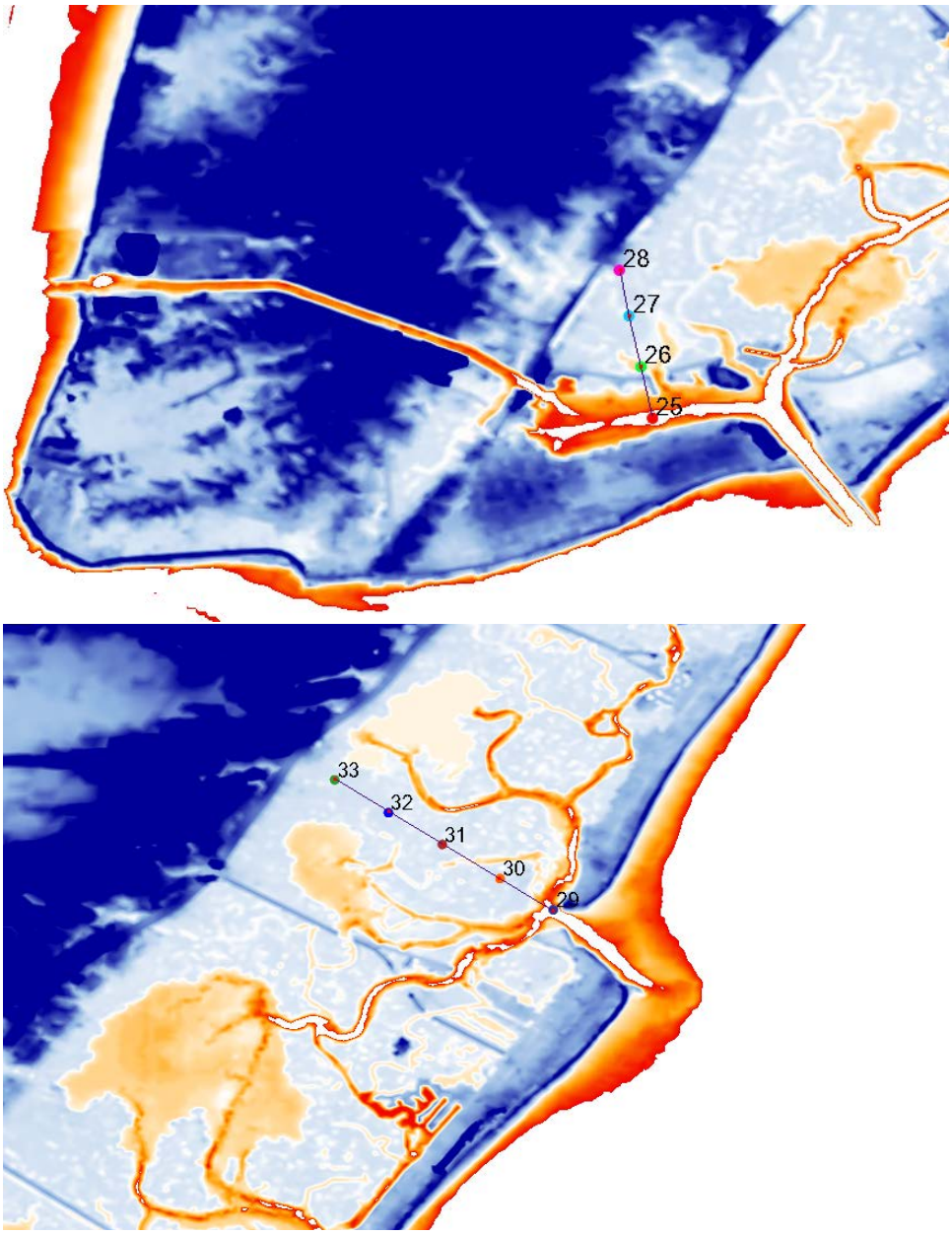

Figure 5-4. Some of the transects considered to investigate the relationship between wet and upland locations.

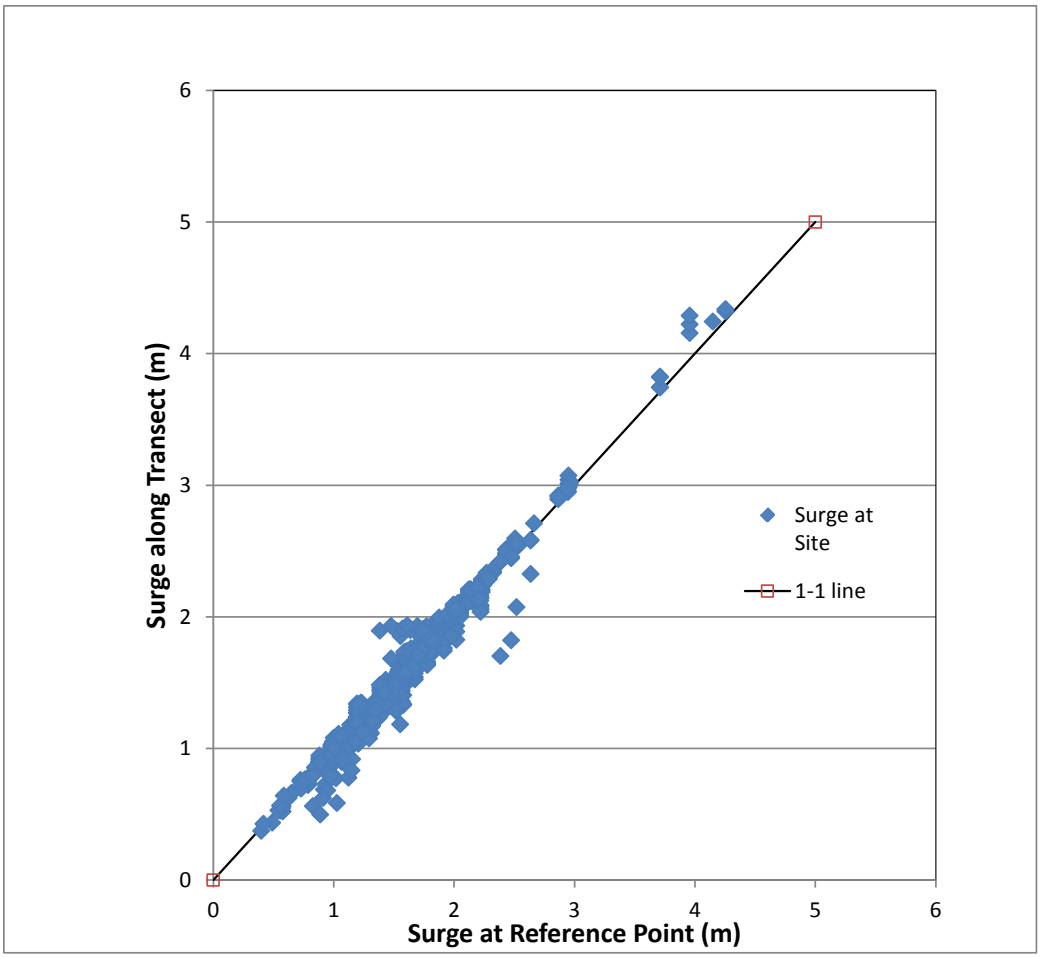

Figure 5-5. Scatter diagram between surge at upland nodes and at the first node in the transect.

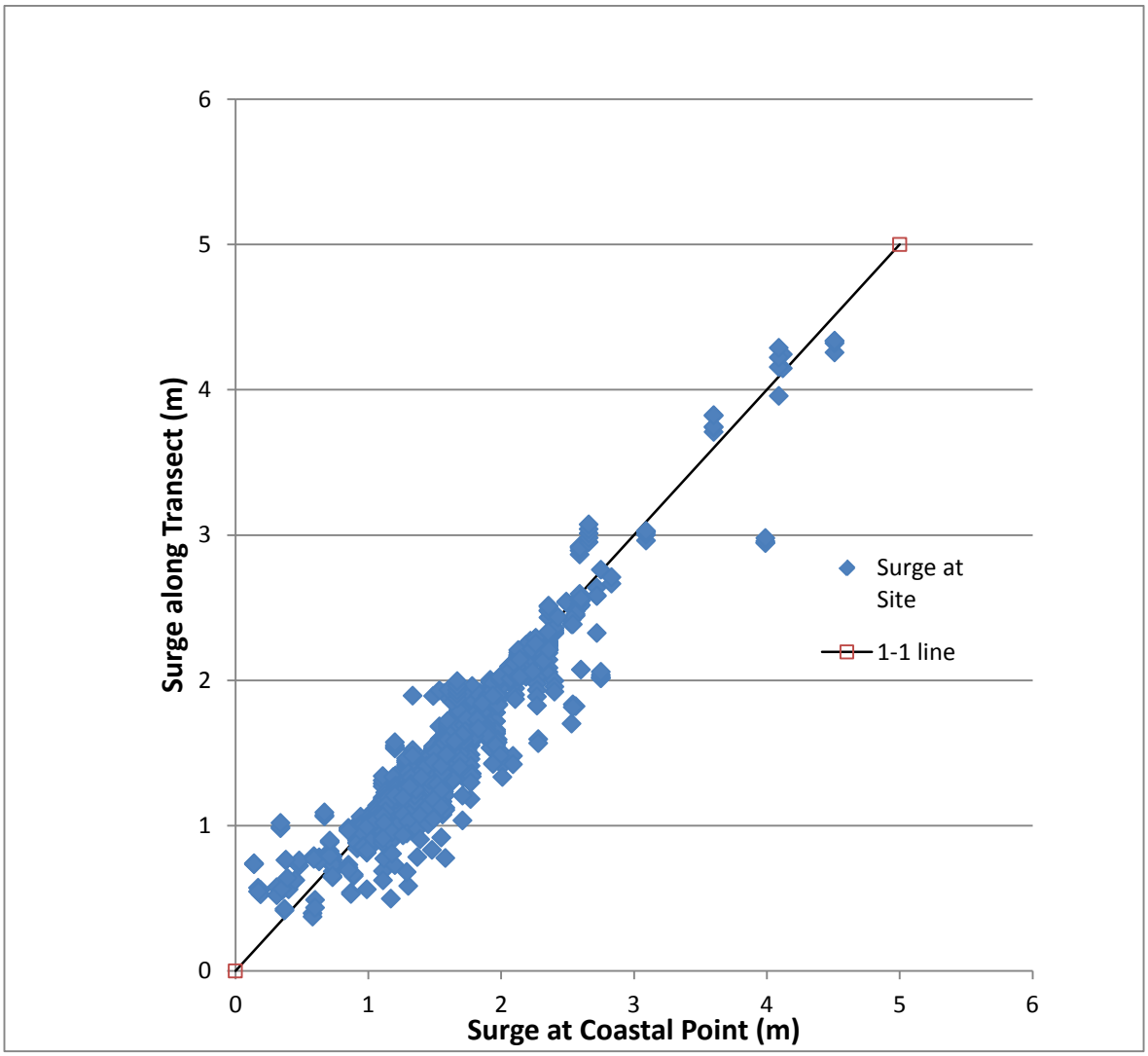

Figure 5-6. Scatter diagram between surge at upland nodes and near coastal node (i.e., the nearest point in Figure 4-1).

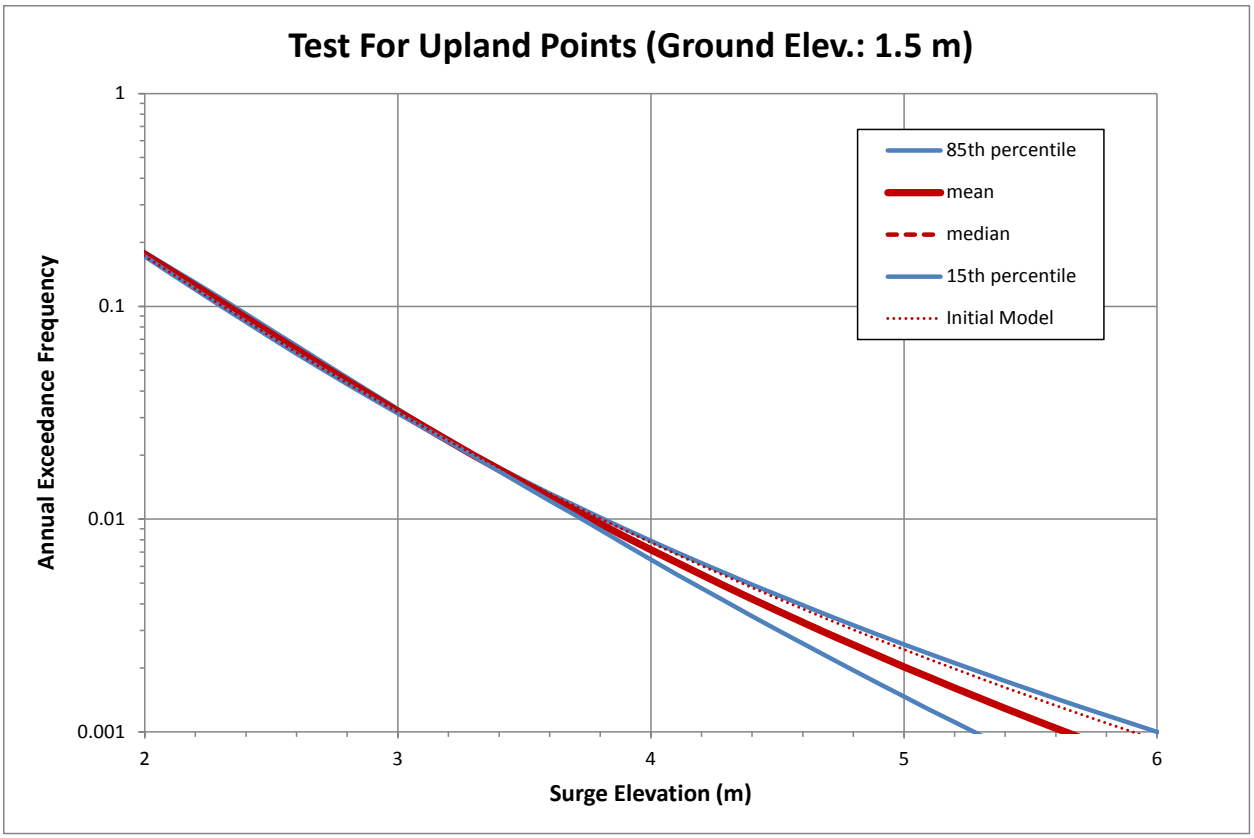

Figure 5-7. Bootstrap results for an upland node with a 1.5-meter (m) ground elevation.

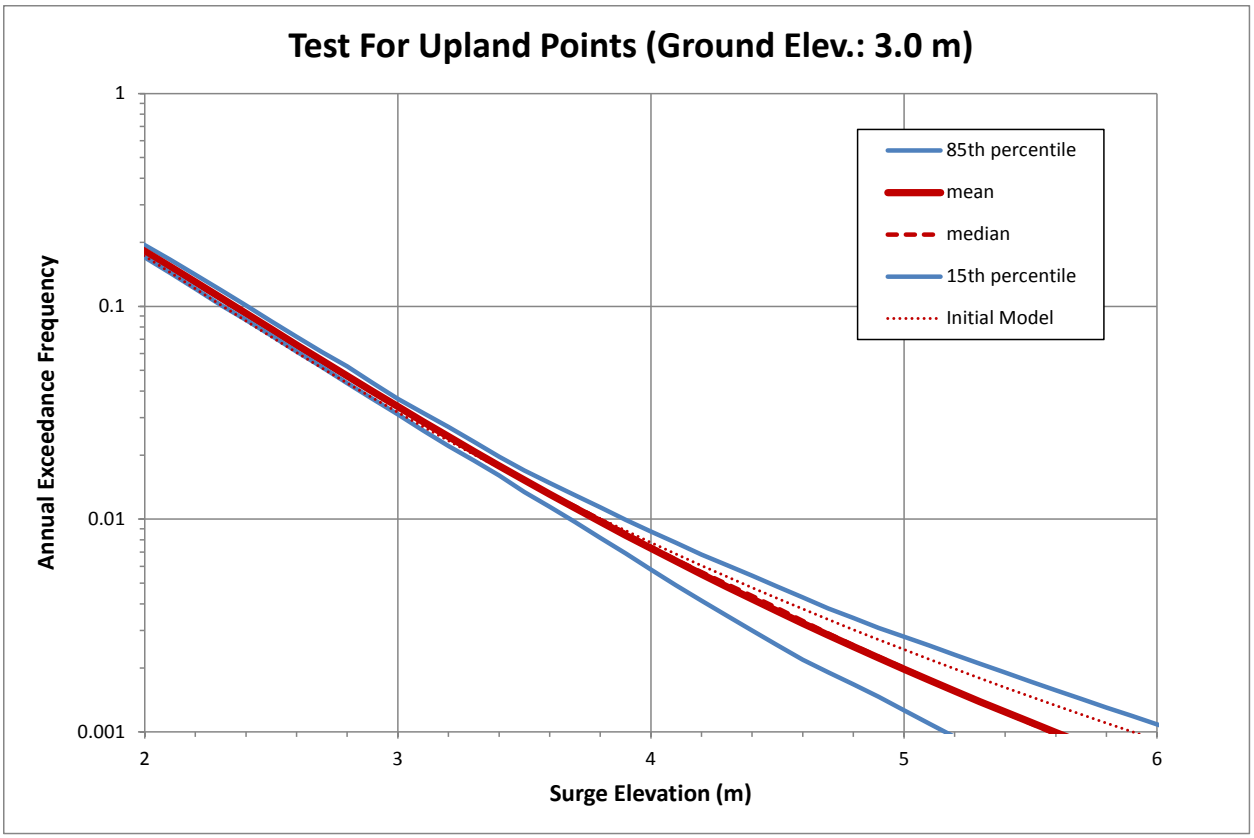

Figure 5-8. Bootstrap results for an upland node with a 3.0-m ground elevation.

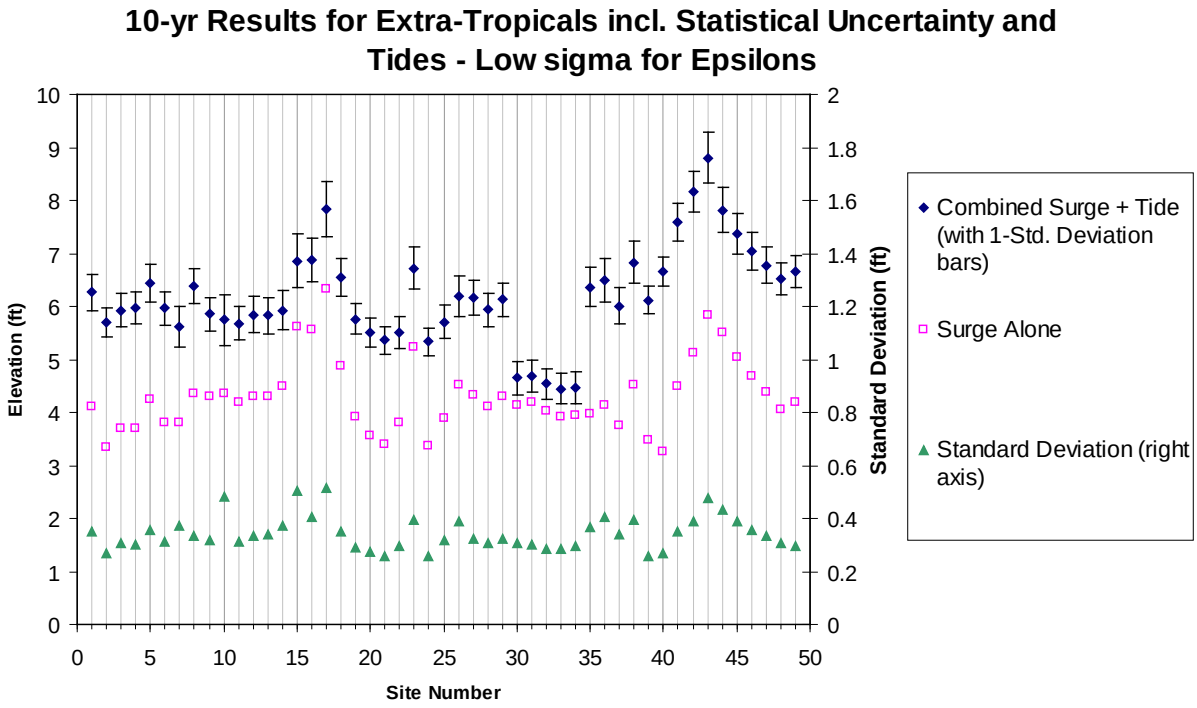

Figure 5-9. Effect of astronomic tide on the 10% annual-chance (10-year) surge from extratropical storms.

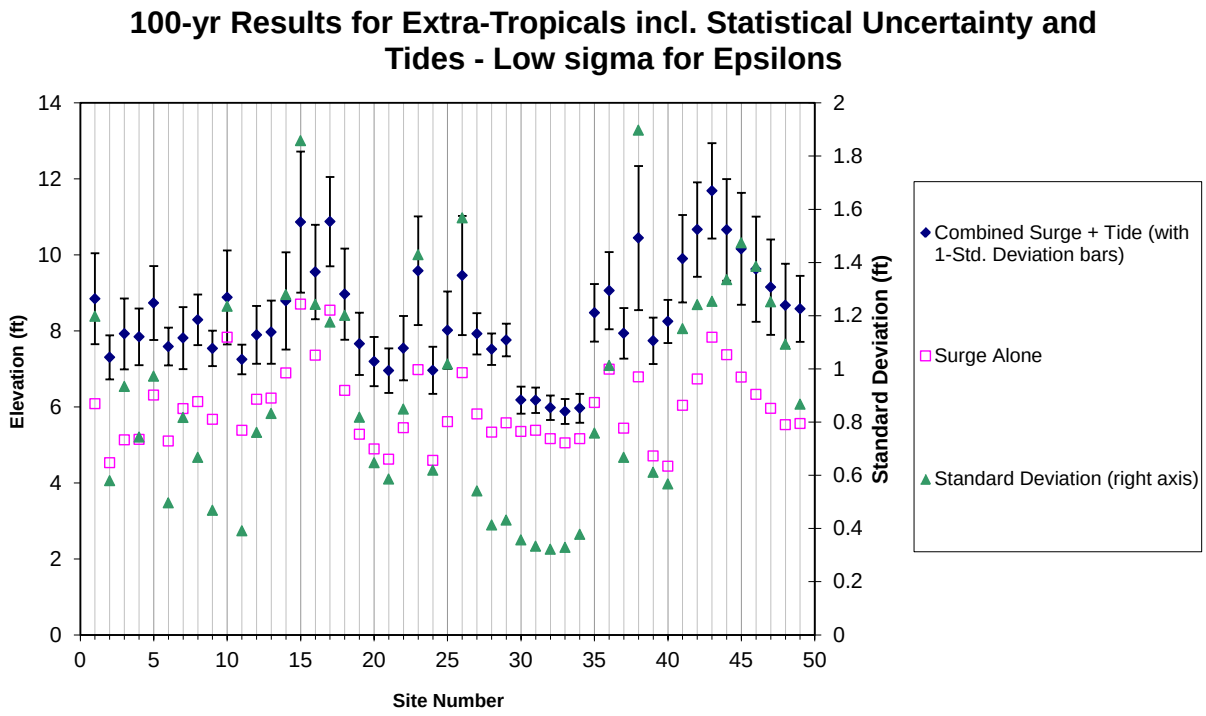

Figure 5-10. Effect of astronomic tide on the 1% annual-chance (100-year) surge from extratropical storms.

SECTION SIX APPROACH FOR SURGE FREQUENCY CALCULATIONS

6.1 INTRODUCTION

This section summarizes the approach to determine stillwater elevations at the desired recurrence intervals using the results from the storm surge model simulations of the JPM-OS and extratropical storms and discusses the key input parameters required for this step. The implementation of this approach is further detailed in the Recurrence Interval Analysis of Coastal Storm Surge Levels and Wave Characteristics Report for this project (RAMPP, 2014b).

6.2 INCLUSION OF THE SECONDARY TERMS

As indicated earlier, the JPM method does not explicitly include all factors affecting storm surge and also has to account for the limitations in the storm characterizations and in the numerical models. These include random departures of real storms from the idealized PBL behavior; random surge variations not captured by the hydrodynamic model; and the random contribution of astronomical tide. These effects are accounted for in the JPM method in a probabilistic manner. To this effect, the relationship given in Equation 4-5 can be expanded to include these factors by inclusion of the term ε:

$$P\left[\eta_{max(1\,yr)} > \eta\right] \approx \sum_{i=1}^{n} \lambda_i P\left[\eta(x_i) + \varepsilon > \eta\right] \tag{6-1}$$

where the random term ε includes four components, all considered Gaussian with zero means, as follows:

ε_1 – represents the astronomical tide level at the coast at the time of landfall. Because this study uses a Monte Carlo approach to include the effect of astronomical tide, including nonlinear tide-surge interactions, the standard deviation of this term is set to zero because this term is not needed.

ε_2 – represents variations in the surge response caused by random variations of the Holland B parameter that are not represented by the JPM-OS storms. Because this study treats the variation of B explicitly in the JPM-OS, the standard deviation of this term is set to zero because this term is not needed.

ε_3 – represents random errors in the computed surge caused by lack of skill of the numerical modeling. This was evaluated by comparing values of computed and measured surge at a large number of points for the validation storms; and was characterized by a standard deviation of 1.28 ft.

ε_4 – represents variations in the surge due to a wide range of departures in the real behavior of hurricane wind and pressure fields that are not represented by the planetary boundary layer (PBL) model. In FEMA (2008), this was evaluated by comparing the results of surge modeling done using handcrafted "best winds" with the findings for the same storms as represented using the PBL model. This effect was characterized by a standard deviation of 1.17 feet. Given the complexities of Atlantic hurricanes, this value is increased by 50 percent (after consultations with OWI), obtaining 1.76 feet. An additional contributor to these secondary factors is the difference between single- and double-exponential wind fields, which contributes a

small additional standard deviation of 0.29 feet. The resulting total standard deviation is then 1.78 feet.

These four components of ε are taken to be independent, and so can be combined into a single term having a standard deviation given by:

$$\sigma_\varepsilon = \sqrt{\sigma_{\varepsilon_1}{}^2 + \sigma_{\varepsilon_2}{}^2 + \sigma_{\varepsilon_3}{}^2 + \sigma_{\varepsilon_4}{}^2} \tag{6-2}$$

obtaining a standard deviation of 2.2 feet.

6.3 MATHEMATICS OF THE SURGE FREQUENCY CALCULATIONS FOR JPM-OS

The approach for surge frequency calculations is described in FEMA (2008) and in Niedoroda et al. (2010). This approach distributes the results for each storm using a Gaussian shape with standard deviation σ_ε, and then calculates exceedance frequencies in the usual manner.

6.4 COMBINATION OF RESULTS FROM TROPICAL AND EXTRATROPICAL STORMS

The approach for combination of results from tropical and extratropical storms is straightforward. It simply consists of adding the annual frequencies (for each value of surge elevation) from the two storm types and then reading off the values of surge elevation associated with the annual exceedance frequencies of interest. The process is illustrated in Figure 6-1. This calculation is often presented in a more complicated form, using formulas derived from Poisson processes or from probabilities of unions and/or intersections. Because the annual frequencies of interest are small (i.e., 10-percent or less), those formulas produce results that are numerically equivalent to those obtained by simple addition.

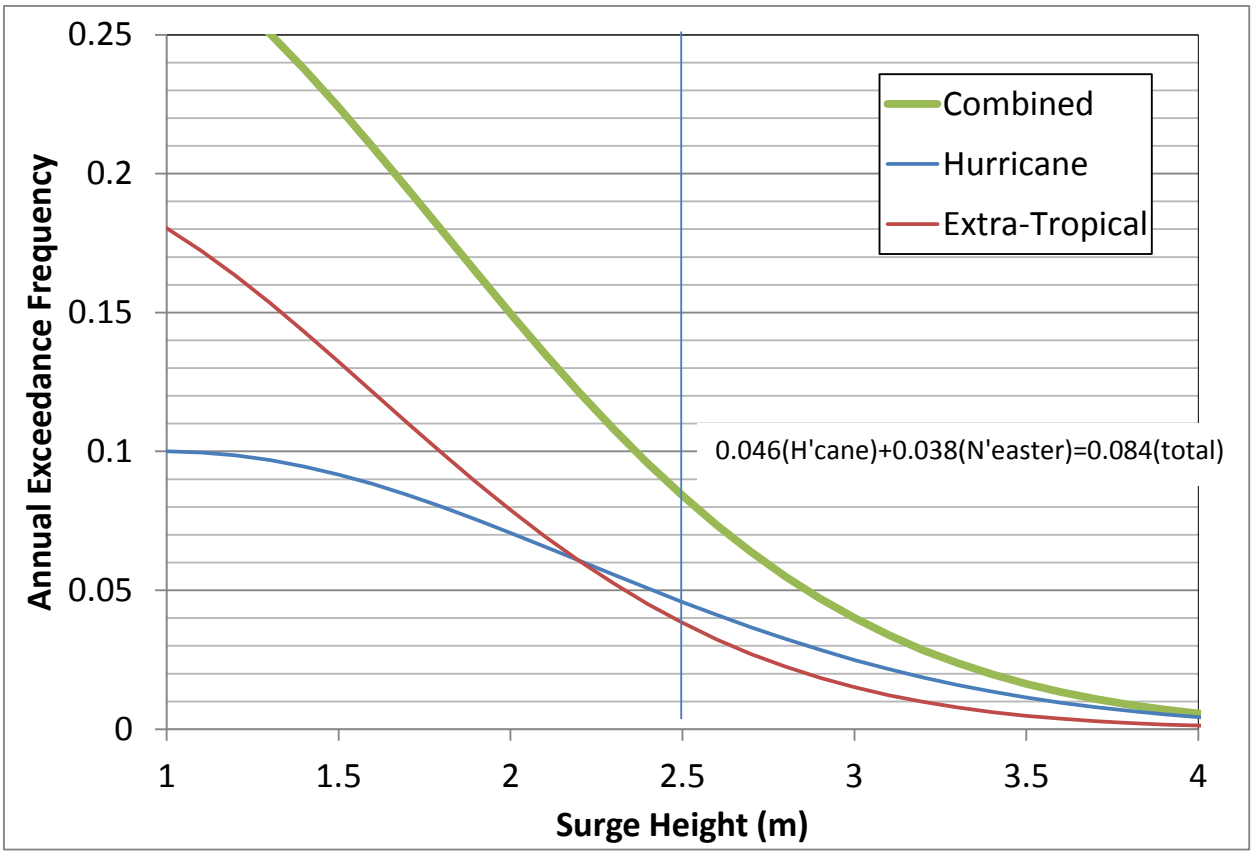

Figure 6-1. Example showing the process for combining surge elevations from tropical and extratropical storms.

SECTION SEVEN REFERENCES

Bell, G. D., and M. Chelliah (2006). Leading tropical modes associated with interannual and multi-decadal fluctuations in North Atlantic hurricane activity. J. Climate. 19, 590-612.

Benjamin, J.R. and C.A. Cornell (1970). Probability, Statistics, and Decision for Civil Engineers. New York, New York: McGraw-Hill.

Blanton, B.O., and P.J. Vickery (2008). North Carolina Coastal Flood Analysis System: Hurricane Parameter Development. Renaissance Computing Institute Technical Report TR-08-06, September.

Borgman, L.E., M.C. Miller, H.L. Butler, and R.D. Reinhard, R. D. (1992). "Empirical simulation of future hurricane storm histories as a tool in engineering and economic analysis." ASCE Proc. Civil Engineering in the Oceans V. College Station, TX. 2-5 November 1992

Chiu, T.Y, and R.G. Dean (2002). Methodology on Coastal Construction Control Line Establishment. Beaches and Shores Resource Center, Institute of Science and Public Affairs, Florida State University. http://bcs.dep.state.fl.us/reports/method.pdf (accessed March 26, 2014).

Chouinard, L. E. (1992). "A Statistical Method for Regional Design Wave Heights in the Gulf of Mexico," OTC 6832, Proceedings of the Offshore Technology Conference, Houston, TX.

Chouinard, L.M., and C. Liu (1997). "Model for Recurrence Rate of Hurricanes in Gulf of Mexico," *Journal of Waterway, Port, Coastal and Ocean Engineering*, Vol. 123, No. 3, pp. 113-119.

Chouinard, L.M., C. Liu, and C. K. Cooper (1997). "Model for Severity Rate of Hurricanes in Gulf of Mexico," *Journal of Waterway, Port, Coastal and Ocean Engineering*, Vol. 123, No. 3, pp. 120-129.

Efron, B. (1982). The Jackknife, the Bootstrap, and other Resampling Plans. Society for Industrial and Applied Mathematics, Philadelphia.

Federal Emergency Management Agency (1988). Coastal Flooding; Hurricane Storm Surge Model. Volume 1, Methodology, Office of Risk Assessment, Federal Insurance Administration, Washington DC.

Federal Emergency Management Agency (FEMA) (2008). Mississippi Coastal Analysis Project: Coastal Documentation and Main Engineering Report. Project reports prepared by URS Group Inc., (Gaithersburg, MD and Tallahassee, FL) under HMTAP Contract HSFEHQ-06-D-0162, Task Order 06-J-0018.

Federal Emergency Management Agency (FEMA) (2008). Joint Probability – Optimal Sampling Method for Tropical Storm Surge Frequency Analysis. Operating Guidance 8-12..

Gray, W.M., (1984). Atlantic seasonal hurricane frequency. Part II: Forecasting its variability, Mon. Wea. Rev., 112, 1649-1668.

Gualdi, S., E. Scoccimarro, A. Navarra (2008). Changes in Tropical Cyclone Activity due to Global Warming: Results from a High-Resolution Coupled General Circulation Model. Journal of Climate, Volume 21, no. 20, pp. 5204-5228

Ho, F.P. and V.A. Myers (1975). Joint Probability Method of Tide Frequency Analysis applied to Apalachiacola Bay and St. George Sound, Florida, NOAA Tech. Rep. WS 18, 43p.

Ho, F.P., J.C., Su, K.L. Hanevich, R.J. Smith, and F.P. Richards (1987). Hurricane Climatology for the Atlantic and Gulf Coasts of the United States, NOAA Technical Report NWS 38, Washington, D.C., April.

Holland, G.J. (1980). "An Analytic Model of the Wind and Pressure Profiles in Hurricanes." Monthly Weather Review: Vol. 108, No. 8, pp. 1212–1218.

Holland, G.J. and P.J. Webster (2007). Heightened tropical cyclone activity in the North Atlantic: natural variability or climate trend? Philosophical Transactions of the Royal Society A, 365(1860), 2695-2716.

Jelesnianski, C.P., J. Chen, and W.A. Shaffer (1992). SLOSH: Sea, lake, and overland surges from hurricanes. NOAA Technical Report NWS 48, NOAA, Washington, DC.

McGuire, R.K., C.A. Cornell, and G.R. Toro (2005). "The Case for Using Mean Seismic Hazard," *Earthquake Spectra,* v. 21, no. 2, p. 879-886.

Myers, V.A. (1975). Storm Tide Frequencies on the NY-NJ Coast, NOAA Tech. Rep. NWS-16, 79 p.

National Oceanic and Atmospheric Administration (1996). The deadliest, costliest, and most intense United States hurricanes of this century (and other frequently requested hurricane facts). NOAA Technical Memorandum NWS TPC-1.

National Oceanic and Atmospheric Administration (2005). The deadliest, costliest, and most intense United States tropical cyclones from 1851 to 2005 (and other frequently requested hurricane facts). NOAA Technical Memorandum NWS TPC-4. Appendix A updated in 2006.

National Oceanic and Atmospheric Administration (2007). The Atlantic Hurricane Database (HURDAT). http://www.aoml.noaa.gov/hrd/hurdat/

Niedoroda, A.W., D.T. Resio, G.R. Toro, D. Divoky, H. Das, and C.W. Reed (2010). "Analysis of the coastal Mississippi storm surge hazard," *Ocean Engineering,* Vol. 37, No. 1, pp. 82-90.

Oceanweather, Inc. (2010). Tropical Cyclone Parameter Analysis and Synoptic Climatology for the FEMA Region II NY/NJ Coastline RAMPP Project. Draft report, May.

Parzen, E. (1962). Stochastic Processes. San Francisco, California: Holden Day.

Patè-Cornell, M.E. (1990). Risk Uncertainties in Public-Sector Safety Decisions: Assessment Methods and Management Implications, in Cox, L.A., and P.F. Ricci (editors), New Risks: Issues and Management. Plenum Press

RAMPP, 2014a, Region II Storm Surge Project - Development of Wind and Pressure Forcing in Tropical and Extratropical Storms, FEMA TO HSFE02-09-J-001, 2014

RAMPP, 2014b, Region II Storm Surge Project - Recurrence Interval Analysis of Coastal Storm Surge Levels and Wave Characteristics, FEMA TO HSFE02-09-J-001, 2014.

Resio, D.T. (2007). *White Paper on Estimating Hurricane Inundation Probabilities* (with contributions from S.J. Boc, L. Borgman, V. Cardone, A. Cox, W.R. Dally, R.G. Dean, D. Divoky, E. Hirsh, J.L. Irish, D. Levinson, A. Niedoroda, M.D. Powell, J.J. Ratcliff, V. Stutts, J. Suhada, G.R. Toro, and P.J. Vickery). Appendix 8-2 (R2007) of US Army Corps of Engineers (2007), Interagency Performance Evaluation Taskforce (IPET) Final Report (Interim). https://ipet.wes.army.mil/NOHPP/_Post-Katrina/(IPET)%20Interagency%20Performance%20Evaluation%20TaskForce/Reports/IPET%20Final%20Report/Volume%20VIII/Technical%20Appendices.pdf

Resio, D.T., and L. Orelup (2006). Climatic Variations in Hurricane Characteristics and their Potential Effects on Waves and Surges in the Gulf of Mexico. Proc. 9th International Workshop On Wave Hindcasting And Forecasting, September.

Risk Engineering, Inc. (2005). Estimation of 10-4 Using Synthetic Storms—Phase II-GoM: Refined Model and Estimates for the Gulf of Mexico. October.

Schloemer, R.W. (1954). Analysis and synthesis of hurricane wind patterns over Lake Okeechobee, FL. Hydromet Rep. 31, 49 pp. [Govt. Printing Office, No. C30.70:31].

Shen, W., 2006: Does the size of hurricane eye matter with its intensity?, Geophys. Res. Let., 33, L18813.

Toro, G.R., C.A. Cornell, V.J. Cardone, and D.B. Driver (2004). "Comparison of historical and deductive methods for the calculation of low-probability seastates in the Gulf of Mexico," *Proc. OMAE-04 Conference*, ASME.

Toro, G.R., A.W. Niedoroda, C.W. Reed, and D. Divoky (2010). "Quadrature-based approach for the efficient evaluation of surge hazard," *Ocean Engineering*, Vol. 37, No. 1, pp. 114-124.

Toro, G.R., D.T. Resio, D. Divoky, A.W. Niedoroda, and C. Reed (2010b). "Effective joint-probability methods of hurricane surge frequency analysis," *Ocean Engineering*, Vol. 37, No. 1, pp. 125-134.

Vickery, P. J., P. F. Skerlj, and L.A. Twisdale (2000). Simulation of Hurricane Risk in the U.S. Using Empirical Track Model. Journal of Structural Engineering, vol. 126, no. 10, October.

Vickery, P.J., and D. Wadhera (2008). Statistical Models of Holland Pressure Profile Parameter and Radius to Maximum Winds of Hurricanes from Flight-Level Pressure and H*Wind Data. Journal of Applied Meteorology and Climatology, vol. 47, October.

Webster, P.J., G.J. Holland, J.A. Curry, and H.R. Chang (2005). "Changes in Tropical Cyclone Number, Duration, and Intensity in a Warming Environment." Science Vol. 309, no. 16, September.

Wen, Y.K. and H. Banon (1991). "Development of Environmental Combination Design Criteria for Fixed Platforms in the Gulf of Mexico," OTC 6540, Offshore Technology Conference, Houston, Texas, May.